Initial studies towards new activators of the BK channel

Lawin Askari

Thesis for the degree Master of Pharmacy
45 credits

Section for Pharmaceutical Chemistry
Department for Pharmacy
Faculty of Mathematic and Natural Sciences

UNIVERSITY OF OSLO

May 2021

Initial studies towards new activators of the BK channel

Lawin Askari

Thesis for the degree Master of Pharmacy
45 credits

Section for Pharmaceutical Chemistry
Department for Pharmacy
Faculty of Mathematic and Natural Sciences

UNIVERSITY OF OSLO

May 2021

2021

Initial studies towards new activators of the BK channel

Lawin Askari

http://www.duo.uio.no/

Acknowledgements

The work on the master´s degree was performed at the Section for Pharmaceutical Chemistry, Department of Pharmacy, University of Oslo, in the LIPCHEM-group. I would like to express my deepest gratitude to my supervisors Professor Trond Vidar Hansen, Associate Professor Anders Vik and Dr. Marius Aursnes for giving me this amazing opportunity to be a part of a great project. I am incredibly grateful for Professor Trond Vidar Hansen for sharing his vast knowledge of organic chemistry, also his encouragement and motivation have been of great help.

I wish to show my gratitude to Dr. Marius Aursnes. I am very grateful for his assistance in the lab and also for sharing his vast knowledge of organic chemistry. His support and conversations were really of great help during stressful times.

I also want to thank Dr. Karoline Primdahl for her assistance with HPLC-analysis, and also for answering any questions I had in the laboratory. Also, I am very grateful for the rest of the LIPCHEM-group and the other master students. Thank you for the support and also the motivation.

Finally, I would like to thank my family and friends for their support, motivation and love. Especially, my parents who have given me a humongous amount of support and love during this time. They have been my biggest role model and my driving force during this period. Also, I am grateful for my little brother who has always found a way to make laugh.

Blindern, May 2021

Lawin Askari

Abstract

Over the years, many studies have been conducted on long-chain ω-3 polyunsaturated fatty acids (PUFAs). The health benefits of PUFAs have gained a lot of attention and therefore believed to be good lead compounds in drug discovery. One of the PUFAs that have been of great interest is docosahexaenoic acid (DHA). DHA has proven to be a good substrate for the activation of the BK (Slo1) channel in vascular smooth muscle cells resulting in vessel relaxation, thus provides lowering of the blood pressure. To achieve more knowledge about the interaction of DHA and the BK channel are very beneficial to be able to optimize structural features and therefore the hypotensive effect.

Eicosapentaenoic acid (EPA) is another PUFA which has structural similarities to DHA, and therefore also very interesting in the activation of the BK channel. Thus, different analogs of EPA will give us insight in which structural and spatial structure is the most optimal for the interaction with the BK channel. Therefore, the aim of this project was to synthesis new analogs of EPA, thus new activators of the BK channel. The synthesis included the synthesis of EPA-oxy acetate, and also introduction of methyl- and ethyl-groups to EPA-oxy-acetate. It was particularly focused on achieving a separation of the enantiomers of the EPA-oxy-acetate analog with the ethyl group. Biological evaluations can provide information about the activating effect these enantiomers have.

Graphical abstract

Synthesis of EPA-oxy-acetate

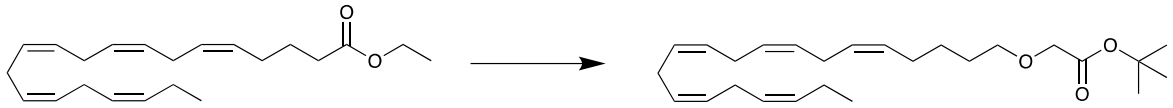

Introduction of methyl group to EPA-oxy-acetate

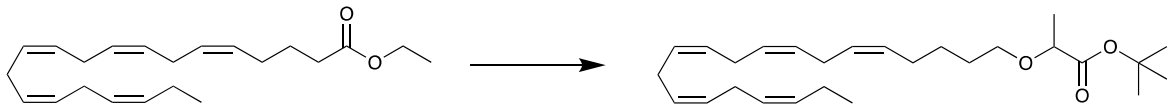

Introduction of ethyl group to EPA-oxy-acetate

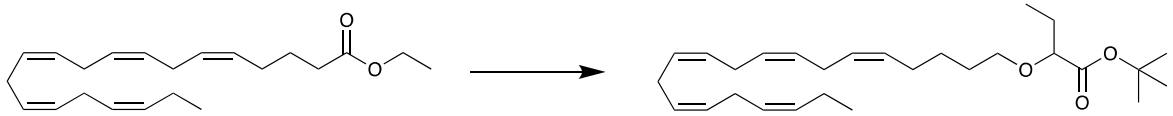

Separation of enantiomers of EPA-oxy-acetate analog with ethyl group

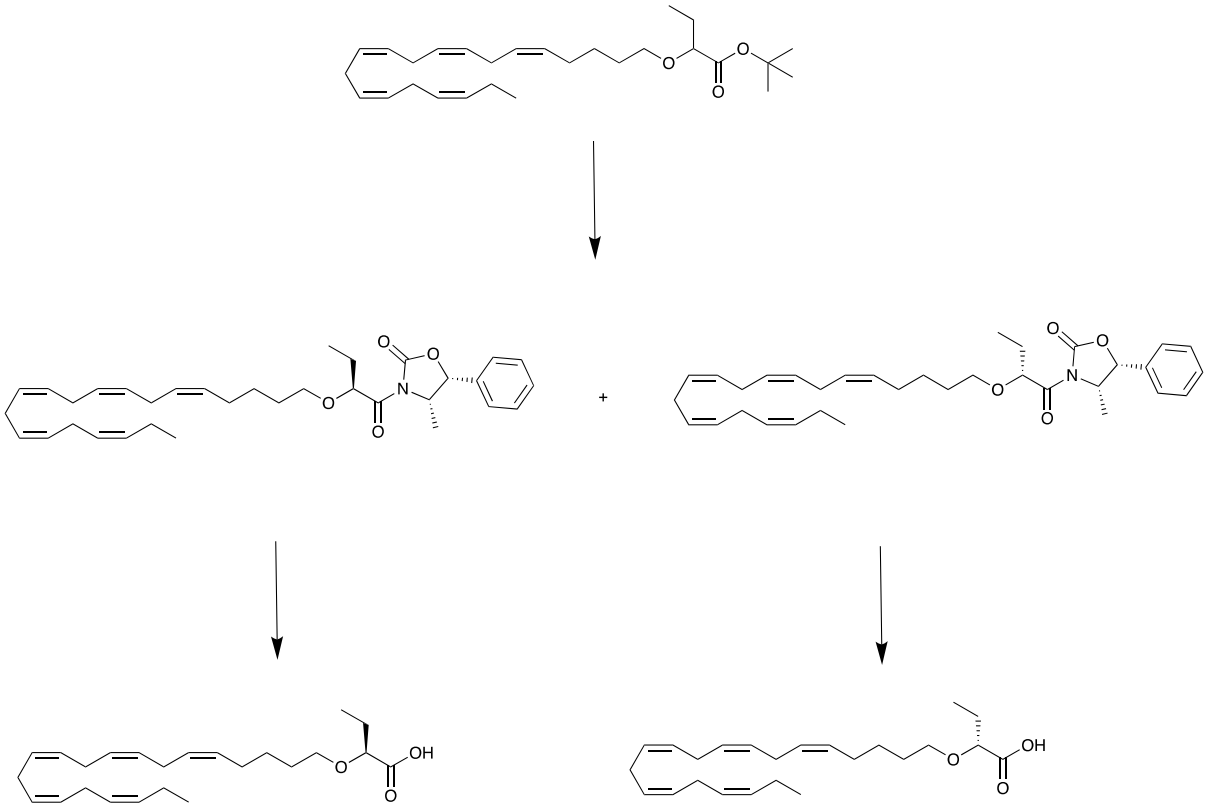

Amid coupling of EPA-oxy-acetate analog with ethyl group

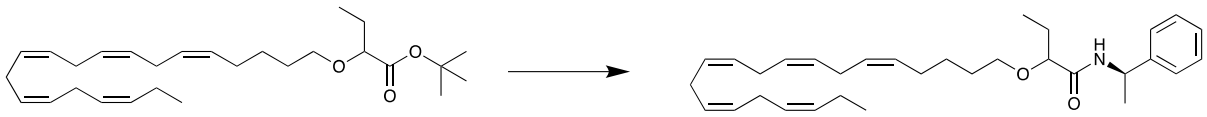

List of abbreviations

AA	Arachidonic acid
ALA	α-Linolenic acid
Acetyl-CoA	Acetyl Coenzyme A
CAM	Cerium ammonium molybdate
CDI	Carbonyldiimidazole
CTD	The cytosolic domain
DCC	*N*,*N*´-Dicyclohexylcarbodiimide
de	Diastereomeric excess
DGAT	Aceyl-CoA:diacylglycerol acyltransferase
DHA	Docosahexaenoic acid
DMAP	4-Dimethylaminopyridine
DMSO	Dimethyl sulfoxide
DPA	Docosapentaenoic acid
dr	Diastereomeric ratio
EC_{50}	Half-maximal effective concentration
EPA	Eicosapentaenoic acid
HPLC	High-performance liquid chromatography
HRMS	High-resolutioon mass spectrometry
LTB_4	Leukotriene B4X
NMDA	*N*-Methyl-D-aspartate
PIP2	Phosphatidylinositol 4,5-biphosphate
PGD	Pore-gate domain
PUFA	Polyunsaturated fatty acid

THF	Tetrahydrofuran
TLC	Thin-layer chromatography
TRP	Transient receptor potential cation channel
VSD	Voltage sensor domain

Table of contents

1 Introduction

1.1 Aim of synthesis

Previous results for the LIPCHEM group have shown that the synthetic PUFAs analogs named 3-oxa n-3 DPA is a potent activator of BK (Slo1) channel[1]. Based on this the following aims are related to this project:

1. Synthesis of EPA-oxy-acetate. The structure is shown in Figure 1.1.

2. Preform initial and further drug structural activity relationship studies using EPA-oxy-acetate where methyl and ethyl group are to be introduced.

3. Prepare the *S*- and *R* -enantiomers of the analog of the EPA-oxy-acetate with an ethyl group.

4. Submit the products to biological evaluations, if time allowed.

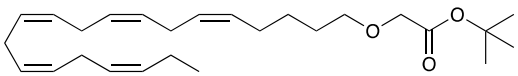

EPA-oxy-acetate (16)

Figure 1.1: Structure of EPA-oxy-acetate **16**.

1.2 An introduction to fatty acids

The basal structure of a fatty acid consists of a hydrocarbon chain and a carboxyl group (-COOH) on the end. The acidic terminal (pKa ∼ 4.8) which is ionized at physiological pH, gives a fatty acid a hydrophilic character. One the other hand, the hydrocarbon chain causes its hydrophobic character, meaning that fatty acids are amphipathic structures. Long-chain fatty acids (LCFAs) are highly insoluble in hydrophilic environment, due to the larger hydrophobic portion.[2]

A fatty acid is a well-known member of the lipid class of natural products biosynthesized via the polyketide pathway. Thus, the structure of fatty acids are as other polyketides derived from

Claisen condensation reactions of acetic acid units, which leads to poly-β-keto chains. Firstly, acetyl-coenzyme A (acetyl-CoA) is carboxylated to malonyl-coenzyme A (malonyl-CoA). The carboxylation takes place with the help of ATP, CO_2 as HCO_3^- (bicarbonate) and the coenzyme biotin. The condensation reaction is repeated several times to extend the chain. The chain reaction branch early for fatty acids. Most fatty acids are straight chained consisting of four to thirty carbon atoms. There are fatty acids with a backbone consisting of odd numbers of carbon atoms, but usually they are even numbers. In the nature, the fatty acids that consist of 16 and 18 carbon atoms are represented most.[3]

Fatty acids can be grouped according to whether they are saturated or unsaturated. Saturated fatty acids do not have any double bonds in the hydrocarbon chain. These are mostly found as solids in the form of glycerides in animal fat. In fish and plants fatty acids are manly in liquid form, thus unsaturated. Unsaturated fatty acids carry one or more double bonds in the hydrocarbon chain, grouped as mono- or polyunsaturated fatty acids, respectively.[2, 3]

1.3 Polyunsaturated fatty acids

The reason for the often occurring "bends" in the hydrocarbon chains in polyunsaturated fatty acids (PUFAs) is due to the configuration of the double bonds, which is usually *Z* (*cis*). Therefore, aggregation and association of these PUFAs are hindered, causing the PUFAs to be liquids and cell membranes containing PUFAs to be more fluidic. In the backbone, the double bonds are typically placed in a non-conjugated order. A way of systematically grouping the fatty acids is according to the number of carbon atoms in the chain, also the configuration and position in the chain of the double bonds. A commonly known grouping is according to the position of the double bond from the methyl group (C-terminus), and they are known as *ω*-3 (omega-3), *ω*-6 (omega-6), and *ω*-9 (omega-9) fatty acids. The position of the double bond is determined by the desaturase enzyme that facilitates the biosynthesis of PUFAs. Different desaturase enzymes are available in the plant and mammalian metabolism. Long chained PUFAs, that fall under the umbrella of *ω*-3 fatty acids, are eicosapentaenoic acid (EPA) (**1**), n-3 docosapentaenoic acid (n-3 DPA) (**2**) and docosahexaenoic acid (DHA) (**3**).[3] The structure of these *ω*-3 PUFAs are shown in Figure 1.2.

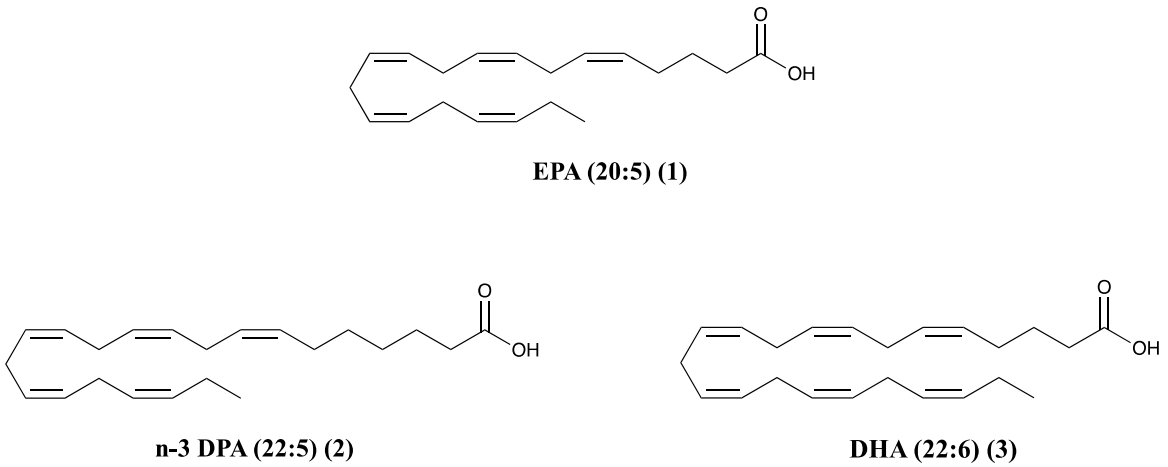

Figure 1.2 Chemical structures of EPA (**1**), n-3 DPA (**2**) and DHA (**3**)

Many studies have been conducted throughout the years researching PUFAs and optimized structures that can be health beneficial. The health benefits of PUFAs will be discussed later on.

1.4 Biosynthesis of polyunsaturated fatty acids

There are several ways unsaturated fatty acids can be synthesized in an organism. In many different organisms unsaturated fatty acids are synthesized from several repeated desaturations of the alkanoic acid, assisted by various types of desaturase enzymes. The initial step of biosynthesis of unsaturated fatty acid is of course the biosynthesis of a saturated fatty acid. Then a double bond is introduced to the hydrocarbon chain in the position between C-9 and C-10, with the stereochemistry *Z* (*cis*). The double bond is often introduced by the Δ^9-desaturase enzyme, which is a commonly occurring desaturase enzyme in many eukaryotic organisms. The mechanism is supported by O_2 as the acceptor at the electron transport chain (ETC) ending, and also by either NADPH or NADH as a cofactor.[3]

A stearoyl derivative has a saturated hydrocarbon chain and is a common start for introducing a double bond and results in an oleic thioester. Mammalian organisms and plants have different biosynthetic routes after the latter mechanism. What differs between mammalian organisms and plants is the different desaturase enzyme they use in the next desaturation and therefor the positioning of the next double bond.[3] New double bonds are introduced towards the carboxyl group in the fatty acid's hydrocarbon chain in mammalian organisms. In plants the new double

bonds are introduced between the methyl terminus and the previous synthesized double bond. Plants contain the Δ^{12} and Δ^{15} desaturase enzymes, which gives them ability to synthesize linolenic acid and α-linolenic acid, that do not occur in mammalian cells. When animals consume plants, they gain linolenic acid and α-linolenic acid, which they can use as building blocks for the synthesis of other unsaturated fatty acids through desaturation and elongation of the hydrocarbon chain.[3]

In Figure 1.3, an overview of the biosynthesis of EPA (**7**), DPA (**8**), DHA (**9**) and arachidonic acid (**13**) is shown. α -linolenic acid is the precursor of EPA, DPA and DHA. A double bond is introduced to α -linolenic acid in the position between C-6 and C-7 by the help of Δ^6-desaturase to give stearidonic acid (**5**). Further, the chain is elongated by the help of C_{18} elongase, which results in an extension of the hydrocarbon chain by two carbons to give eicosatetraenoic acid (**6**). The Δ^5-desaturase enzyme introduces a new double bond between C-5 and C-6 in the hydrocarbon chain of eicosatetraenoic acid (**6**), which results in EPA (**7**). EPA itself has numerous health benefits which will be discussed in Chapter 1.5. From EPA, there are two more significant routes. Adding one more malonyl-CoA to EPA (**7)** in a condensation reaction will elongate the hydrocarbon chain by two carbons by the help of C_{20} elongase, which results in DPA (**8**). Introducing one more double bond to DPA in the position C-4 and C-5 by Δ^4-desaturase results in DHA (**9**). Also, EPA is the precursor of the prostaglandins 3-series. Linolenic acid is the precursor for the prostaglandins 1-series and arachidonic acid (**13**), thereby also the prostaglandins 2- series. The hydrocarbon chain of linolenic acid is elongated by the addition of a malonyl-CoA molecule in a Claisen condensation reaction, by the help of C_{18} elongase and Δ^5-desaturase which introduces a double bond between C-5 and C-6.[3]

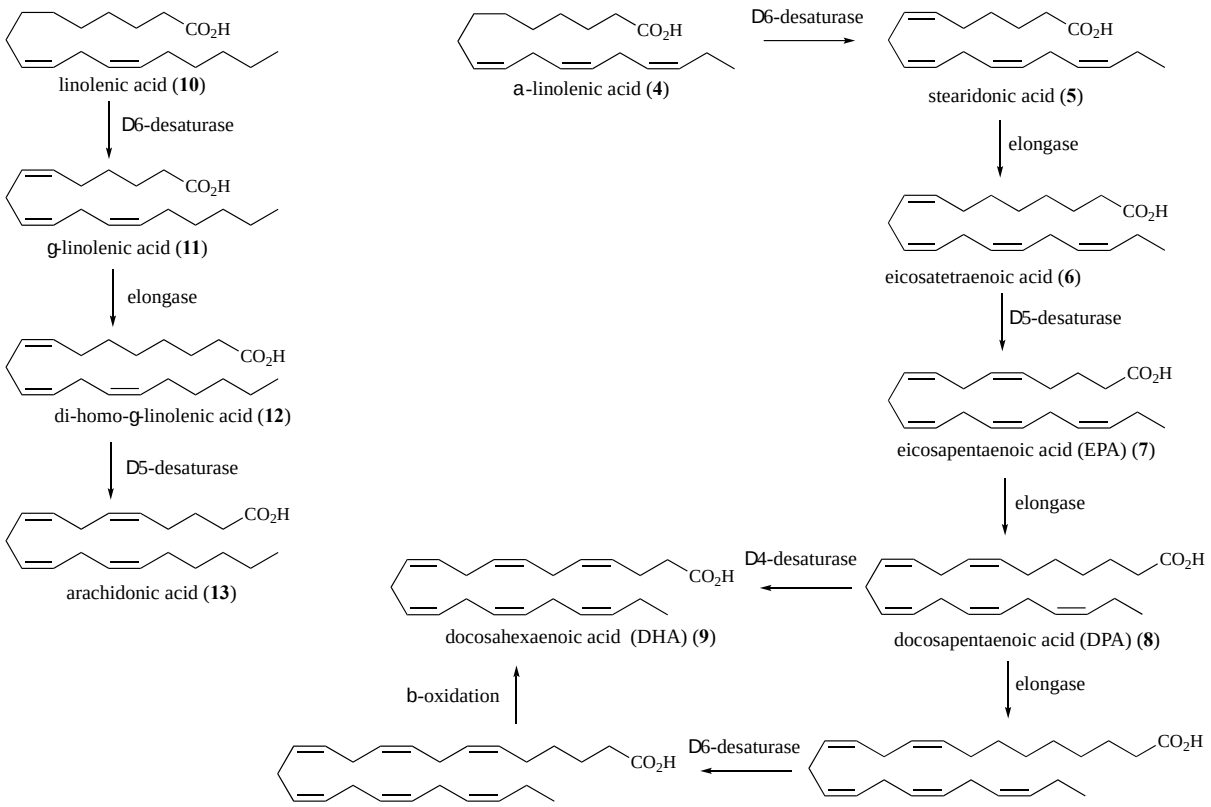

Figure 1.3 A simplified overview of the biosynthesis of eicosapentaenoic acid (**7**), docosapentaenoic acid (**8**), docosahexaenoic acid (**9**) and arachidonic acid (**13**).[3] For simplicity, the free acids are drawn.

1.5 Health benefits of ω-3 Polyunsaturated fatty acids

Eicosapentaenoic acid (EPA) and docosahexaenoic acid (DHA) are both members of the PUFA family. It is well-known that ω-3 polyunsaturated fatty acids (PUFAs), derived from marine-based fish, have health benefits. Health benefits against cardiovascular diseases (CVDs) are the commonly associated with these ω-3 PUFAs. Furthermore, these fatty acids also have anti-inflammatory and hypotriglyceridemic effect. Also, different studies that have been conducted, have shown encouraging results on several other effects these ω-3 PUFAs have, including anticancer, antioxidant and antiarthritis effects.[4]

PUFAs are of great significance in the synthesis of various physiological mediators. Examples of these mediators are the eicosanoids and also arachidonic acid. Furthermore, they serve as structural components for cellular lipids and EPA has an important role as a component specifically in nerve cell lipids. Two major classes of essential PUFAs are the n-6 and ω-3 PUFAs. These are known as essential fatty acids and therefore must be consumed as a part of

the diet, since these cannot be produced by the human body. High concentrations of the ω-3 PUFA linoleic acid is available in seed, leafy vegetables plants, nuts and as well in legumes. As discussed earlier, linoleic acid is an important precursor for EPA and n-3 DPA. Not only linoleic acid, but both EPA and n-3 DPA can be derived as oil from cold-water fish.[5]

Reduction of cardiovascular mortality and morbidity is highly thought of relating to an increased intake of very long chain ω-3 fatty acids. In fact, reduction of mortality has been shown by supplementation studies done. Due to the founds and the contouring researchers of the benefits of long-chain ω-3 fatty acids, both governmental and nongovernmental recommendation of increasing the intake of fish has been released. The recommendation suggests an intake of at least two fish meals per week, and favorably at least one being oily fish.[6] Reduction of ischemic heart disease by eating fish routinely is supported by epidemiological evidence. Also, taking PUFAs as supplement to a diet has also been favorably to the patients who had myocardial infarction recently. However, the mechanism of action on triglyceride concentrations is still unknown.[7]

In 1994, a lipid-regulating agent, marketed under the name Omacor® (Pronova BioPharma) was introduced to the Norwegian market, and two years later it was introduced to the European market.[8] It became the first ω-3 fatty acid drug that was approved by both the EU and US Food and Drug Administration (FDA). Omacor® is formulated as a capsule containing 380 mg of the ethyl ester of DHA and 460 mg of the ethyl ester of EPA, respectively.[9]

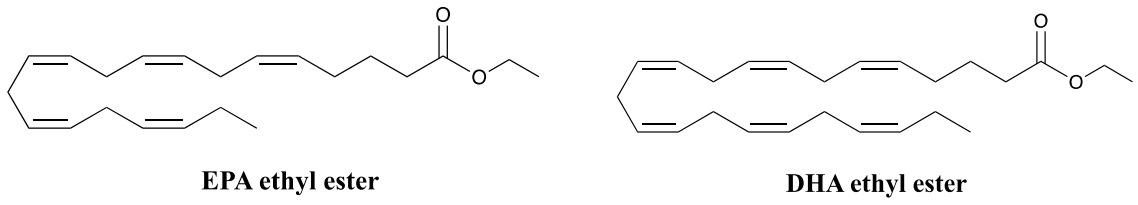

EPA ethyl ester **DHA ethyl ester**

Figure 1.4 Structures of EPA ethyl ester and DHA ethyl ester

Inhibition of acyl CoA:1,2-diacylglycerol acyltransferase and also increased peroxisomal B-oxidation in the liver is thought to be the potential mechanisms of actions. However, it is not fully understood. It is believed that Omacor® has the potential to reduce the synthesis of triglycerides (TGs) in the liver. The reason for this, is that EPA and DHA are poor substrates

for the enzyme glycerol-3-phospate acyltransferase (GPAT) that participate in the synthesis of TGs.[10, 11]

FDA has approved the use of the ethyl ester of EPA named as icosapent ethyl, marketed as Vascepa® in the USA. The ethyl ester is in fact de-esterfied when administered orally and results in EPA in free acid state.[12, 13]

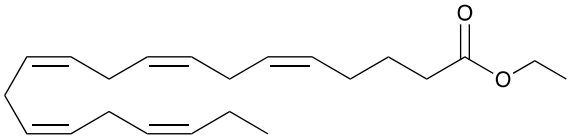

Icosapent ethyl (EPA-EE)

Figure 1.5 Structure of Icosapent ethyl (EPA-EE)

The approved indication is as an adjunct to give a reduction of TG levels in adult patients with severe hypertriglyceridemia which is defined as >500 mg/dL (>5.65 mmol/L). A second approved indication is the use of Vascepa® as an adjunct to maximally tolerated statin therapy with the aim of reducing the risk of stroke, coronary revascularization, myocardial infarction and unstable angina in cases where hospitalization may be necessary for adult patients with high levels of TG (>500 mg/dL), and also established cardiovascular disease or diabetes mellitus and two or more additional risk factors for cardiovascular disease.[12, 13]

A patent was filed for by BASF AS and approved in 2019,[14] for several fatty acid derivatives with the aim for treating steatohepatitis. Among these structures, the separation of the enantiomers of EPA-oxy-acetate with an ethyl group, was included. Herein, the synthesis of these enantiomers was desired to be able to research further their impact on the BK channels in blood vessels.

1.6 Fatty acids and ion channel function

The plasma membrane of cells has an important role in controlling influx and efflux of different molecules and functions as a barrier. Some molecules can move in and out of the cells by passive diffusion, while others need active transport. This depends of course on the molecular size, and the lipophilicity and hydrophilicity of the molecule. Ion channels is one of the main classes of membrane proteins and operates by passive diffusion. Meaning molecules can pass through these very small pores in the membrane, which creates an opportunity for inorganic ions, which pass through the hydrophobic lipid bilayer. Ion channels have ion selective, therefore only the ions that with the right charge and size is able to go through the channel. An important characteristics of ion channels is the fact that they are not always open, but rather gated. Therefore, they switch from being open and closed when influenced by a stimulus. There are many different stimuli that can trigger a conformational change in ion channels, and each ion channel has their specific stimulus. If the stimulus can trigger an opening in an ion channel is the membrane potential, then the class of ion channel is known as voltage-gated ion channels. Changes in the membrane potential is detected by the voltage sensors which are specialized charges protein domain within the ion channel. A few specific ions indirectly influence the opening and closing of the voltage-gated ion channels. This is related to the fact that these ions have an impact on the membrane potential, when small changes are detected by the sensitive voltage sensors a change in the conformation will happen.[15]

30 years ago, the principle of "force-from-lipids" (FFL) was demonstrated. This principle explains that large anisotropic forces acquired from changes in the lipid bilayer, can be the driving force to conformational rearrangements, thereby ion channel gating. It has been demonstrated by structure-function studies that direct interaction lipids and protein could have an impact on the channel gating. Ion channel function can be modulated by PUFAs and also their derivatives. The FFL principle can be applied to many different ion channels.[16, 17]

PUFAs carry many different roles as important components of the membrane lipid membrane. They have an important role of regulating membrane protein function. Also, they have an impact on regulation of receptor signaling, gene expression and membrane remodeling.[16] The two different ways PUFAs can do such an impact are indirectly or directly. Firstly, it might be their ability to alter the mechanical properties of the membranes. It can also be caused by their ability to directly bind to the membrane protein. It has been demanding to recognize which one it is, and therefore numerous studies have been conducted. Studies conducted by Cordereo-

Morales *et al*. in 2018,[16] conveyed that fatty acids have the ability to regulate different ion channels. However, they could not conclude how much impact they have *in vivo* despite the usage of different models and conditions, since the studies where not conducted in the membrane environment.[16] This shows how much more research is needed and also in work to determine the impact fatty acids can have on ion channels.

Ion channels that are prone to modulation indirectly by lipids are NMDA, C. elegans mechanoreceptor complex, TRP and TRPL. The *N*-methyl-D-aspartate (NMDA) receptor is modulated by arachidonic acid (AA) and the effect it gives off is potentiation, leaving an impact on cognitive functions and neural signaling. PIP2 has an activation effect on the TRP and TRPL ion channels leaving an impact on the sensory transduction.[16, 18] Ion channels that are known to be prone to modulation by lipids are the BK channel, TRPV1 and pLGIC. DHA has proven to have the ability to modulate directly both the BK channel and pLGIC, however it will activate BK channel enhance desensitization pLGIC. Another substrate that will enhance activation of the BK channel is leukotriene B4 (LTB_4). LPA and anandamide will lead to the activation of the TRPV1 channels.[16] PUFAs have been proven to regulate pain by activating the TRPA1 and TRP vanilloid 1 (TRPV1). The PUFAs EPA, DHA and AA have been proven to have the ability to regulate pain by leaving activating TRPA1 channels. TRPV1 is activated by the lipid metabolite lysophosphatidic acid (LPA) and the endogenous metabolite anandamide but inhibited by EPA and DHA and thereby prevent inflammatory pain.[16, 18] BK channels will be discussed in more detail in the next chapter.

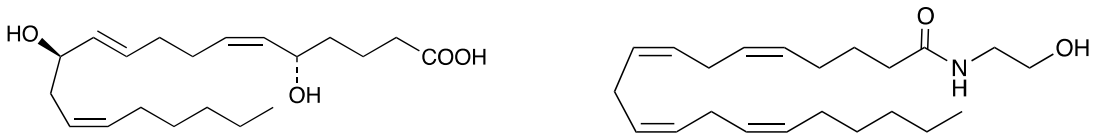

Leukotriene B4 (LTB_4) **Anandamide**

Figure 1.6 Structure of leukotriene B4 (LTB_4) and anandamide

Ion channels modulated directly and/or indirectly by lipids			
Type of interaction	**Ion channel**	**Lipid**	**Effect on function**
Indirect	NMDA	AA	Potentiation
	TRP and TRPL	PIP_2 depletion	Activation
	C. elegans mechanoreceptor complex	AA-containing phospholipids	Enhance activation
	TRPV4	EEQ-containing phospholipids	Enhance activation
Direct	pLGIC	DHA	Enhance desensitization
	BK	DHA	Activation
	BK	LTB4	Enhance activation
	TRPV1	LPA Anandamide	Activation

Figure: 1.7 An overview of some of the PUFAs and their effect on different ion channels. This table is based on a table in an article by Cordero-Morales *et al.* in 2018.[16]

A different study, conducted by Larsson *et al.* in 2020,[19] has demonstrated physiological regulation of the Kv7.1-Kv7.3 channels by PIP2 and also later by free fatty acids as EPA, DHA, AA, ALA and LA. The Kv7.1 - Kv7.3 are members of the Kv7 family, which are voltage-gated potassium channels, and the five different isomers are expressed in many different tissues. Demonstrated PUFAs as modulators of Kv7 channels. The Kv7 family are voltage-gated potassium channels, and the five different isomers are expressed in many different tissues. Dysfunctional Kv7 channels are linked to different disorders, such as cardiac arrhythmia, hearing impairment and epilepsy. It has been shown that free fatty acids, meaning unesterified, have the ability to modulate Kv7 channels by leading to an increase in current amplitude. Thereby, the opening of the Kv7 channel and also increased maximum conductance is shown in some cases. It was observed that the degree of anionic character impacted the degree of the shift toward negative voltages. A cationic character was observed to shift the voltage positively. PUFAs are also believed to be able to indirectly effect the Kv7 channels by effecting the bilayer or by giving active metabolites of the corresponding PUFA as AA which gives the metabolites prostaglandins and leukotrienes.[19]

1.7 BK (Slo1) channel and polyunsaturated fatty acids

Large-conductance Ca^{2+}- and voltage-activated K+ (BK) channels are also known as Slo1, $K_{Ca}1.1$ and MaxiK channels. Ion channels are membrane proteins which have an important function in cell communication and contributes by mediating passive ion transport. An ion flux down an electrochemical gradient is allowed upon an activation of the pores. Thereby, ions are allowed inside or outside of the cell membrane. BK channels is one important example.[1] Intracellular Ca^{2+} activates the BK channels by binding to the allosteric site, also membrane depolarization will give an activation and opening of the channel.[1, 20] Which then leads to an efflux of K^+. Other ligands that are able to activate the channel are Mg^{2+}, heme, protons, ethanol, carbon monoxide (CO), and PUFAs.[20] An important feature of the BK channels is the fact of the large conductance of -250 pS, which in fact 10-20 times larger than the typical conductance for a Kv channel, meaning that opening of few BK channels will result in change in the membrane voltage.[21]

The human gene called *Slo* or *KCNMA1* is the only gene responsible for the encoding of the BK channels. BK channels are expressed in most human cell which explains the reason behind its participation in many different physiological processes. Among the physiological processes there are regulation of the vascular tone, meaning they have an impact on the contraction of the smooth muscle. Due to their impact on the vascular system they are proven to have a connection to vascular diseases as hypertension, subrachnoid hemorrhage (SAH) stroke.[20, 22] It has also been proven that BK channels are well represented in the neural cells in the central nervous system (CNS) and have an important role by regulating the release of neurotransmitters and neural excitation. Therefore, the BK channels are also proven to be involved in the pathogenesis of Alzheimer's disease and epilepsy.[20, 22, 23] Other processes they are able to regulate are regulation of the bladder tone and hearing, and again also involved in pathogenesis of diseases relating to these physiological processes. In fact, they also involved several other physiological processes and also pathogenesis of diseases relating to these.[20, 22]

The channel itself consists of two subunits, which are the α and β subunits. The α subunit is the pore-forming unit and is also part of the voltage-dependent potassium (Kv) channel family. A characteristic of those channels are the six transmembrane domains (S1-S6). When the cell membrane is depolarized the S4 will move across electric field and conveys energy to mediate channel opening.[20] The reason for this, is that the fact it carries positively charged residues.[24]

The β-subunit consists of β1- β4 which are transmembrane proteins.[21] Four Slo1 subunits make up for the BK channel. Three main structural domains have three different important functions, and they are the pore-gate domain (PGD), the voltage sensor domain (VSD) and the large cytosolic domain (CTD). PGD is the domain located in the center of the channel. It has an impact and control the ion selectivity, and therefore also the permeation of K^+ by opening and closing. The CTD takes up the role of a chemical sensor as it detects intracellular Ca^{2+} ions and also other ligands. Lastly, the VSD is the domain that senses changes in the membrane potential. In summary, the VSD is affected by depolarization and the CTD is affected by Ca^{2+}, accordingly the PGD gets activated.[20] The membrane spanning domains are the PGD and VSD. S1-S4 are components of VSD, while PGD consist of S5-S6. The S0 segment is important for modulation of the β-subunit.[24] RCK1 and RCK2 as can be seen on the illustration in Figure 1.8, play the role of regulators of K^+ conductance.

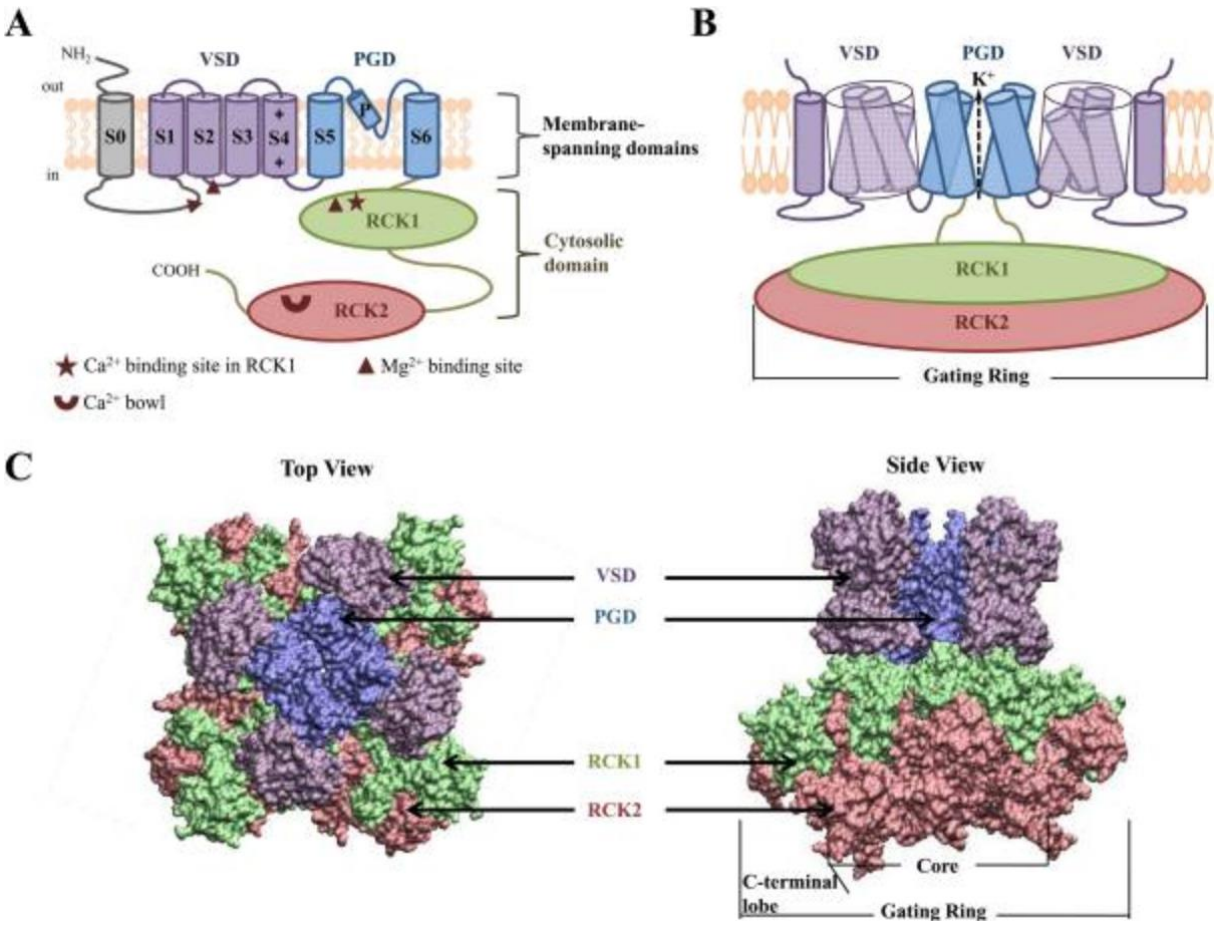

Figure 1.8 Illustration of the BK channel. This picture is taken from an article by S.Lee *et al.*[24]

Experiments with different PUFA derivatives by the usage of unnatural amino acid. The results from this study indicate that a direct ion-dipole interaction is made between Tyr318 in the BK channel with the carboxylate group of DHA. The unnatural amino acid they used was phenylalanine-based which has a pKa by 1.24 (at 25℃) and, is therefore a zwitterion at physiological pH. They also could conclude that only LTB_4 out of all LTs has the ability to enhance impact of the BK channel with only nanomolar concentrations needed. Unlike DHA, LTB4 require an optimal concentration of Ca^{2+} to give a significant effect. Figure 1.9 illustrates the results that was taken from this study, which is that BK with $\beta 1$ subunit and DHA supplies favors opening of the ion channel.[16]

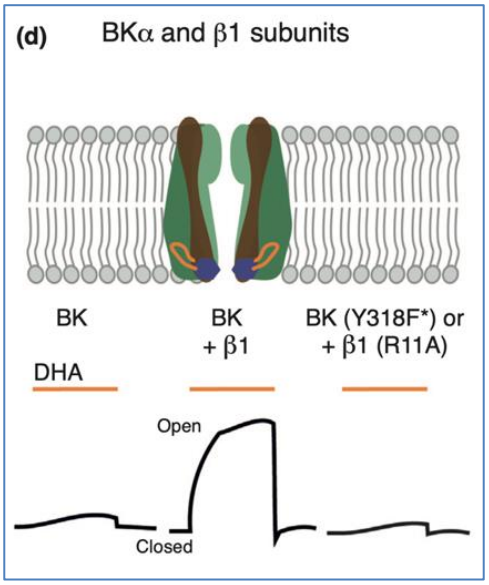

Figure 1.9 Illustration of the BK channel and $\beta 1$ subunit taken from an article by Cordero-Morales *et al.*[16] Note that Y318 = Tyr318.

Several studies on particularly docosahexaenoic acid (DHA) were conducted by Tian *et al.* in 2016[1]. The purpose of the study was to gain a better understanding how the BK channel is activated by DHA and determine the impact on an atomic level. The interaction between the BK channel and DHA was studied in two different methods. Firstly, the structure of DHA was manipulated. Also, the composition of the BK channels was manipulated. Several discoveries were made in both of the strategies.[1]

Electrophysiological monitoring on the BK channel show that the open conformation of the channel is favored by DHA. In fact, is not dependent on the activation of the Ca^{2+} sensors. It was found that the tyrosin residue Tyr318 in hSlo1 is the essential structural moiety, which is needed for DHA to be able to mediate effect. Even though the, the interactions are not yet

discovered, it is believed to be caused by an ion-dipole bond which is the observed interaction between DHA and residues on the VSD that are of positive character. This is too supported by studies done on DHA ethyl ester which suggested that the negatively charged carboxyl acid was need for the activation of the Slo1 BK channels and also in a hypotensive effect in mice. The study concluded that an ion-dipol interaction is essential between the free fatty acid of DHA and the OH group of Tyr318. Also, the hydrophobic chain of the PUFAs plays a role for the degree of affinity.[1]

1.8 Synthetic methods

1.8.1 DCC – coupling agent

In organic synthesis a very commonly used coupling agent throughout years has been DCC (dicyclohexyl carboiimide). Introduced by Sheehan and Hess in 1955,[25] DCC has since been used to form amide linkages in peptide synthesis. It is through the *O*-acylisourea active intermediate that the formation of an amide is created. Due to its very reactive nature and the difficulty of isolation, its able to react nucleophiles. This includes of course amines and thereby leads to the formation of an amide bond alongside the formation of dicyclohexyllurea. Stoichiometrically equimolar concentrations of the reagents are used in this method. The reaction takes place at 0℃ temperature and followed by leaving at ambient temperature overnight. However, if *N*-acylurea is wished to be avoided, then low temperature is ideal.[26] In fact, DCC has been used as a condensing agent to form an amide bond in the synthesis of penicillin.[27]

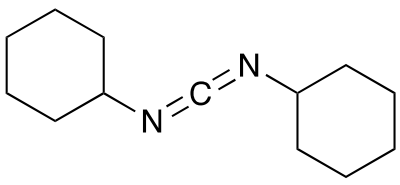

DCC
N,N'-Dicyclohexyl carboiimide

Figure 1.10 Structure of DCC.

1.8.2 Chiral resolution and Evan´s auxiliary

The differences in physical properties forms the basis for the separation of different compounds that are normally used. That is not a luxury the enantiomers have due to the same physical properties they have.[28, 29] Therefore, other approaches for separation must be assessed. The separation of enantiomers from a racemate is also called resolution.[28] Different methods that are available are for instance separation by chiral column chromatography, crystallization or by the help if chiral resolving agents.[28] A very popular approach for obtaining individual enantiomers is asymmetric synthesis. Stereoselective synthesis and asymmetric synthesis are two terms used interchangeably, and it comprises the chemical reactions that induced a formation of one or more chirality elements to a molecule. Stereoisomeric products are thereby produced, but in unequal amounts.[29] An important and often used tool in asymmetric synthesis the chiral oxazolidinones.[30] In order to eventually determine which is the most optimal enantiomer of EPA ethyl acid **10** in the stimulation of BK channels, synthesis using chiral oxazolidinones was of interest to this project.

Evans oxazolidinones was first reported by Evans and co-workers in 1981. Whereas the oxazolidinones was used in enantioselective aldol condensation, where the appropriate purification methods reported, were based on flash chromatography and molecular distillation. The article concluded that the oxazolidinone indeed gives satisfactory results in enantioselective aldol condensations as a chiral auxiliary. The easy removal and the recycling without inducing racemization, are some advantages reported of the usage of oxazolidinones as chiral auxiliaries.[31]

(4*S*,5*R*)-4-methyl-5-phenyloxazolidin-2-one was used in the separation of the enantiomers of the racemic EPA fatty acid **10** with the coupling agent DCC, and with aid from the catalyst 4-dimethylaminopyridine (DMAP). The procedure was based on a synthetic preparation performed by BASF AS in Norway.[14] In the first step, DCC is coupled with the EPA fatty acid **10**. The carboxylic acid group of the EPA fatty acid **10** is depronated by DCC. The *O*-acylisourea is then generated, which is an active acyl transfer reagent. Next, as seen in Scheme 1.1, a leaving group is kicked out by the nuclephilic nitrogen atom in DMAP, which is reacting in on the carbonyl carbon atom.[32]

The (4*S*,5*R*)-4-methyl-5-phenyloxazolidin-2-one carries a good nucleophile generated by deprotonation. A nucleophilic attack on the carbon carbonyl kicks out the DMAP and results in

the EPA fatty acid **10** coupled with the (4*S*,5*R*)-4-methyl-5-phenyloxazolidin-2-one. The molecule carries two stereocenters, and the product is a racemic mixture of the two diastereomers, which have different physical properties. Therefore, this gives the opportunity to separate by purification.

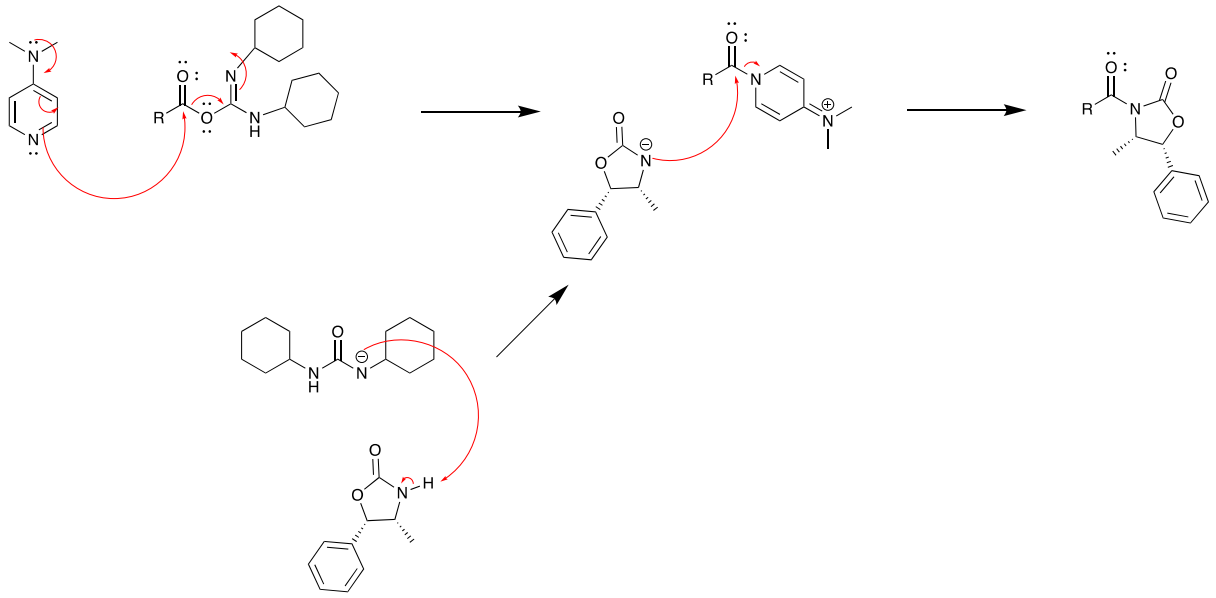

Scheme 1.1 The simplified mechanism of the last step of the synthesis of compounds (2*S*,4*S*,5*R*)-diastereomer-17 and (2*R*,4*S*,5*R*)-diastereomer-18. The R-group is representing EPA fatty acid **10**.

2 Results and Discussion

NMR analysis was done in advance to assure the purity of the EPA-ethyl ester. Three different EPA ether **7**, **8** and **16** were successfully synthesized. Furthermore, the hydrolysis of the EPA ether **8** to EPA acid **10** was successful. Then the attachment of the oxazolidine auxiliary, followed by the separation of the *S*- and *R*-enantiomer, was achieved. Also, an attempt of hydrolysis of the *R*-enantiomer was done, but unfortunately no product was obtained, which will be discussed further. An outline of the latter syntheses is displayed in Scheme 2.1. In addition, the *tert*-butyl ether **5** was prepared, but not in satisfactory purity, therefore the commercially available *tert*-butyl ethers, were used in the preparation of the different EPA ethers **7**, **8** and **16**. Lastly, an amidation of the EPA acid **10** was done, but unfortunately not in satisfactory purity.

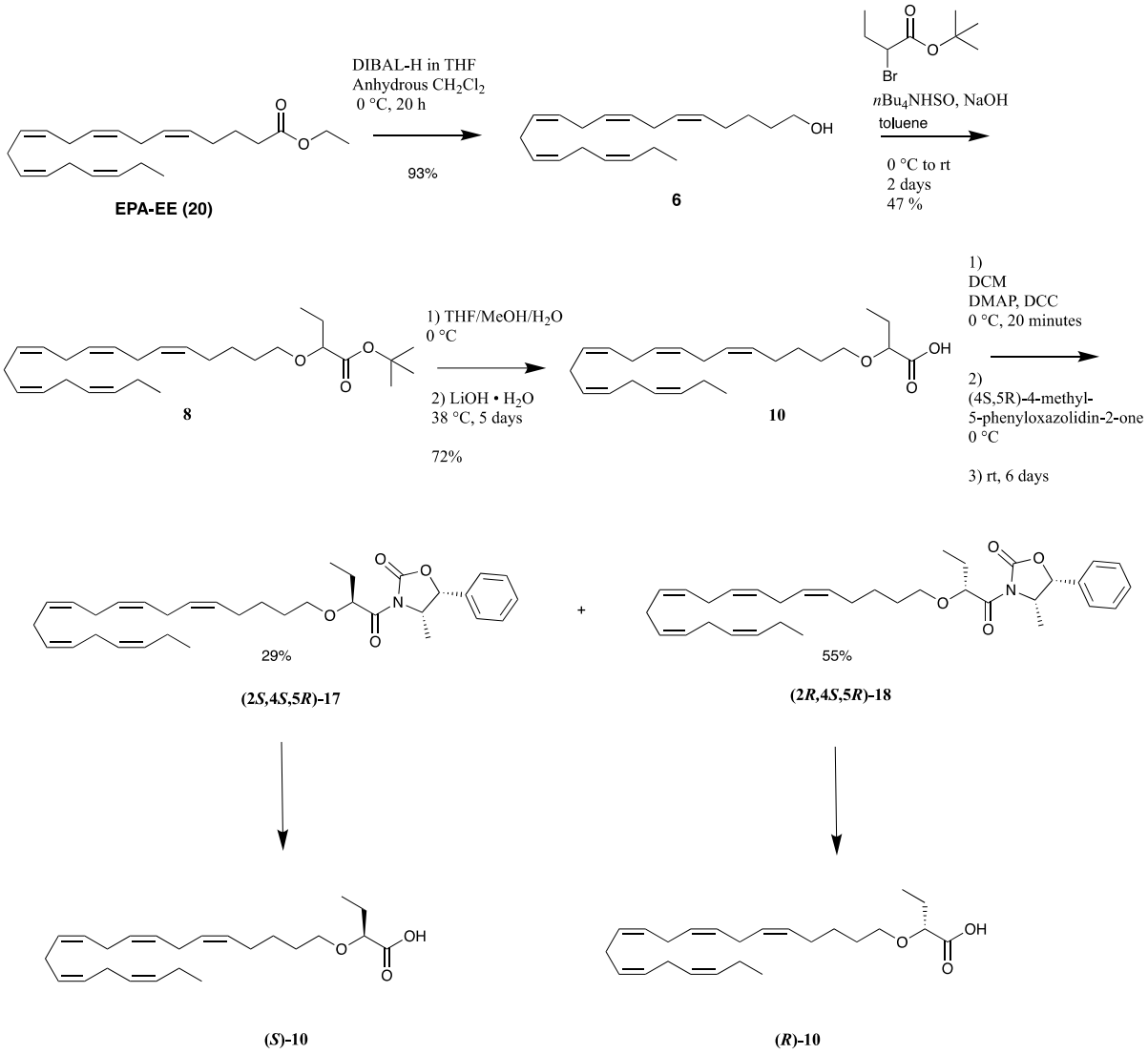

Scheme 2.1 An outline of the complete synthesis of (***S***)**-10** and **(*R*)-10**.

2.1 Synthesis of EPA alcohol 6

In the first step the EPA-ethyl ester (**20**) was reduced with DIBAL-H to give the EPA alcohol **6**. The method reported by Itoh.T *et al*. in 2011,[33] used the DIBAL-H reduction on the DHA ethyl ester.[33] DHA ethyl ester and EPA ethyl ester only differ in the length of hydrocarbon chain, therefore we expect the procedure to give similar results. In Scheme 2.2, the mechanism of the reduction of EPA ethyl ester using DIBAL-H is shown. DIBAL-H is often used in the reduction of esters down to aldehydes, due to its mild nature, also due to mechanistic reasons. Since it was desired to reduce the ethyl ester down to a primary alcohol, three equivalents of DIBAL-H were used. The first equivalent of DIBAL-H lead to a reduction of the ester to an aldehyde. The next equivalent lead to a reduction of the aldehyde to a primary alcohol, while the third and last equivalent ensured that all the aldehyde is reduced to the primary alcohol. The reaction was carried out in an anhydrous environment at 0°C. The reaction was stirred overnight, and then quenched at 0°C.

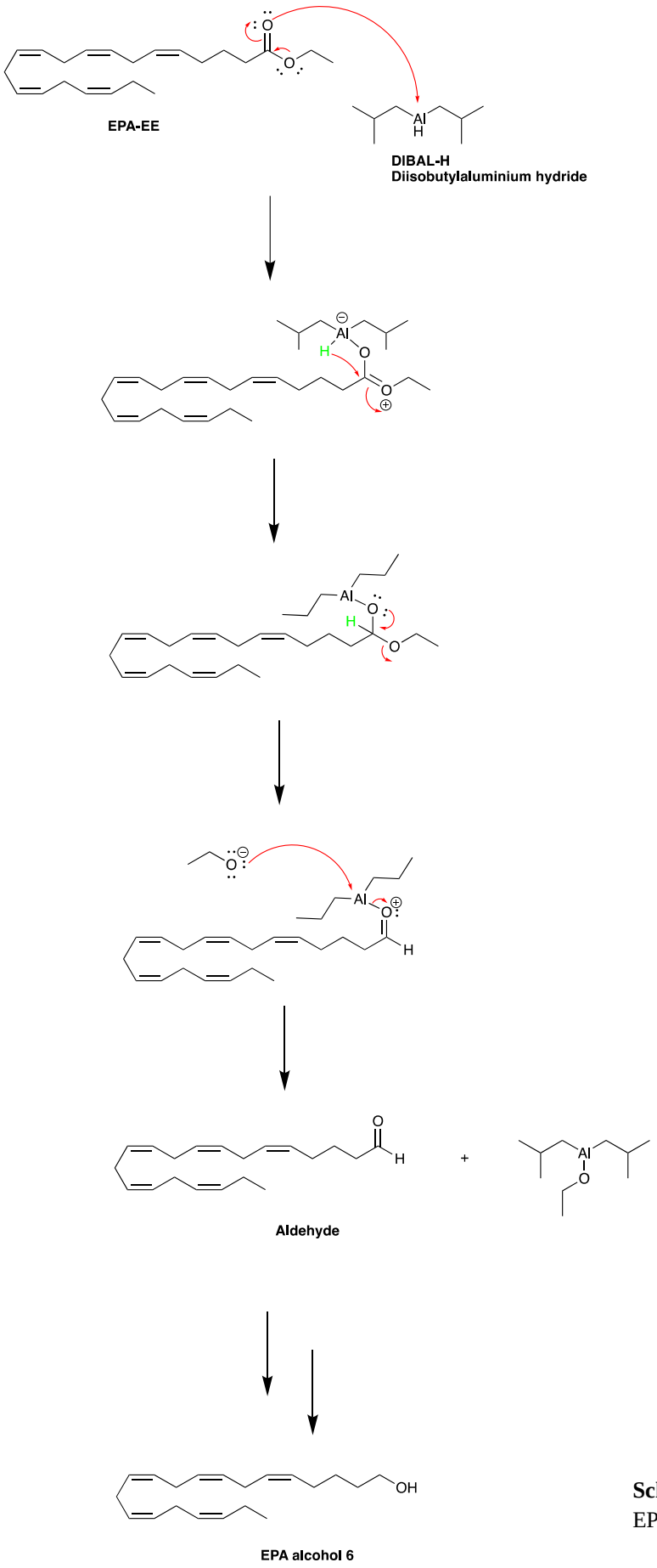

Scheme 2.2 An outline of the reaction between EPA-EE (**20**) and DIBAL-H.

The crude product was purified by flash column chromatography on silica gel to obtain the desired product, EPA alcohol **6** in 93% yield. The recorded ^{1}H- and ^{13}C-NMR, which are available in the appendix (Figure 6.1 and 6.2), confirmed that the EPA alcohol **6** was indeed synthesized. Also, the MS- and HRMS-spectra back up that the desired product was obtained. In the upcoming sections, both NMR- and MS-spectra are discussed in more detail.

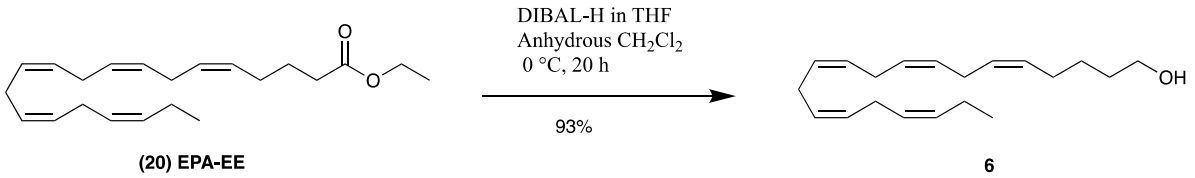

Scheme 2.3 The DIBAL-reduction of EPA-EE (**20**) to compound **6.**

2.2 Characterization of EPA alcohol 6

NMR interpretation

The number of protons in the ^{1}H NMR spectrum (Figure 6.1) is in accordance with the total number of protons in EPA alcohol **6**. The proton of the alcohol group usually causes a very broad singlet caused by hydrogen-deuterium exchange and therefore is not expected to be see in the spectrum. The triplet occurring at 3.65 ppm (2H), arise from the two protons that are attached to the α-carbon to the alcohol group. This signal is a triplet and integrates for two protons, which indicates two protons at the neighbor carbon and the chemical shift is within the expected rage. It is due to the electron-withdrawing inductive effect exerted from the oxygen atom which deshields the two protons and therefore the signal occurs downfield. This signal is a strong indication that the reduction of compound **20** to compound **6** has been successful. The triplet occurring at 0.98 ppm (3H) indicates a methyl group. The two multiplets occurring at 1.42 – 1.46 ppm (2H) and 1.56 – 1.62 ppm (2H) most likely belong to the protons in the C-3 and C-4 positions. The protons attached to the ß-carbon in position C-3 and closer to the electron-withdrawing oxygen atom, are most likely occurring more downfield at 1.56 – 1.62 ppm. The multiplet occurring at 2.14-2.03 ppm (4H) indicates the protons an allylic position, which are C-4 and C-16. The multiplet occurring at 2.77-2.90 ppm (8H) corresponds to the range of chemical shift for allylic protons and the signal integrates for the correct number of protons. The signal with chemical shift at 5.28-5.46 ppm (10H) corresponds well with the range for olefinic hydrogens in the hydrocarbon chain. The signal occurs downfield due to the anisotropic effect from the π-electrons in the alkenes.

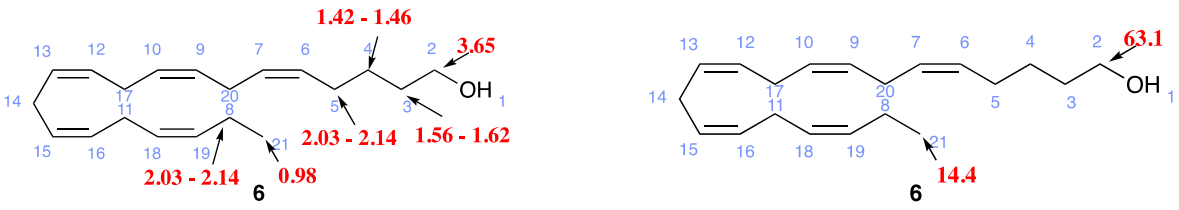

Figure 2.1 Assignment for ^{1}H NMR and ^{13}C NMR for EPA alcohol **6**.

The ^{13}C NMR spectrum (Figure 6.2) of EPA alcohol **6** shows is in agreement with the total number of carbon atoms in compound **6**, which is 20 carbon atoms. A good indication that the reduction down to alcohol has been successful is the peak occurring at 63.1 ppm, which is within the range of chemical shift for a sp^3 hybridized carbon attached to an oxygen atom. The peak at 14.4 ppm belongs to the carbon in the methyl terminus. The signals occurring at 20.7 ppm, 25.7 ppm, 25.8 ppm (3C), 25.9 ppm, 27.1 ppm and 32.5 ppm belong to the sp^3 hybridized carbon atoms in the allylic positions and the two methylene groups in the positions C-3 and C-4. The rest of the downfield peaks correspond with the range for sp^2 hybridized carbon atoms. Another good indication that the ethyl ester is reduced completely to an alcohol, is that there are no peaks in the range of chemical shifts for carbonyls.

The data were compared to the NMR spectra of the DHA alcohol.[33] The signals have similar chemical shift and also the splitting is similar, the only difference is as expected the number of protons. Therefore, it was logical and useful to use these data for comparison.

MS- and HRMS characterization

The calculated molecular mass of the sodium adduct of compound **6** and the base peak of 311.234 *m/z* shown in the recorded MS (electrospray) spectrum (Figure 6.18) for compound **6**, are in agreement. The recorded HRMS spectrum (Figure 6.19), for compound **6** shows a base peak of 311.2345 *m/z*, which also corresponds with the calculated molecular mass of sodium adduct of compound **6**. The error is 0.2 ppm, which is within the error criteria for HRMS of 10 ppm and therefore acceptable.

2.3 Synthesis of EPA ethers

Three different EPA ethers **7**, **8** and **16** were synthesized according to a procedure from a previous master thesis by Pangopoulos in 2016,[34] with small modifications. The only difference is that toluene/H_2O was used instead of DCM/H_2O. In procedure used by Pangopoulos in 2016,[34] the reaction was on performed on n-3 DPA to synthesize the 3-oxa n-3 DPA. The following procedure was used because it is well-established and have previously given good results on a similar compound. The use of different *tert*-butyl bromoacetate reactants with different branching, was exploited to obtain the desired *tert*-butyl ester with the desired branching.

The mechanism of the reaction is shown in Scheme 2.4. The alcohol group on the EPA chain may be reversibly deprotonated by hydroxide anion under phase-transfer conditions using tetrabutylammonium bisulfate (*n*-Bu_4NHSO) salt. *n*-Bu_4N+ functions as the cation of said hydroxide anion, effectively making the resulting base soluble in the organic phase.[35] The *tert*-butyl group provides steric hindrance, which results in a nucleophilic attack on the α-carbon atom.[34] The bromide provides as a good leaving group and it is an activated position. A transesterification would take place if the reactant lacked some form of steric hindrance, because then the nucleophilic attack would also be on the carbonyl carbon atom.[34]

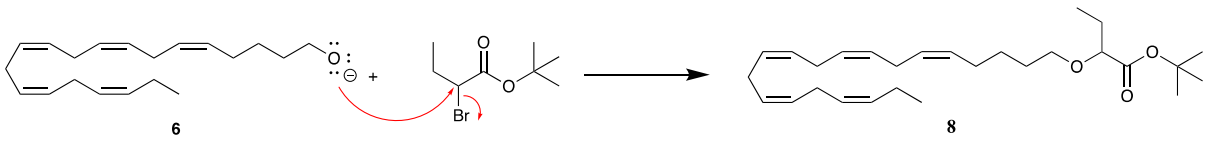

Scheme 2.4 The nucleophilic attack of the hydroxide group from the EPA alcohol **6** on the *tert*-butyl bromoacetate to synthesis EPA ethyl ether **8**. A similar mechanism happens for the synthesis of EPA ethyl ether **7** and **16**.

2.3.1 Synthesis of EPA ethyl ether 8

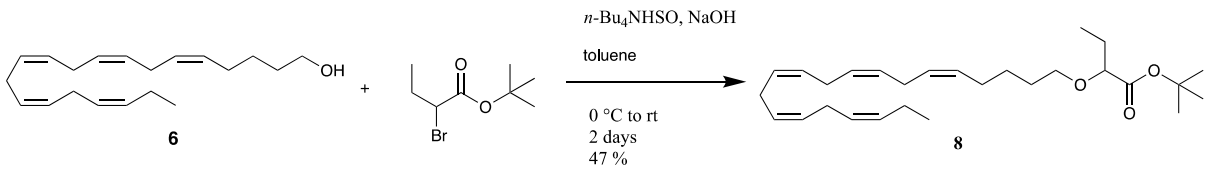

Scheme 2.4 Synthesis of EPA ethyl ether **8**

The procedure for the synthesis of EPA ethyl ether **8**, was based on the same procedure as mentioned, from previous master thesis by Pangopoulos in 2016.[34] However, one element was modified in this procedure, to try to obtain a better yield. An excess of the *tert*-butyl bromoacetate was used, instead of the 1.49 equivalents that used in the previously mentioned procedure. However, the recorded ^{1}H NMR spectrum accounted for many more protons, and that gave some difficulties during analysis and processing of the spectrum. A sample of the synthesized compound was spotted on a TLC plate alongside a sample of the *tert*-butyl bromoacetate, and a co-spot of *tert*-butyl bromoacetate and synthesized compound **8**. The eluent used was 5% EtOAc:Hexane. The TLC plate was visualized under UV light and also with $KMnO_4$ stain. Under the UV light, the spots on TLC plate indicated that there was still unreacted the *tert*-butyl bromoacetate in synthesized product. However, the same observation was not detected with $KMnO_4$ stain. Therefore, *tert*-butyl bromoacetate was most likely interfering with the signals for EPA ethyl ether **8** in the recorded NMR spectra. Despite knowing that the compound was indeed synthesized, the product was purified once more by flash column chromatography on silica gel. Therefore, it can be concluded that there is no point of adding more equivalent of *tert*-butyl bromoacetate to try to better the yield, and that procedure was already optimal.

The crude product was purified by flash column chromatography on silica gel to obtain the desired product EPA ether **8** in 47 % yield. The recorded ^{1}H- and ^{13}C -NMR, which are available in the appendix (Figure 6.3 and 6.4), confirmed that the EPA ethyl ether **8** was indeed synthesized. Also, the MS- and HRMS-spectra back up that the desired product was obtained. In the upcoming sections, both NMR- and MS-spectra are discussed in more detail.

2.3.2 Characterization of EPA ethyl ether 8

NMR interpretation

The number of protons in the ^{1}H NMR spectrum (Figure 6.3) is in accordance with the total number of hydrogen atoms in **8**, which are 46. A strong indication that the *tert*-butyl group has been attached to the EPA alcohol **6** hydrocarbon chain is the singlet at 1.47 ppm, which integrates for 9 protons. These 9 protons belong on the *tert*-butyl group. Also, the neighbor carbon does not have any protons which results in a singlet. Another good indication is the signal occurring at 0.97 ppm (6H), which is a triplet of doublet. This is caused by the methyl

group on the C-terminus and also the three protons on C-25. The signal is most likely an overlap of two triplets. The single hydrogen on the C-22 next to the ether group gives a signal at 3.32 ppm (1H). This signal occurs more downfield due to the electron-withdrawing inductive effect from the oxygen in the ether group. The α-protons on the C-2 causes the multiplet at 3.52 – 3.66 ppm (2H), because they are deshielded due to the inductive effect from the oxygen atom in the ether group. The multiplet at 2.02 – 2.14 ppm (4H) accounts for the four protons on the allylic positions in C-5 and C-8. The protons on the methylene group in position C-3 and C-4 give the signals 1.67 – 1.75 ppm (2H) and 1.59 – 1.64 (2H). The protons on the C-3 most likely cause the more downfield signal at 1.67 – 1.75 ppm (2H) due the electron withdrawing effect from the oxygen atom in the ether group. The mulitplet at 2.74 – 2.92 ppm (8H) indicates the eight protons in the allylic positions C-20, C-17, C-14 and C-11 in the hydrocarbon chain. Lastly, the multiplet at 5.20 – 5.59 ppm (10H) belongs to the ten olefinic protons in the positions C-6, C-7, C-9, C-10, C-12, C-13, C-15, C-16, C-18 and C-19.

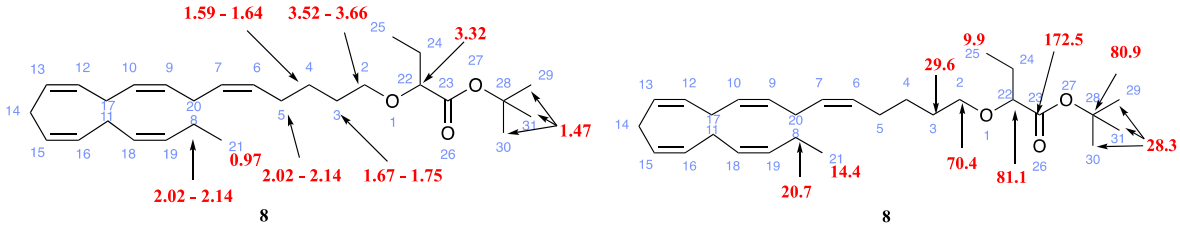

Figure 2.2 Assignment for ^{1}H NMR and ^{13}C NMR for EPA ethyl ether **8**

The ^{13}C NMR spectrum (Figure 6.4) of EPA ethyl ether **8** is in agreement with the total number of carbon atoms in compound **8**, which is 28 carbon atoms. The signal that occurs at 172.5 ppm indicates the highly deshielded carbon atom in the carbonyl and confirmed the existence of the carbonyl group in the compound. The signal occurring at 28.3 ppm belongs to the three chemical equivalent carbon atoms at the *tert*-butyl group and is also a good indication that the synthesis was successful. There are three signals occurring in the range of chemical shifts for carbon atoms attached to an electron-withdrawing group, which is in this case is the oxygen in the ether group and in the ester group. The signal occurring at 81.1 ppm indicates the carbon atom, C-22 between the carbonyl group and the ether group. The signal at 80.9 ppm is most likely caused by the carbon atom C-28 in the *tert*-butyl group. The carbon atom C-2 between the ether group and the hydrocarbon chain is causing a signal at 70.4 ppm. The 10 olefinic carbon atoms are causing 10 signals in the range for sp^2 hybridized carbon atoms. The signals

are occurring at 132.2 ppm, 130.2 ppm, 128.7 ppm, 128.6 ppm, 128.4 ppm, 128.3 ppm, 128.1 (2C), 128.0 ppm and 127.2 ppm. They occur downfield due to the deshielding effect coming from the π – electrons in the alkenes which causes the anisotropic effect. The rest of the 8 carbon atoms are sp^3 hybridized and causes the signals that are the most upfield due to the shielded effect. The methyl groups C-25 and C-21, gives the signals at 9.9 ppm and 14.4 ppm respectively. The signal occurring at 29.6 ppm is caused by the β-carbon at C-3. The reason for this is that this carbon atom still has a small impact from the electron-withdrawing oxygen and therefore the signal occurs more downfield than for the other sp^3 hybridized. The rest of the signals occurring at 27.2 ppm, 26.4 ppm, 26.3 ppm, 25.8 ppm (3 carbons) and 25.7 ppm belong to the sp^3 hybridized C-4, C-5, C-11, C-14, C-17, C-20 and C-24. However, it is difficult to differ which one of these three signals are caused by which of the seven mentioned carbon atoms.

The recorded ^{1}H NMR spectrum is in agreement with previously recorded ^{1}H NMR spectrum.[14] There is no recorded ^{13}C NMR available for this compound. The ^{13}C NMR data are in accordance with the structure.

MS- and HRMS characterization

The calculated molecular mass of the sodium adduct of compound **8** and the base peak of 453.334 *m/z* shown in the recorded MS (electrospray) spectrum (Figure 6.20) for compound **8**, are in agreement. The recorded HRMS spectrum (Figure 6.21), for compound **8** shows a base peak of 453.3338 *m/z*, which also corresponds with the calculated molecular mass of sodium adduct of compound **8**. The error is 0.2 ppm, which is within the error criteria for HRMS of 10 ppm and therefore acceptable.

2.3.3 Synthesis of EPA methyl ether 7

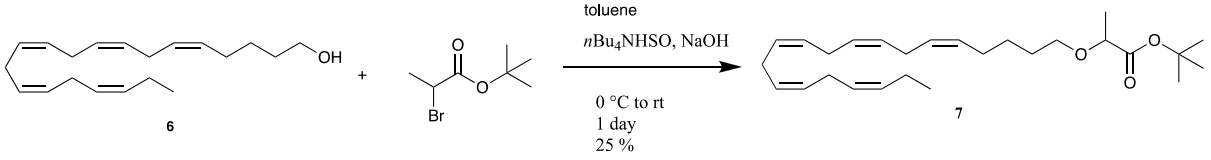

Scheme 2.5 Synthesis of EPA ethyl ether **7**

The same procedure, described previously, was used for the synthesis of EPA ethyl ether **7**, as seen in Scheme 2.5. The crude product was purified by flash column chromatography on silica gel to obtain the desired product EPA ether **7** in 25 % yield. The recorded ^{1}H- and ^{13}C -NMR, which are available in the appendix (Figure 6.5 and 6.6), confirmed that the EPA ether **7** was indeed synthesized. Also, the MS- and HRMS-spectra back up that the desired product was obtained. In the upcoming sections, both NMR- and MS-spectra are discussed in more detail.

2.3.4 Characterization of EPA methyl ether 7

NMR interpretation

The number of protons in the ^{1}H NMR spectrum (Figure 6.5) is in accordance with the total number of protons in EPA ethyl ether **8**, which is a total of 44 protons. The most eye-catching signals is the singlet at 1.47 ppm (9H) which indicates a *tert*-butyl group. The doublet occurring at 1.35 ppm (3H) indicates that a methyl group has been added. The quartet occurring at 3.80 ppm (1H) is caused by the proton on the carbon C-22 between the ether and carbonyl group. The three neighboring protons causes the seen splitting pattern. The two protons on the carbon C-2 next to the ether group are not equivalent, thus gives two different signals at 3.35 ppm (1H) and 3.55 ppm (1H). The reason for this is that they actually are diastereotopic, which is caused by the stereogenic center at C-22. These signals also share the same coupling constant at 6.5 Hz and also at 8.9 – 9.0 Hz, which indicates that they indeed are coupled. The splitting pattern of each of these signals are doublet of triplet, which is caused by the single proton on the C-22 which splits the signal into a doublet. The doublets of triplets caused by the two neighboring protons on C-3. The multiplet at 5.27 – 5.44 ppm (10H) is caused by the olefinic protons in the hydrocarbon chain, and the multiplet occurring at 2.77 – 2.89 ppm (8H) is caused by the allylic protons in the hydrocarbon chain. The rest of the signals are allocated to the correct protons in Figure 2.3.

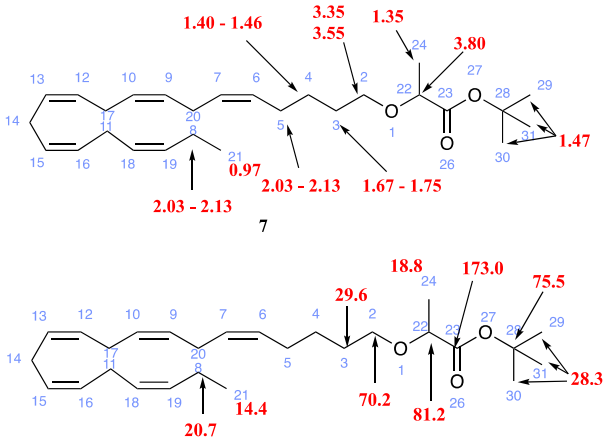

Figure 2.3 Assignment for ^{1}H NMR and ^{13}C NMR for EPA ethyl ether **7**

The ^{13}C NMR spectrum (Figure 6.6) of EPA methyl ether **7** is in agreement with the total number of carbon atoms in compound **7**, which is 27 carbon atoms. The signal that occurs at 173.0 ppm confirms the existence of the carbonyl group. The signal occurring at 28.2 ppm indicates the three equivalent carbon atoms at the *tert*-butyl group. Due to the electron withdrawing effect from the oxygen, the signal to C-28 occurs at 75.6 ppm. For the same reason, the signal to the carbon C-2 occurs at 70.2 ppm. The signal at 81.2 ppm is caused by the carbon C-22. The signals that occur at 132.2 ppm, 130.2 ppm, 128.7 ppm, 128.6 ppm, 128.4 ppm, 128.3 ppm, 128.1 ppm (3C) and 127.2 ppm accounts for the 10 olefinic carbon atoms. The signals occurring at 27.2 ppm, 26.3 ppm, 25.8 ppm (3C), 25.7 ppm and 20.7 ppm, belongs to the sp^3 hybridized C-4, C-5, C-11, C-14, C-17, C-20 and C-24. However, it cannot be determined with great certainty which signal belongs to the exact carbon atoms. The rest of the signals are allocated to the correct carbon atoms in Figure 2.3.

There is no reference data available for this compound. The data are in accordance with structures and previous synthetic routes made in the LIPCHEM group.

MS- and HRMS characterization

The calculated molecular mass of the sodium adduct of compound **7** and the base peak of 439.318 *m/z* shown in the recorded MS (electrospray) spectrum (Figure 6.22) for compound **7**, are in agreement. The recorded HRMS spectrum (Figure 6.23), for compound **7** shows a base peak of 439.3182 *m/z*, which also corresponds with the calculated molecular mass of sodium adduct of compound **6**. The error is 0 ppm.

2.3.5 Synthesis of EPA-oxy-acetate 16

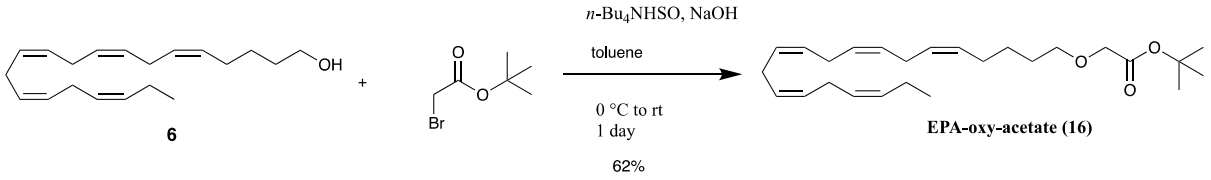

Scheme 2.6 Synthesis of EPA-oxy-acetate **16**

The EPA-oxy-acetate **16** was synthesized using the latter procedure based on method presented by previous master thesis by Pangopoulos in 2016.[34] The crude product was purified by flash column chromatography on silica gel to obtain the desired product EPA ethyl ether **16** in 62% yield. The recorded ^{1}H- and ^{13}C -NMR, which are available in the appendix (Figure 6.7 and 6.8), confirmed that the EPA-oxy-acetate **16** was indeed synthesized. Also, the MS- and HRMS-spectra back up that the desired product was obtained. In the upcoming sections, both NMR- and MS-spectra are discussed in more detail

2.3.6 Characterization of EPA-oxy-acetate 16

The number of protons in the ^{1}H NMR spectrum (Figure 6.7) is in accordance with the total of protons in EPA ethyl ether **16**, which is a total of 42 protons. As expected, a signal occurring at 1.48 ppm (9H) which indicates the nine protons on the *tert*-butyl group. The splitting pattern is a singlet, which confirms that there are none neighboring protons. Another good indication that the synthesis was successful is the signal occurring at 3.94 ppm (2H), which belongs to the two protons one the C-22. The reasons this signal occurs downfield is the electron-withdrawing oxygen atom in the ether group and the carbonyl group. The multiplet occurring at 5.27 – 5.44 ppm (10H) is caused by the olefinic protons in the hydrocarbon chain. The multiplet that occurs at 2.76 – 2.89 ppm (8H) is caused by the allylic protons in the hydrocarbon chain. The rest of the signals are allocated to the correct protons in Figure 2.4.

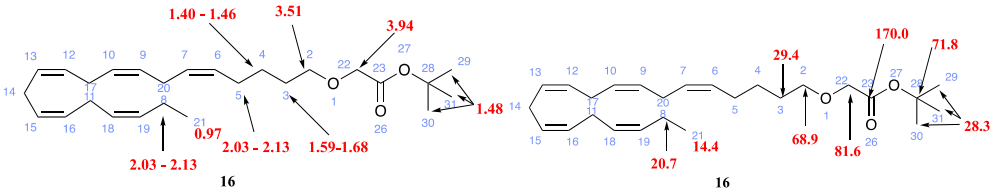

Figure 2.4 Assignment for ^{1}H NMR and ^{13}C NMR for EPA-oxy-acetate **16.**

The ^{13}C NMR spectrum (Figure 6.8) of EPA ethyl ether **16** is in agreement with the total number of carbon atoms in the compound **16**. The signal that occurs at 170.0 ppm confirms the existence of the carbonyl group. The signal occurring at 28.3 ppm confirms the existence of the three chemical equivalent carbon atoms on the *tert*-butyl group. Signal to the carbon in the *tert*-butyl group, which is attached to the oxygen, occurs downfield at 69.9 ppm due to the electron-withdrawing effect from the oxygen. For the same reason, the carbon C-2 causes a signal at 68.9 ppm. The signal occurring at 81.6 ppm is caused by C-22. The 10 olefinic carbon atoms in the hydrocarbon chain causes the signals at 127.2 ppm, 128.1 ppm, 128.1 (2C) ppm, 128.3 ppm, 128.36 ppm, 128.6 ppm, 128.7 ppm, 130.1 ppm and 132.2 ppm. While the rest of the carbons are sp^3 hybridized and their signals occur at 14.4 ppm, 20.7 ppm, 25.7 ppm, 25.8 ppm (3C), 26.2 ppm and 27.1 ppm. However, it cannot be determined with great certainty which signal belongs to the exact carbon atoms. The rest of the signals are allocated to the different carbons in Figure 2.4.

There is no reference data available for this compound. The data are in accordance with structure.

MS- and HRMS characterization

The calculated molecular mass of the sodium adduct of compound **16** and the base peak of 425.303 *m/z* shown in the recorded MS (electrospray) spectrum (Figure 6.24) for compound **16**, are in agreement. The recorded HRMS spectrum (Figure 6.25), for compound **16** shows a base peak of 425.3025 *m/z*, which also corresponds with the calculated molecular mass of sodium adduct of compound **16**. The error is 0.2 ppm, which is within the error criteria for HRMS of 10 ppm and therefore acceptable.

2.4 Hydrolysis of EPA ethyl ether 8 to EPA acid 10

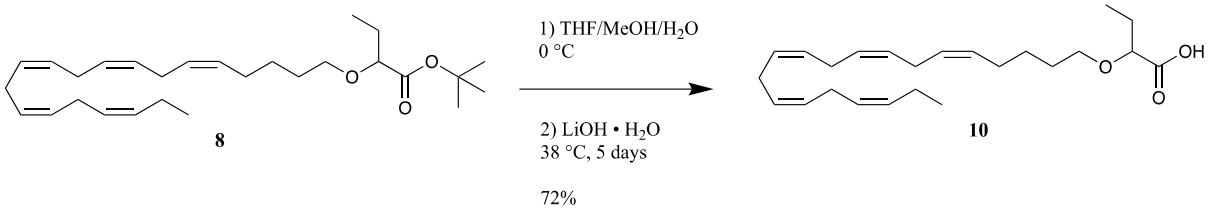

8 **10**

Scheme 2.7 The synthesis of EPA acid **10.**

The procedure for the hydrolysis of EPA ethyl ether **8** to EPA acid **10** was based on the well-established procedure from the article by M. G. Jakobsen in 2012.[36] The crude product was purified by flash column chromatography on silica gel to obtain the desired product EPA acid **10** in 52% yield. The recorded ^{1}H- and ^{13}C -NMR, which are available in the appendix (Figure 6.9 and 6.10), confirmed that the EPA acid **10** was indeed synthesized. Also, the MS- and HRMS-spectra backs up that the desired product was obtained. In the upcoming sections, both NMR- and MS-spectra are discussed in more detail.

2.5 Characterization of EPA acid 10

NMR interpretation

The number of protons in the ^{1}H NMR spectrum (Figure 6.9) is in accordance with the total number of 37 protons in EPA acid **10**, which matches the total of protons in compound **10** that will cause visible signals in a ^{1}H NMR spectrum. The signal for the proton in the carboxylic acid is most likely too broad to be seen in the spectrum caused by hydrogen-deuterium exchange. The first indication that the hydrolysis was successful is that the signal for the *tert*-butyl group occurring at 1.47 ppm (9H) is not there anymore, meaning it has been cleaved off. As discussed earlier, the signal belonging to the single proton on the α-carbon in C-22, occurs downfield at 3.84 – 3,91 ppm (1H) due to the electron-withdrawing effect from the carboxylic group through its resonance structure. The multiplets occurring at 1.43 – 1.50 ppm, 1.62 – 1.65 ppm and 1.77 – 1.90 ppm each account for two protons. These signals most likely are caused by the methylene groups in the positions C-3, C-4 and C-24. The signal occurring at 2.03 – 2.14 ppm is caused by the four protons at the allylic positions C-5 and C-8. The multiplet occurring at 2.75 – 2.91 ppm (8H) accounts for the eight protons in the positions C-11, C-14, C-17 and C-20. As expected, the ten protons in the olefinic positions in the hydrocarbon chain results in

a multiplet occurring downfield at 5.29 – 5.46 ppm (10H). The rest of the signals are allocated to the belonging protons in the molecule as seen in Figure 2.5.

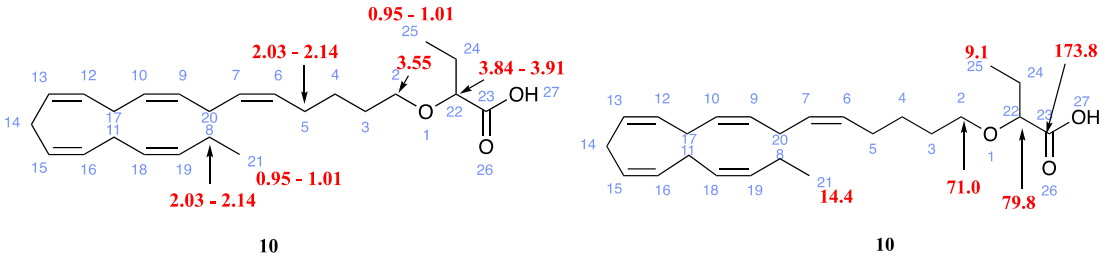

Figure 2.5 Assignment for ^{1}H NMR and ^{13}C NMR for EPA acid **10.**

The signals of the ^{13}C NMR spectrum (Figure 6.10) of EPA ether **10** in total accounts for 24 carbon atoms, which matches the total number of carbon atoms in the compound **10**. The carbon atom in the carbonyl group is still present, which confirmed by the signal that occurs at 173.8 ppm. The downfield signals occurring at 127.2 ppm, 128.0 ppm, 128.3 ppm (2C), 128.4 ppm, 128.5 ppm (2C), 128.7 ppm, 129.7 ppm and 132.2 ppm are caused by the ten carbon olefinic carbons atoms in the hydrocarbon chain. The upfield signals occurring at 20.7 ppm, 25.3 ppm, 25.8 ppm (3C), 26.2, ppm, 27.0 ppm and 29.4 ppm are caused by the ten carbon allylic carbons atoms in the hydrocarbon chain and also C-22. The signals from the C-4 and C-24 most likely occur more downfield at 29.4 ppm and 27.0 ppm. However, it cannot be determined with great certainty which signal belongs to the exact carbon atoms. The rest of the signals are allocated to the belonging protons in the molecule which is seen in Figure 2.5.

The recorded ^{1}H NMR spectrum is in agreement with previously recorded ^{1}H NMR spectrum.[14] There is no recorded ^{13}C NMR available for this compound. The ^{13}C NMR data are in accordance with the structure.

MS- and HRMS characterization

The calculated molecular mass of the sodium adduct of compound **10** and the base peak of 397.271 *m/z* shown in the recorded MS (electrospray) spectrum (Figure 6.26) for compound **10**, are in agreement. The recorded HRMS spectrum (Figure 6.27), for compound **10** shows a base peak of 397.2713 *m/z*, which also corresponds with the calculated molecular mass of sodium adduct of compound **10**. The error is 0.1 ppm, which is within the error criteria for HRMS of 10 ppm and therefore acceptable.

2.6 Synthesis of (2*S*,4*S*,5*R*)-diastereomer-17 and (2*R*,4*S*,5*R*)-diastereomer-18

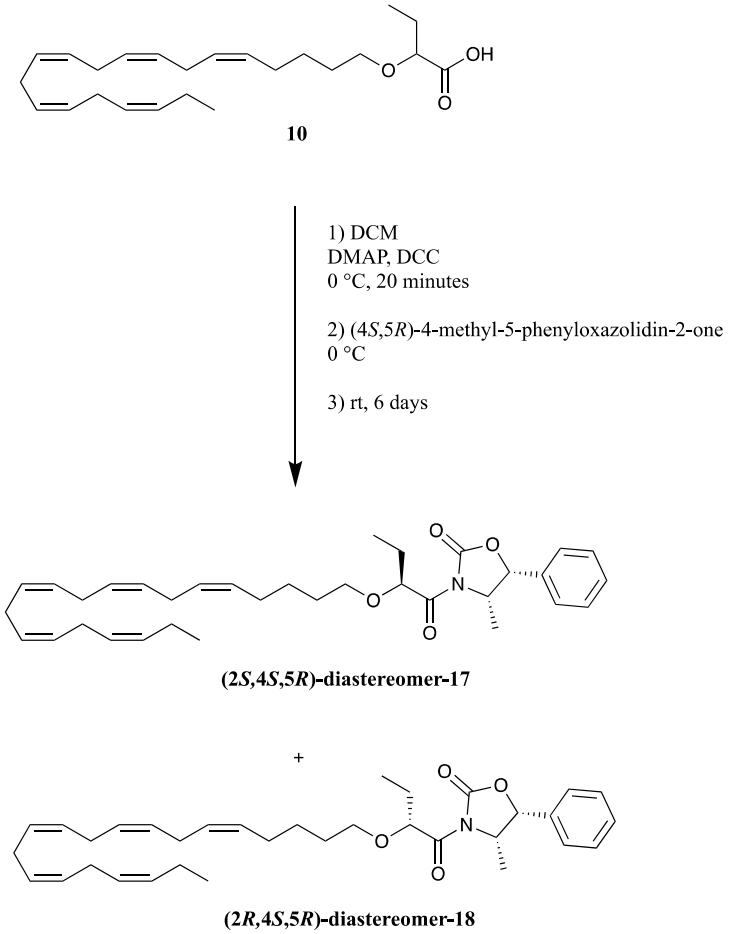

Scheme 2.8 Synthesis of EPA (**2*S*,4*S*,5*R*)-diastereomer-17** and **(2*R*,4*S*,5*R*)-diastereomer-18**

The **(2*S*,4*S*,5*R*)-diastereomer-17** and **(2*R*,4*S*,5*R*)-diastereomer-18** were synthesized and separated following the procedure described in a patent by BASF AS in 2019.[14] The reaction was facilitated by the use of the coupling agent DCC. A chiral auxiliary, (4*S*,5*R*)-4-methyl-5-phenyloxazolidin-2-one, was introduced to compound **10.** A more detailed description of the mechanism is presented in Chapter 1.2. The reaction was carried out in anhydrous environment under argon, and at 0° C. The reaction was stirred for 6 days instead of 5 days, simply because that was appropriate in terms of time. Shortly a turbid mixture was observed as described in the patent by BASF AS.[14] In the reported procedure,[14] the DMAP was used in superstochiometric amounts even though stochiometric amounts should be enough. However, it was decided to follow the reported procedure. The reaction mixture was then filtrated and concentrated by the use of reduced pressure to ensure that the precipitate was omitted. As seen in Scheme 2.8, the product consisted of two diastereomers. Meaning, they have different R_f-values, which was

exploited in the further separation. Despite that the R_f-values were not previously reported, the same eluent system was used to record some Rf-values and get a feeling of when to expect the diastereomers to elute. Since, the eluent system gave an acceptable separation it was decided to use the same system in the purification and separation of the diastereomers by flash chromatography on silica gel. The eluent which was used, was 15:85 EtOAc:Heptane. Several purifications were needed to be able to achieve high degree of diastereomeric purity. A more detailed description of the purification and process of it is discussed in Chapter 2.8.

The desired products **(2*S*,4*S*,5*R*)-diastereomer-17** and **(2*R*,4*S*,5*R*)-diastereomer-18** were obtained in 28 % yield and 55 % yield, respectively. The recorded ^{1}H- and ^{13}C-NMR, which are available in the appendix (Figure 6.11 and 6.12 for **(2*S*,4*S*,5*R*)-diastereomer-17** and Figure 6.13 and 6.14 for **(2*R*,4*S*,5*R*)-diastereomer-18**) confirmed that both products were synthesized and separated. Also, the MS- and HRMS-spectra back up that the desired products were obtained. The HPLC chromatograph also supports the results and are discussed furthermore in Chapter 2.7. In the upcoming sections, NMR- and MS-spectra and HPLC-chromatogram are discussed in more detail.

2.6.1 Characterization of (2*S*,4*S*,5*R*)-diastereomer-17

NMR interpretation

The number of protons in the ^{1}H NMR spectrum (Figure 6.11) is in accordance with the total number of 47 protons in the compound **(2*S*,4*S*,5*R*)-diastereomer-17**. Firstly, the two multiplets 7.35 – 7.46 ppm (3H) and 7.27 – 7.32 ppm (2H) confirms the existence of a phenyl group in the compound. They appear even more downfield than the olefinic protons in the hydrocarbon chain. The reason for this is simply anisotropic effect due to the π-electrons in the aromatic ring, which gives a strong deshielding effect. All five protons are not chemically equivalent, and therefore will result in different signals. There are two protons in *ortho* position to the electron donating methine group. Therefore, they are a little more shielded than the protons in the *meta* and *para* position. The two protons in the *ortho* position will give a signal that is a little more upfield, which is the multiplet at 7.27 – 7.32 ppm (2H). The signal at 7.35 – 7.46 ppm (3H) belongs to the three protons in the *meta* and *para* position. Even though, the two protons in the *meta* position are not chemically equivalent with the proton in the *para* position, the signal is most likely a result of two overlapping signal.

The doublet at 5.73 ppm (1H) has a very significant role. In the recorded ^{1}H NMR, only one doublet is visible indicating that the product is diastereomerically pure. The diastereomeric purity (de) will be assessed further in the HPLC analysis in Chapter 2.7. The signal comes from the proton on C-29. The reason for its appearance at a more downfield chemical shift, is the deshielding effect from both the carbonyl and also the phenyl group with its π-electrons. The coupling constant J is 7.5 Hz, which indicates that it is coupled with the three protons on the ethyl group in position C-25. As it will be discussed in Chapter 2.8, numerous purifications of the product were needed to achieve the recorded ^{1}H NMR.

The diastereotropic protons next to the ether group in C-2, causes two signals in the splitting pattern doublet of triplet with the coupling constant 8.9 Hz, which indicates that they are coupling. However, the signal 4.81 – 4.92 ppm (2H) seems to be an overlap of two signals. It is very likely an overlap between the signals for the single proton on C-22 and C-28. In the NMR characterization of **(2*R*,4*S*,5*R*)-diastereomer-18**, two separated peaks are visible in the latter area. The signal for the olefinic protons in the hydrocarbon chain is still in the same range, which is 5.29 – 5.46 ppm (10H). The signal for the allylic protons in the hydrocarbon chain is also still in the same range and the signal occurs at 2.75 – 2.91 ppm (8H). The signals 1.81 – 1.93 (m, 1H), 1.61 – 1.74 (m, 3H), 1.42 – 1.52 (m, 2H), belongs to the protons on C-3, C-4 and C-24. The rest of the peaks are assigned to the belonging protons in the compound, as seen in Figure 2.7.

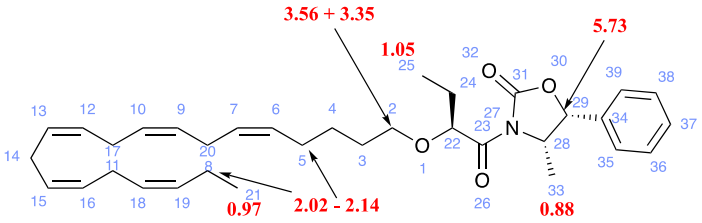

Figure 2.6 Assignment for ^{1}H NMR for *compound* ***(2S,4S,5R)*-diastereomer-17.**

The signals in the recorded ^{13}C NMR (Figure 6.12), which account for the 34 carbon atoms in the compound. The existence of the two carbonyl groups is confirmed by the peaks at 173.2 ppm and 152.8 ppm. The C-23 gives a more downfield signal at 173.2 ppm compared to the C-31, which causes the signal at 152.8 ppm. The reason for this is that C-31 is more shielded due to the neighboring oxygen atom and nitrogen atom.

The signal for C-28 next to the electronegative nitrogen is as expected at 54.7 ppm. The reason this carbon atom causes a signal a little more upfield than the carbon atoms connected to oxygen

atoms, is simply due to the electronegativity differences. A nitrogen atom is less electronegative than an oxygen atom and therefore the inductive effect is a little weaker, thereby the carbon atom is less deshielded.

The signal at 79.4 ppm is likely to be caused by the C-29. When comparing the ^{13}C NMR for **(2*S*,4*S*,5*R*)-diastereomer-17** with the ^{13}C NMR for **(2*R*,4*S*,5*R*)-diastereomer-18** (Figure 6.14), it is the latter signal which is clearly a bit different. The allylic carbon atoms and the sp^3 hybridized carbon atoms are as expected giving the signals at 20.7 ppm, 25.7 ppm, 25.8 ppm (3C), 26.3 ppm, 26.4 ppm and 27.1 ppm. The signals at 10.1 ppm, 14.4 ppm and 14.7 ppm are caused by the sp^3 hybridized methyl groups C-21, C-25 and C-33. The ten olefinic carbon atoms in the hydrocarbon chain and the six sp^2 hybridized carbons atoms in the aromatic ring give as expected the signals at 125.8 ppm (2C), 127.2 ppm, 128.1 ppm (3C), 128.4 ppm, 128.6 ppm, 128.7 ppm, 128.9 ppm (2C), 129.0 ppm, 130.2 ppm, 132.2 ppm and 133.4 ppm. The rest of the signals are assigned to the belonging carbon atoms in the compound, as seen in Figure 2.8.

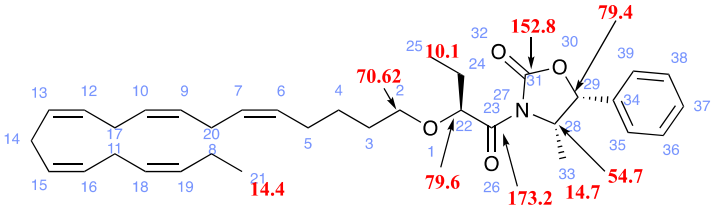

Figure 2.7 Assignment for ^{13}C NMR for *compound* ***(2S,4S,5R)*-diastereomer-17.**

The recorded ^{1}H NMR spectrum is in agreement with previously recorded ^{1}H NMR spectrum.[14] There is no recorded ^{13}C NMR available for this compound. The ^{13}C NMR data are in accordance with the structure.

2.6.2 Characterization of (2*R*,4*S*,5*R*)-diastereomer-18

NMR interpretation

The number of protons in the ^{1}H NMR spectrum (Figure 6.13) is in accordance with the total number of 47 protons in the compound **(2*R*,4*S*,5*R*)-diastereomer-18**. The doublet occurring at 5.69 ppm (1H) has a very significance role. When comparing the ^{1}H NMR spectra for the two diastereomers **(2*S*,4*S*,5*R*)-diastereomer-17** and **(2*R*,4*S*,5*R*)-diastereomer-18**, the proton on C-29 give two doublets with two different chemical shifts. In some of the ^{1}H NMR spectra of

the fractions after purification of the product, both doublets were occurring, meaning that the product was not diastereometrically pure enough.

The signal for the olefinic protons in the hydrocarbon chain is still in the same range, which is 5.23 – 5.468 ppm (10H). The signal for the allylic protons in the hydrocarbon chain is also still in the same range and the signal occurs at 2.74 – 2.89 ppm (8H). The signals 1.78 – 1.89 (m, 1H), 1.60 – 1.75 (m, 3H), 1.40 – 1.51 (m, 2H), belongs to the protons on C-3, C-4 and C-24. The rest of the peaks are assigned to the belonging protons in the compound, as seen in Figure 2.9.

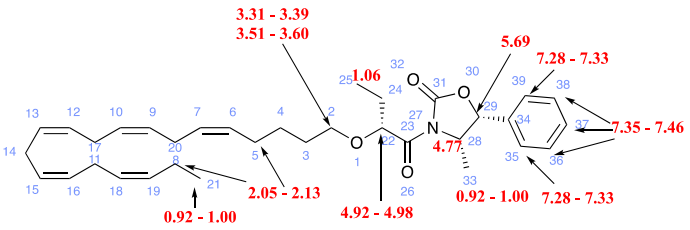

Figure 2.8 Assignment for ^{1}H NMR compound **(2*R*,4*S*,5*R*)-diastereomer-18**

The signals in the recorded ^{13}C NMR (Figure 6.14), account for the 34 carbon atoms in the compound. The allylic carbon atoms and the sp^3 hybridized carbon atoms are as expected giving the signals occurring at 20.7 ppm, 25.7 ppm, 25.8 ppm (3 carbons), 26.2 ppm, 26.7 ppm and 27.1 ppm. The ten olefinic carbon atoms in the hydrocarbon chain and the six sp^2 hybridized carbons atoms in the aromatic ring give as expected the signals at ranging from125.73 ppm to 133.19 ppm. The rest of the peaks are assigned to the belonging protons in the compound, as seen in Figure 2.10.

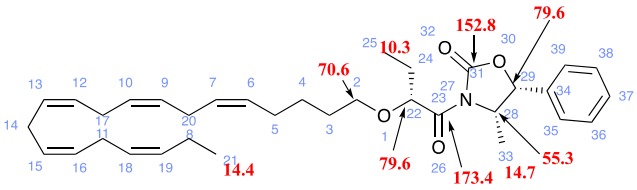

Figure 2.9 Assignment for ^{13}C NMR compound **(2*R*,4*S*,5*R*)-diastereomer-18**

The recorded ^{1}H NMR spectrum is in agreement with previously recorded ^{1}H NMR spectrum.[14] There is no recorded ^{13}C NMR available for this compound. The ^{13}C NMR data are in accordance with the structure.

2.6.3 Other characterizations of (2*S*,4*S*,5*R*)-diastereomer-17 and (2*R*,4*S*,5*R*)-diastereomer-18

MS- and HRMS characterization

In the recorded MS (electrospray) spectrum for both **(2*S*,4*S*,5*R*)-diastereomer-17** and **(2*R*,4*S*,5*R*)-diastereomer-18** (Figure 6.28 and Figure 6.30), a base peak of 556.340 *m/z* is seen, which is in agreement with the calculated molecular mass of sodium adduct of the compound. The recorded HRMS spectrum (Figure 6.29), for compound **(2*S*,4*S*,5*R*)-diastereomer-17** shows a base peak of 556.3397 *m/z*, which also corresponds with the calculated molecular mass of sodium adduct of compound **(2*S*,4*S*,5*R*)-diastereomer-17**. The error is 0.1 ppm, which is within the error criteria for HRMS of 10 ppm and therefore acceptable. The recorded HRMS spectrum (Figure 6.31), for compound **(2*R*,4*S*,5*R*)-diastereomer-18** shows a base peak of 556.3396 *m/z*, which also corresponds with the calculated molecular mass of sodium adduct of compound **(2*S*,4*S*,5*R*)-diastereomer-17**. The error is 0.2 ppm, which is within the error criteria for HRMS of 10 ppm and therefore acceptable.

Specific optical rotation

The calculated specific optical rotation of compound **(2*S*,4*S*,5*R*)-diastereomer-17** is $[\alpha]_D^{20}$= 26.9 (c = 0.01, EtOH). There is no previous recorded value of specific optical rotation of compound **(2*S*,4*S*,5*R*)-diastereomer-17**

The calculated specific optical rotation of compound **(2*R*,4*S*,5*R*)-diastereomer-18** is $[\alpha]_D^{20}$= -35.1 (c = 0.01, EtOH). There is no previous recorded value of specific optical rotation of compound **(2*R*,4*S*,5*R*)-diastereomer-18**.

2.7 HPLC analysis of (2*S*,4*S*,5*R*)-diastereomer-17 and (2*R*,4*S*,5*R*)-diastereomer-18

For determination of the diastereomeric excess (*de*) of **(2*S*,4*S*,5*R*)-diastereomer-17** and **(2*R*,4*S*,5*R*)-diastereomer-18**, High Performance Liquid Chromatography (HPLC) was utilized. The racemic mixture was used as a standard. Five different analysis was conducted. Firstly, a HPLC analysis was conducted of the racemic mixture. Next, HPLC analysis was conducted on each of the purified diastereomer. Lastly, each of the latter HPLC samples were spiked with the standard to achieve a clearer and more affirmative calculation of the enantiomeric excess. In prior to the HPLC analysis, an ultraviolet-visible spectroscopy (UV-

Vis) was recorded to be able to determine the wavelength at which the compound has its highest degree of absorption. The UV-Vis spectrometer is found in the appendix (Figure 6.41), which show that the λ_{max}, the wavelength the racemic mixture has its strongest absorbance is 197 nm. Therefore, the HPLC analyses were carried out at $\lambda = 197$ nm.

As expected, three distinct peaks are present in the obtained HPLC chromatogram for the racemic mixture of **(2*S*,4*S*,5*R*)-diastereomer-17** and **(2*R*,4*S*,5*R*)-diastereomer-18**, as seen in Figure 2.10 also in the appendix (Figure 6.35). The Thin Layer Chromatography (TLC) of the racemic mixture displayed three closely spots in a row. The TLC plate indicated that the **(2*S*,4*S*,5*R*)-diastereomer-17** was eluted first, followed by **(2*R*,4*S*,5*R*)-diastereomer-18** and lastly an impurity. The **(2*S*,4*S*,5*R*)-diastereomer-17** was expected to elute out first according to the previously synthesized.[14] Therefore, a similar pattern was expected in the obtained HPLC chromatograph, which was confirmed. The peak with retention time R_T = 40.85 min belongs to the **(2*S*,4*S*,5*R*)-diastereomer-17**, while the peak with retention time R_T = 43.66 min belongs to the **(2*R*,4*S*,5*R*)-diastereomer-18**.The HPLC chromatogram confirms that it is a 1:1 mixture of both of the diastereomers: **2*S*,4*S*,5*R*)-diastereomer-17** and **(2*R*,4*S*,5*R*)-diastereomer-18.**

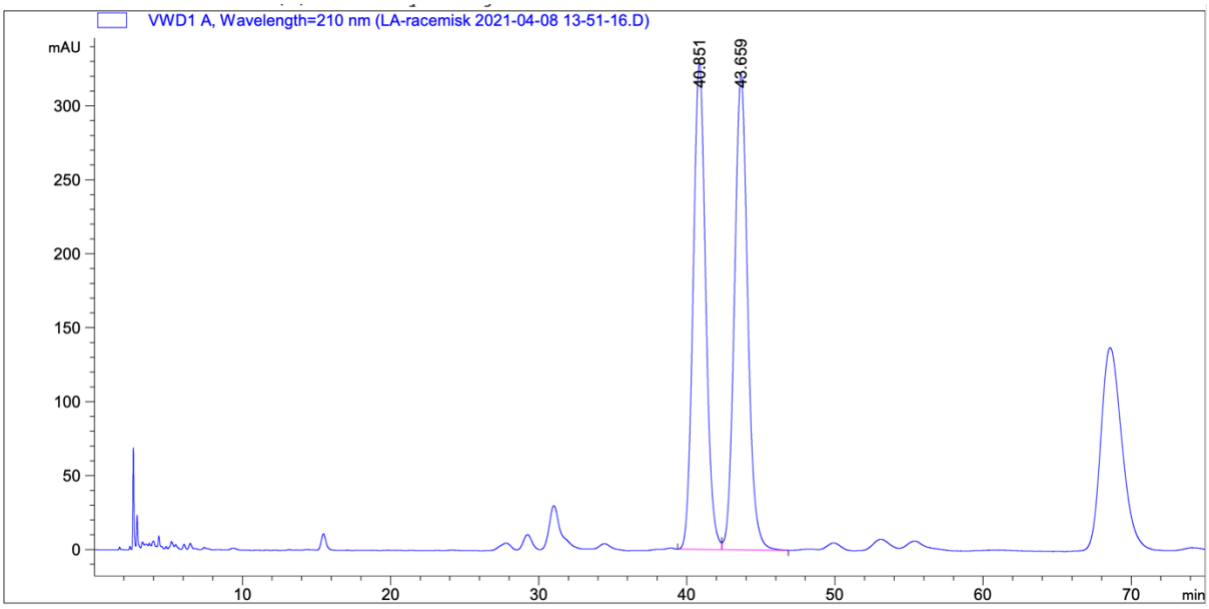

Peak #	RetTime [min]	Type	Width [min]	Area [mAU*s]	Height [mAU]	Area %
1	40.851	BV	0.9089	1.93871e4	329.28293	49.2430
2	43.659	VB	0.9518	1.99832e4	321.22903	50.7570
Totals :				3.93702e4	650.51196	

Figure 2.10 HPLC-chromatogram of the racemic mixture of **(2*S*,4*S*,5*R*)-diastereomer-17** and **(2*R*,4*S*,5*R*)-diastereomer-18**

The obtained HPLC chromatograph of the of **(2*S*,4*S*,5*R*)-diastereomer-17** is shown in Figure 2.11 and in the appendix (figure 6.36). The chromatograph displays one major peak with retention time R_T = 40.55 min and a minor peak with retention time R_T = 44.45. The retention times are close enough to the retention time for two peaks in the obtained HPLC chromatograph for the racemic mixture. The major peak is most likely the recorded signal of the **(2*S*,4*S*,5*R*)-diastereomer-17**, while the minor peak most likely belongs to the **(2*R*,4*S*,5*R*)-diastereomer-18**. The third peak of the impurity does not appear in the chromatograph, which indicates it has been separated during purification.

The diastereomeric excess (*de*) for **(2*S*,4*S*,5*R*)-diastereomer-17** is estimated to approximately 98%, which, is based on integrals of these two peaks. The diastereomeric ratio (*dr*) of **(2*S*,4*S*,5*R*)-diastereomer-17** is estimated to be 96:1. Therefore, it is concluded that the sample of the **(2*S*,4*S*,5*R*)-diastereomer-17** holds a satisfactory and high degree of diastereomeric purity.

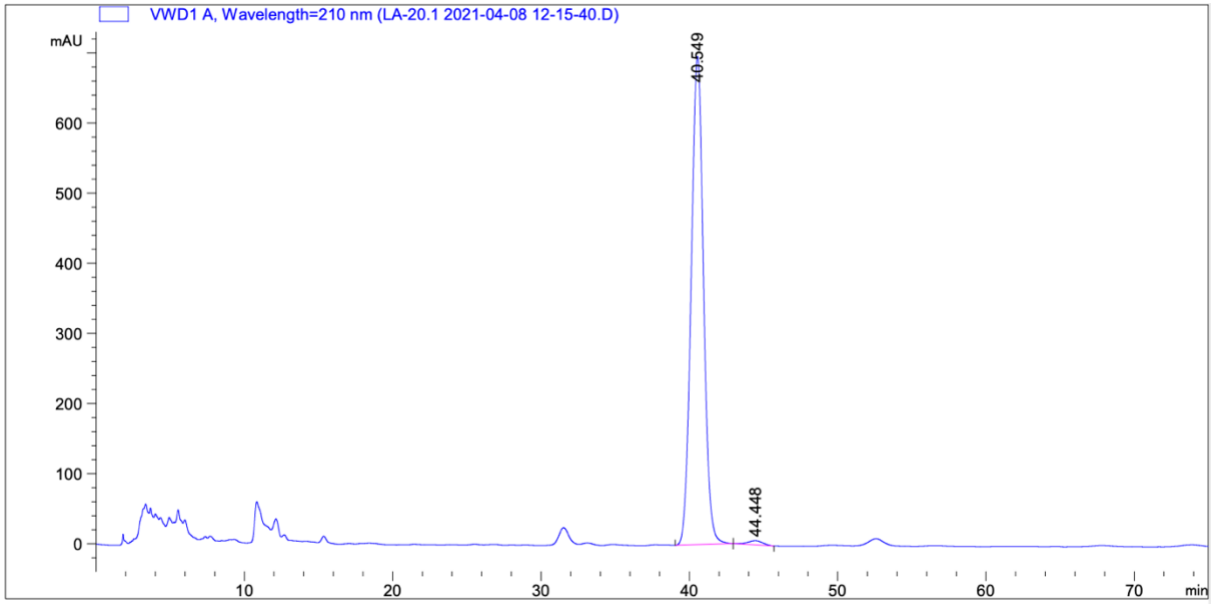

Peak #	RetTime [min]	Type	Width [min]	Area [mAU*s]	Height [mAU]	Area %
1	40.549	BB	0.8955	4.03007e4	696.00183	98.9708
2	44.448	BB	0.9794	419.10123	6.01130	1.0292
Totals :				4.07198e4	702.01313	

Figure 2.11 HPLC-chromatogram of **(2*S*,4*S*,5*R*)-diastereomer-17**

The **(2*S*,4*S*,5*R*)-diastereomer-17** sample was spiked with the sample of the racemic mixture. To achieve a 1:1 ratio of the two samples, almost double the amount of the racemic mixture

was added to the spiked sample. The obtained HPLC chromatogram is shown in Figure 2.12 and in the appendix (figure 6.37). The major peak has a retention time R_T = 40.30 min, and the minor peak next to it has a retention time R_T = 43.06 min. As expected, the peaks of the impurities and the third biggest peak is again appearing in the chromatograph. The HPLC chromatogram confirms that the major peak with the retention time R_T = 40.30 min is indeed **(2*S*,4*S*,5*R*)-diastereomer-17**, and that peak with retention time R_T = 43.06 min is indeed **(2*R*,4*S*,5*R*)-diastereomer-18**.

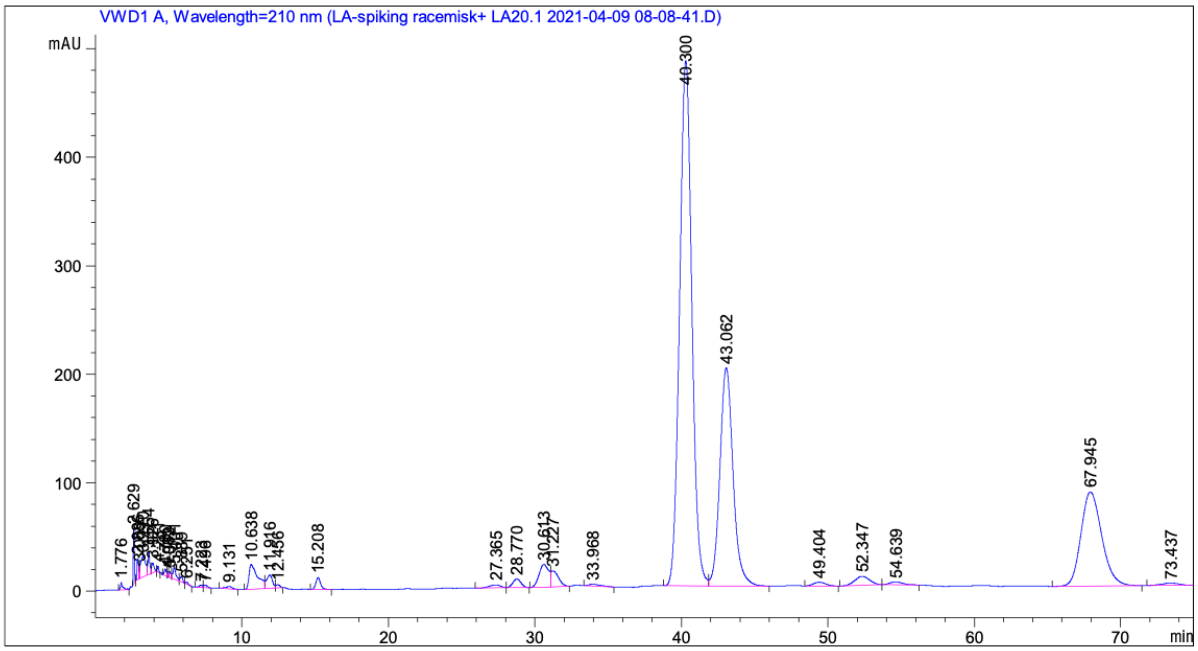

Peak #	RetTime [min]	Type	Width [min]	Area [mAU*s]	Height [mAU]	Area %
27	40.300	BV	0.8951	2.80414e4	483.90482	50.1943
28	43.062	VB	0.9555	1.26257e4	201.08484	22.6001

Figure 2.12 HPLC-chromatogram of **(2*S*,4*S*,5*R*)-diastereomer-17** spiked with the racemic mixture

The obtained HPLC chromatograph of the **(2*R*,4*S*,5*R*)-diastereomer-18** displays major one major peak with retention time R_T = 43.19 min and a minor peak with retention time R_T = 40.29. The obtained HPLC chromatogram is shown in Figure 2.13 and also in the appendix (figure 6.38). The major peak is **(2*R*,4*S*,5*R*)-diastereomer-18**, which was confirmed. The third peak of the impurity does not appear in the chromatograph, which indicates it has been separated during purification. The diastereomeric excess (*de*) for the **(2*R*,4*S*,5*R*)-diastereomer-18** is

estimated to approximately 98%, which, is based on integrals of these two peaks. The diastereomeric ratio (*dr*) of **(2*R*,4*S*,5*R*)-diastereomer-18** is estimated to be 120:1. Therefore, it is concluded that the sample of the **(2*R*,4*S*,5*R*)-diastereomer-18** holds a satisfactory and high degree of diastereomeric purity.

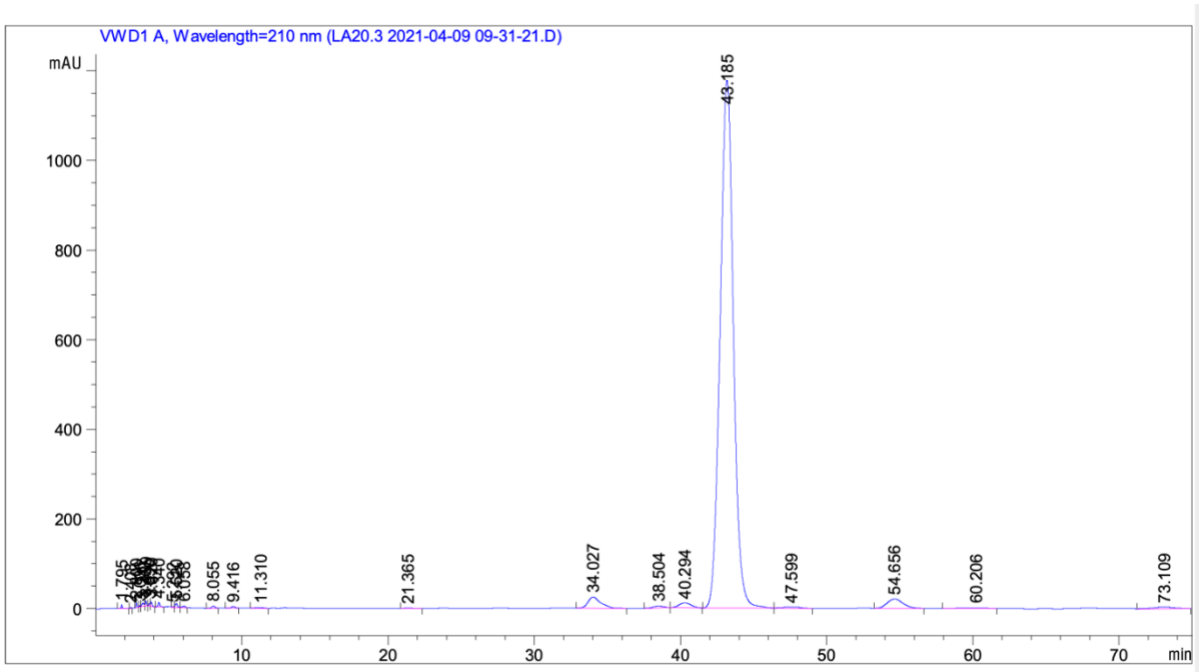

Peak #	RetTime [min]	Type	Width [min]	Area [mAU*s]	Height [mAU]	Area %
19	40.294	BB	0.8608	607.48969	10.71001	0.7636
20	43.185	BB	0.9627	7.38369e4	1177.23792	92.8142

Figure 2.13 HPLC-chromatogram of compound **(*R*)-17**

The **(2*R*,4*S*,5*R*)-diastereomer-18** sample was also spiked with the sample of the racemic mixture. To achieve a 1:1 ratio of the two samples, almost triple the amount of the racemic mixture was added to the spiked sample. The obtained HPLC chromatogram is shown in Figure 2.14 and in the appendix (figure 6.39). The major peak has a retention time R_T = 40.30 min, and the minor peak next to it has a retention time R_T = 43.10 min. As expected, the peaks of the impurities and the third biggest peak is again appearing in the chromatograph The HPLC chromatogram confirms that the major peak with the retention time R_T = 40.34 min is indeed **(2*S*,4*S*,5*R*)-diastereomer-17**, and that peak with retention time R_T = 43.11 min is indeed **(2*R*,4*S*,5*R*)-diastereomer-18**.

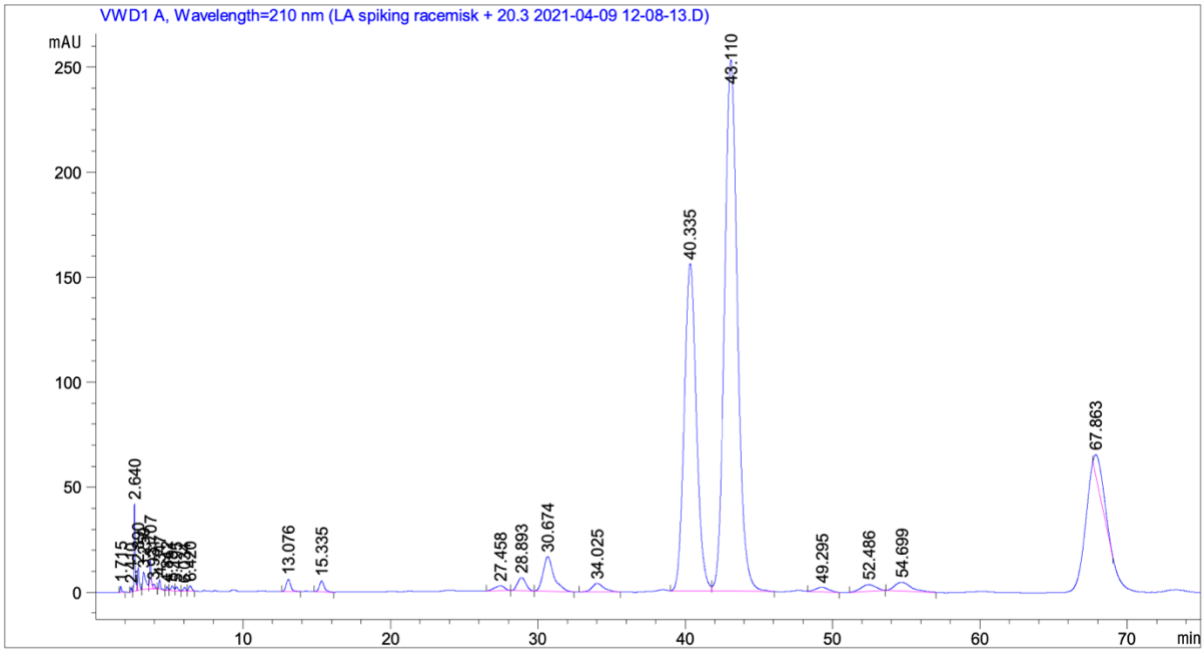

Peak #	RetTime [min]	Type	Width [min]	Area [mAU*s]	Height [mAU]	Area %
20	40.335	BV	0.8837	8932.92383	155.85475	31.7720
21	43.110	VB	0.9453	1.55449e4	252.84682	55.2888

Figure 2.14 HPLC-chromatogram of **(2*R*,4*S*,5*R*)-diastereomer-18** spiked with the racemic mixture

2.8 Chromatographic purification of (2*S*,4*S*,5*R*)-diastereomer-17 and (2*R*,4*S*,5*R*)-diastereomer-18

The product from the reaction was purified several times by flash column chromatography on silica gel. According to the patent by BASF AS[14] **(2*S*,4*S*,5*R*)-diastereomer-17** would be eluted first, followed by the **(2*R*,4*S*,5*R*)-diastereomer-18**. The eluent used for the purification was the same used in the reported procedure[14], which is EtOAc:Heptane 15:85. The eluent provided acceptable separation and was therefore used.

A Thin Layer Chromatography (TLC) analysis was performed to get an idea of when to expect the compounds to elute. As it can be seen on the TLC-plate (Figure 2.15), there was three major spots detected, by $KMnO_4$ stain and also weakly seen under UV light. The first spot was believed to be **(2*S*,4*S*,5*R*)-diastereomer-17** and the second spot was believed to be **(2*R*,4*S*,5*R*)-diastereomer-18**. The third spot was believed to be either impurties or possibly urea. The

column that was used was smallest column available which was 10 mm in diameter and height was 12 cm, to be able to obtain optimal separation because there was a small amount of product.

Small amounts of EPA acid **10** was used in the synthesis of **(2*S*,4*S*,5*R*)-diastereomer-17** and **(2*R*,4*S*,5*R*)-diastereomer-18**. In the first batch, the fractions that were collected were approximately 5 mL. However, for the next purifications it was decided that smaller amounts were needed to be collected to achieve products that were had high degree of diastereomeric purity, therefore fractions of approximately 2 mL were collected. The fractions of **(2*S*,4*S*,5*R*)-diastereomer-17** that looked diastereomeric pure on the TLC-plate were collected together, and fractions of (**2*R*,4*S*,5*R*)-diastereomer-18** that looked diastereomeric pure were collected together. The fraction that did not seem to diastereomeric pure on the TLC-plate, were collected together and purified again. If there was any uncertainty as to whether a fraction was diastereomeric pure or not, the fraction was collected separately, and the purity was checked by ^{1}H NMR-spectroscopy.

A challenging element of the purification process was that some fractions looked diastereomeric pure on the TLC-plate, however the recorded ^{1}H NMR spectrum indicated that the product was not diastereomeric pure. Several chromatographic purifications were repeated, to achieve products that were diastereomeric pure. Another challenging part of this process was that it was very time consuming for several reasons. Firstly, many purifications were needed. Secondly, fractions of very small amounts were collected, meaning the process was slowed down. Also, the R_f-values were so close to each other that sometimes it was difficult to decide from a visualizing a TLC-plate whether the fraction was diastereomeric pure or not. Sometimes the spots were very unclear and light, which made it challenging. Also, in some cases the spots were overlapping. Therefore, it was very important to work precisely when spotting samples on the TLC-plate. An optimal system was developed, however it concluded that to be able to achieve the diastereomers in satisfactory and with a high degree of diastereomeric purity.

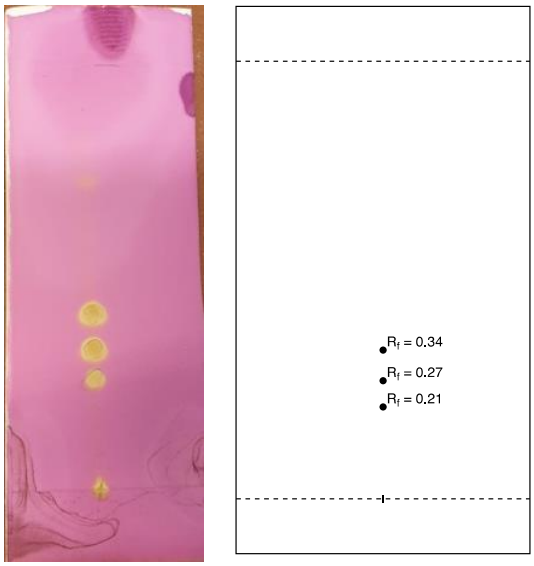

Figure 2.15 To the left is the TLC-plate of the reaction mixture and to the right is a simplified illustration of the TL- plate with the R_f-values to the three most dominant spots.

2.9 Synthesis of EPA amide 19

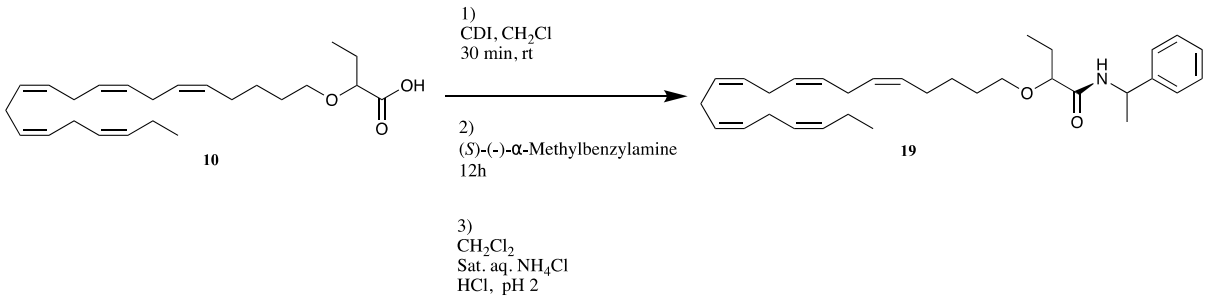

Scheme 2.9 Synthesis and separation of EPA amide **19**

Compound **19** was synthesized from EPA **10** using a well-established method reported by Johannson *et al.*[37] for amide coupling of PUFAs. The method takes basis in activating the acid group by using carbonyl diimidazole (CDI), then the amine of choice was (*S*)-(-)-*α*-methylbenzylamine. In this synthesis the amine used was (*S*)-(-)-*α*-methylbenzylamine to synthesize the desired compound **19.** The use of CDI has several benefits versus DCC[37], which was the coupling agent used in the synthesis of **(2*S*,4*S*,5*R*)-diastereomer-17** and **(2*R*,4*S*,5*R*)-diastereomer-18**.

The aim for this synthesis, was to obtain the diastereomers and a HPLC chromatogram. Then, the **(2*S*,4*S*,5*R*)-diastereomer-17** and **(2*R*,4*S*,5*R*)-diastereomer-18** hydrolyzed to the free fatty acids **(2*S*,4*S*,5*R*)-diastereomer-17** and **(2*R*,4*S*,5*R*)-diastereomer-18,** which would then be

coupled with the same benzylamine That way a HPLC analysis of compound **19** would be compared to each of the HPLC analysis of compound **(*S*)-10** and **(*R*)-10.** That could give an answer to whether the enantiomers had gone through an epimerization during storage or not.

The crude product was purified by microscale flash chromatography on silica gel to obtain the desired product EPA **19**. The recorded ^{1}H- and ^{13}C NMR is available at the appendix (Figure 6.15 and 6.16), confirmed that the EPA **19** is indeed synthesized. However, the ^{1}H NMR is partially characterized. The compound consists of diastereomers, which could be reason for the complex NMR spectra, and therefore very challenging to gain information from. Also, there might be some impurties even after purification, and that is supported by the HPLC chromatogram and also the MS spectra. There was also conducted a HPLC-analysis of the product, but a satisfactory chromatogram was not achieved despite running the analysis at λ_{max}, the absorbance at 201 nm. The MS- and HRMS-spectra confirms that the desired product was obtained, however most likely the yield do not reflect the actual yield of the pure product. In the upcoming sections, MS-spectra are discussed in more detail, and the HPLC -analysis. The reported results from using the same method for the synthesis of different fatty acid amides claims high degree of purity[37]. A second attempt would confirm the purity of the compound more certainly.

MS- and HRMS characterization

The calculated molecular mass of the sodium adduct of compound **19** and the base peak of 500.350 *m/z* shown in the recorded MS (electrospray) spectrum (Figure 6.32) for compound **19**, are in agreement. The recorded HRMS spectrum (Figure 6.33), for compound **19** shows a base peak of 500.3498 *m/z*, which also corresponds with the calculated molecular mass of sodium adduct of compound **19**. The error is 0.1 ppm, which is within the error criteria for HRMS of 10 ppm and therefore acceptable.

HPLC analysis

Several attempts to attain a chromatograph of compound **19** was made, with the expectation of detecting two peaks in 50:50 ratio caused by the two diastereomers. The UV spectroscopy, which is found in the appendix (Figure 6.42), indicated that the wavelength that the compound was showing the strongest absorbance is at 201 nm. Therefore, the UV absorbance was changed to 201 nm for the HPLC analysis, to optimize the system. Unfortunately, a satisfactory HPLC chromatogram was not obtained. It might be some impurities disturbing the peaks. The best

obtained HPLC chromatogram is seen Figure 2.16 and also in the appendix (Figure 6.40). The aim of this particular synthesis was to a obtain a product that could be used in later HPLC analysis for comparisons, and the HPLC analysis was not very helpful it can be concluded that there is no point of using this route. However, a second attempt might be rational choice.

```
Data File C:\Chem32\2\Data\LA22.8 2021-03-29 15-16-00.D
Sample Name: LA22.8

======================================================================
Acq. Operator    : SYSTEM
Sample Operator  : SYSTEM
Acq. Instrument  : LC1260-1                        Location :    P1-A-01
Injection Date   : 3/29/2021 3:16:44 PM
                                                   Inj Volume : 10.000 µl
Acq. Method      : C:\CHEM32\2\METHODS\uio-test.M
Last changed     : 3/29/2021 3:50:06 PM by SYSTEM
                   (modified after loading)
Analysis Method  : C:\CHEM32\2\METHODS\uio-test.M
Last changed     : 4/21/2021 2:57:18 PM by SYSTEM
                   (modified after loading)
Sample Info      : 1 ml/min, C-18 column, 80% i MeOH in H2O, UV-201
```

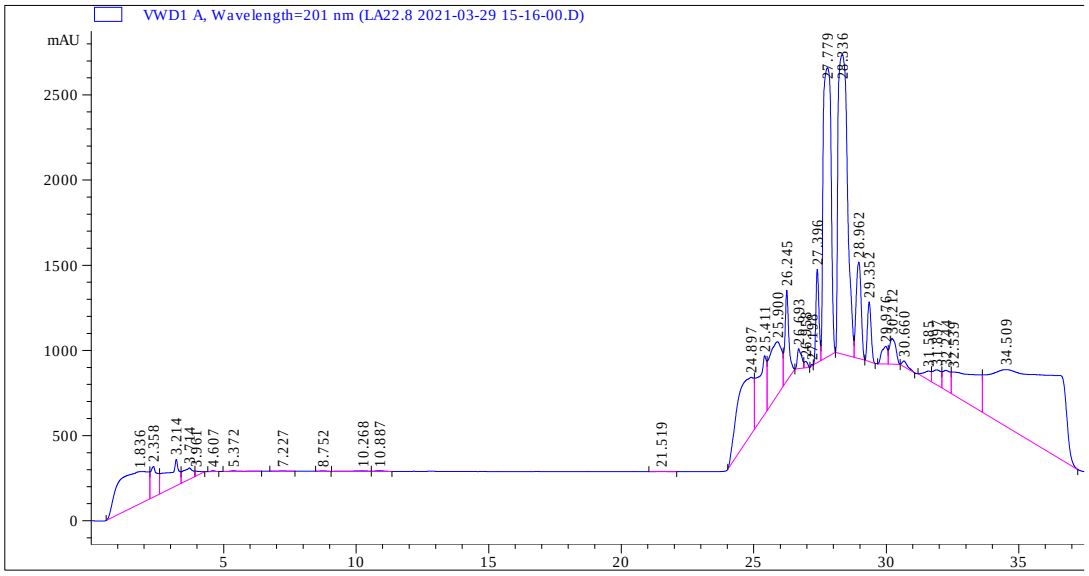

Figure 2.16 HPLC-chromatogram of compound **19**

2.10 Synthesis of *tert*-butyl 2-bromobutanoate 5

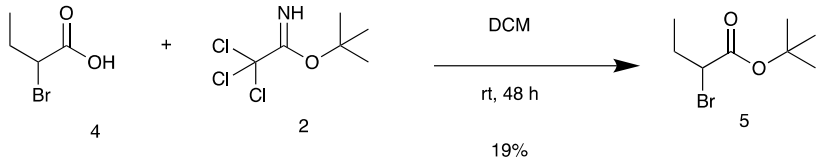

Scheme 2.10 Synthesis of *tert*-butyl 2-bromobutanoate **5**

Tert-butyl 2-bromobutanoate **5** was synthesized with the aim of using it for the syntheses of EPA ethyl ether **8**. The procedure was based on a previous synthetic method in the article by Mahajani *et al*,[38] also in the LIPCHEM-group. However, *tert*-butyl 2-bromobutanoate **5** was not obtained of desired purity. The recorded ^{1}H NMR is found in Figure 6.17 in the appendix. Furthermore, it was preferred to use a commercially available *tert*-butyl 2-bromobutanoate.

2.11 Attempted of synthesis of EPA acid (*R*)-10

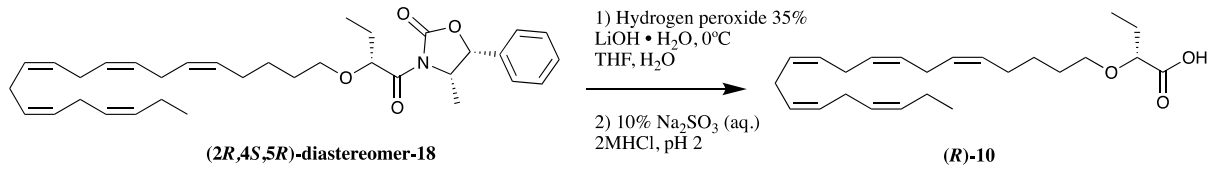

Scheme 2.11 Attempted synthesis of **(*R*)-10**

An attempt was made to synthesis EPA acid **(*R*)-10** following the procedure described in a patent by BASF AS in 2019.[14] A small amount of **(2*R*,4*S*,5*R*)-diastereomer-18** was used for the reaction. A TLC-analysis was conducted on the reaction mixture, which indicated that there was possibly some product. Unfortunaly, during micro-scale flash chromatography no product was obtained. Given the time, there was not much time left for a new attempt. However, a good amount product of both **(2*S*,4*S*,5*R*)-diastereomer-17** and **(2*R*,4*S*,5*R*)-diastereomer-18** are left. Further attempts on the synthesis of both **(*S*)-10** and **(*R*)-10** are preferred.

3 Summary, Conclusions and Future Studies

Given the time, EPA-oxy-acetate was synthesized successfully. Also, methyl and ethyl group were introduced to EPA-oxy-acetate. The separation of the EPA-oxy-acetate with an ethyl group was successfully done in satisfactory purity. The synthesized products should be submitted to biological evaluations. However, the hydrolysis back to free acid form was attempted. Unfortunately, there was not left any time for another attempt. The synthesized products should be submitted to biological evaluations. It was also attempted to make the compound **19**, for further research on the enantiomers. However, desired results were not achieved.

Future studies will be related obtaining the two enantiomers of compound **10,** when these two enantiomers have been obtained structural and stereochemical integrity will be obtained. If sufficient enantiomeric purity of each enantiomer has been obtained biological evaluations will be performed. Altogether, new knowledge on structure functions of synthetically modified PUFAs as BK channels blockers will be gained. Such knowledge is useful towards developing new remedies for treatment of cardiovascular diseases.

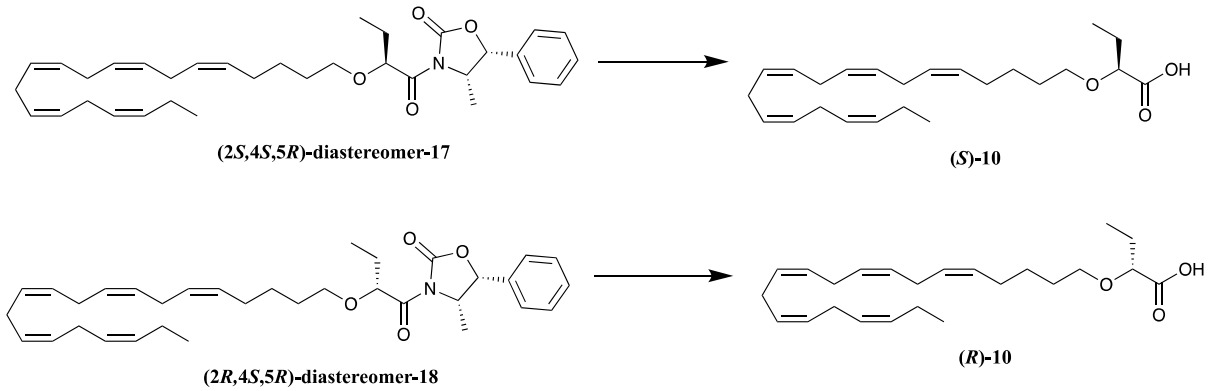

Figure 3.1 The synthesis of **(*S*)-10** and **(*R*)-10.**

In additions other analogs as shown in Figure 3.2 is also in interest.

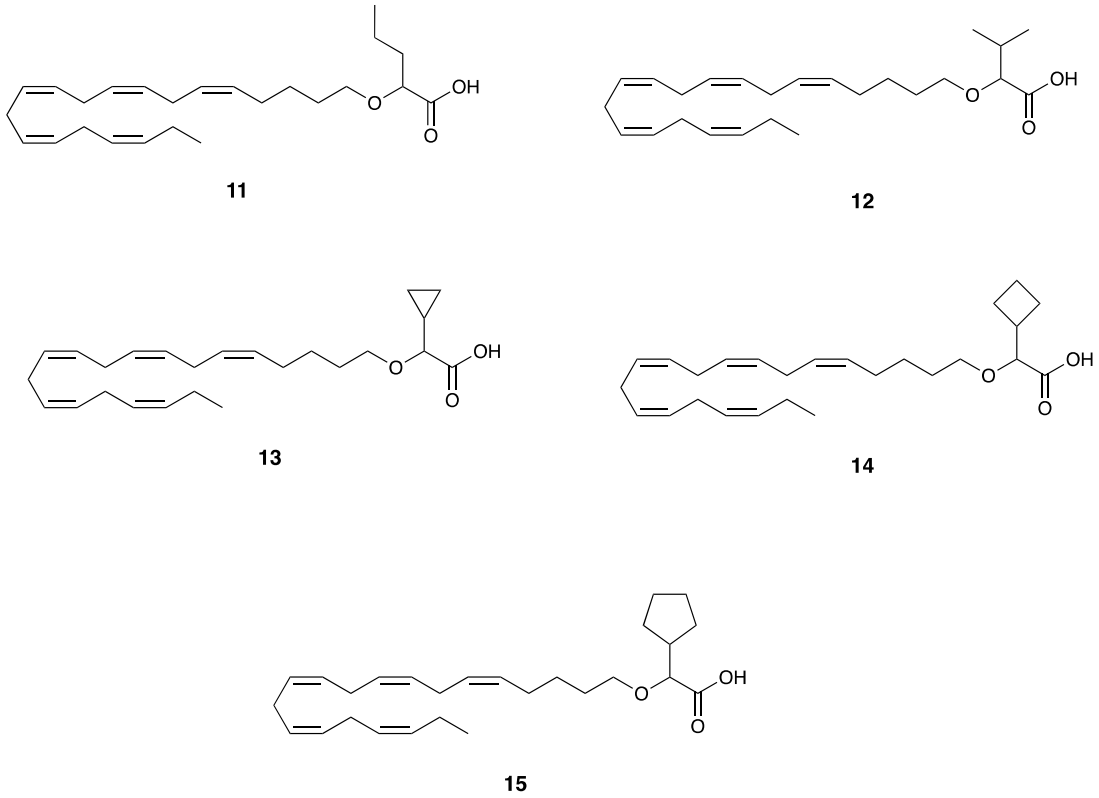

Figure 3.2 Structures of other analogs of EPA fatty acid.

4 Experimental

4.1 Materials and apparatus

Unless otherwise stated, all commercially available reagents and solvents were used in the form they were supplied without any further purification. The yields that are reported are based on isolated material. Using Schlenk techniques, sensitive reactions were performed under argon atmosphere. To minimize exposure to light, reactions flask was covered with aluminum foil when sensitive reactions were performed. All thin layer chromatography (TLC) were performed on silica gel 60 F254 aluminum-backed plates and flash column chromatography was performed on silica gel 60 (40-63 μm), both produced by Merck. Visualizing reagents used for thin layer chromatography (TLC) were UV light, potassium permanganate ($KMnO_4$) and cerium-ammonium-molybdate (CAM).

NMR spectra were recorded on a Bruker AVIII400 spectrometer at 101 MHz for ^{13}C NMR and 400 MHz for ^{1}H NMR. Chemical shifts are reported in parts per million (δ) relative the central carbon solvent resonance in ^{13}C NMR ($CDCl_3$ = δ 77.16 ppm) and to the central residual protium solvent resonance in ^{1}H NMR ($CDCl_3$ = δ 7.26). The coupling constants (*J*) are reported in hertz. Anton Paar MCP 100 polarimeter was used for measurement of optical rotations, using 0.2 mL cell with 1.0 dm path lengths.

Micromass Prospec Q or Micromass QTOF 2 W spectrometer was used for recording the mass spectra at 70 eV. ESI was used as the method of ionization. Micromass Prospec Q or Micromass QTOF 2 W spectrometer was used for recording the high-resolution mass spectra at 70 eV. ESI was used as the method of ionization. High-resolution mass spectra were recorded at the Department of Chemistry, University of Oslo. HPLC-analyses were performed using a C_{18} stationary phase (Eclipse XBD-C_{18}), 4.6 x 250 mm, particle size 5 μm, from Agilent Technologies). Agilent Technologies Cary 8485 UV-VIS spectrophotometer using quartz cuvettes, was used for the recording of the UV/Vis spectrum.

4.2 Experimental procedures

4.2.1 Synthesis of EPA alcohol 6

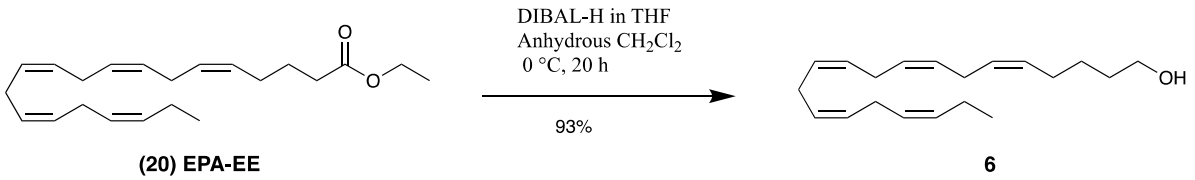

(20) EPA-EE **6**

EPA ethyl ester **20** (3.011 mg, 9.11 mmol) was transferred to a flame dried round-bottom flask. Dry CH_2Cl_2 (21.1 mL) was and stirred. Dry 1.0 M DIBAL-H in THF (27.1 mL, 27.1 mmol) was added to the solution at 0 °C, and the reaction mixture stirred overnight in a refrigerator. 1 M aq. HCL (70 mL) was added to the reaction mixture at 0 °C to quench the reaction. EtOAc:Hexane (1:1, 40 mL) was then added, the mixture was stirred for 20 minutes. Furthermore, the aqueous was extracted with EtOAc (5 x 30 mL). The organic layers were combined and dried over Na_2SO_4 and the solvent was removed *in vacuo*. The crude product was purified by flash chromatography on silica gel (EtOAc/hexane 1:5) and the EPA alcohol **6** was obtained as a yellow oil. **Yield**: 2.44 g (93%); **TLC** (EtOAc/hexane 1:5, $KMnO_4$ stain) R_f = 0.37; **^{1}H NMR** (400 MHz, $CDCl_3$) δ 5.28 – 5.46 (m, 10H), 3.65 (t, *J* = 6.5 Hz, 2H), 2.77 – 2.90 (m, 8H), 2.03 – 2.14 (m, 4H), 1.56 – 1.62 (m, 2H), 1.42 – 1.46 (m, 2H), 0.98 (t, *J* = 7.5 Hz, 3H); **^{13}C NMR** (101 MHz, $CDCl_3$) δ 132.2, 130.1, 128.7, 128.5, 128.4, 128.3, 128.2 (2C), 128.0, 127.2, 63.1, 32.5, 27.1, 25.9, 25.8 (3C), 25.7, 20.7, 14.4. **HRMS (ESI)**: calculated for $[M+Na]^+$: 311.2345, found: 311.2345.

The spectral data were in agreement with structure. There is no reference data available for this compound, however the data was compared to the NMR spectra of the DHA alcohol.[33] The signals have similar chemical shift and also the splitting is similar, the only difference is as expected the number of protons. Therefore, it was logical and useful to use these data for comparison.

4.2.2 Synthesis of EPA ethyl ether 8

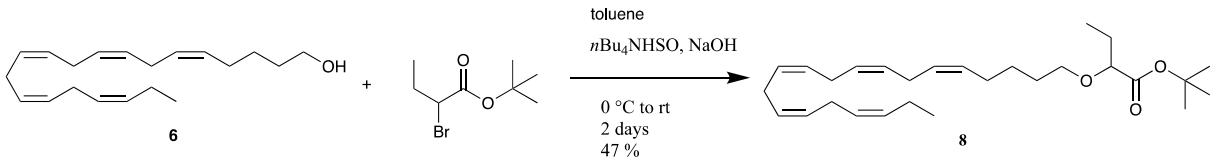

The EPA alcohol **6** (2.36 g, 8.2 mmol) was dissolved in toluene (106 mL). While stirring, 50% NaOH (106 mL) was added to the reaction mixture 0 °C. *n*Bu_4NHSO_4 (0.278 g, 0.82 mmol) was added and the reaction was stirred for 1 hour. Next, *tert*-butyl 2-bromobutanoate (2.27 mL, 12.3 mmol) was added dropwise to the solution. The reaction mixture was stirred at ambient temperature overnight. Then, *tert*-butyl 2-bromobutanoate (0.78 mL, 4.2 mmol) was added again dropwise and the reaction mixture was stirred overnight. The biphasic solution was separated and the aqueous was extracted with diethyl ether (5 x 30 mL). The organic layers were combined and dried over Na_2SO_4 and the solvent was removed *in vacuo*. The crude product was purified by flash chromatography on silica gel (EtOAc/hexane 5:95) and the unsaturated *t*-butyl ester **8** was obtained as a yellow oil. **Yield**: 1.64g (47%); **TLC** (5% EtOAc/hexane, $KMnO_4$ stain and UV light) R_f = 0.38; **^{1}H NMR** (400 MHz, $CDCl_3$) δ 5.20 – 5.59 (m, 10H), 3.52 – 3.66 (m, 2H), 3.32 (dt, *J* = 9.0, 6.5 Hz, 1H), 2.74 – 2.92 (m, 8H), 2.02 – 2.14 (m, 4H), 1.67– 1.75 (m, 2H), 1.59 – 1.64 (m, 2H), 1.47 (s, 9H), 1.41 – 1.46 (m, 2H), 0.97 (td, *J* = 7.5, 5.2 Hz, 6H); **^{13}C NMR** (101 MHz, $CDCl_3$) δ 172.5, 132.2, 130.2, 128.7, 128.6, 128.4, 128.3, 128.1 (2C), 128.0, 127.2, 81.1, 80.9, 70.4, 29.6, 28.3 (3C), 27.2, 26.4, 26.3, 25.8 (3C), 25.7, 20.7, 14.4, 9.9. **HRMS (ESI)**: calculated for $[M+Na]^+$: 453.3339, found: 453.3338.

The recorded ^{1}H NMR spectrum is in agreement with previously recorded ^{1}H NMR spectrum.[14] There is no recorded ^{13}C NMR available for this compound. The ^{13}C NMR data are in accordance with the structure.

4.2.3 Synthesis of EPA ethyl ether 7

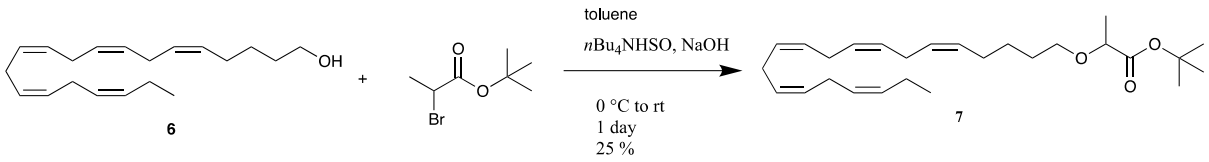

The EPA alcohol 6 (0.165 g, 0.52 mmol) was dissolved in toluene (6.8 mL). At 0 °C, 50% NaOH (6.82 mL)) was added to the reaction mixture while stirring. *n*Bu_4NHSO_4 (0.018 g, 0.052 mmol) was added and the reaction was stirred for 1 hour. Subsequently, *t*-butyl 2-bromopropanoate (0.13 mL, 0.163 g, 0.78 mmol) was added dropwise to the stirred solution. The reaction mixture was stirred at ambient temperature overnight. Hexane:H_2O (1:1, 27 mL) was then added to the reaction mixture .The biphasic solution was separated and the aqueous was extracted with diethyl ether (4 x 10 mL). The organic layers were combined and dried over Na_2SO_4 and solvent were removed aqueous *in vacuo*. The crude product was purified by flash chromatography on silica gel (EtOAc/hexane 5:95) and the unsaturated *t*-butyl ester 7 was obtained as a yellow oil. **Yield**: 0.060 g (25 %); **TLC** (EtOAc/hexane 5:95, $KMnO_4$ stain) R_f = 0.33; **^{1}H NMR** (400 MHz, $CDCl_3$) δ 5.27 – 5.44 (m, 10H), 3.80 (q, *J* = 6.8 Hz, 1H), 3.55 (dt, *J* = 8.9, 6.5 Hz, 1H), 3.35 (dt, *J* = 9.0, 6.5 Hz, 1H), 2.77 – 2.89 (m, 8H), 2.03 – 2.13 (m, 4H), 1.59 – 1.66 (m, 2H), 1.47 (s, 9H), 1.40 – 1.46 (m, 2H), 1.35 (d, *J* = 6.8 Hz, 3H), 0.97 (t, *J* = 7.5 Hz, 3H); **^{13}C NMR** (101 MHz, $CDCl_3$) δ 173.0, 132.2, 130.2, 128.7, 128.6, 128.4, 128.3, 128.1 (3C), 127.2, 81.2, 75.6, 70.2, 29.6, 28.2 (3C), 27.2, 26.3, 25.8 (3C), 25.7, 20.7, 18.8, 14.4. **HRMS (ESI)**: calculated for $[M+Na]^+$: 439.3183, found: 439.3182.

There is no reference data available for this compound. The spectral data were in agreement with previous synthetic routes made in the LIPCHEM group.

4.2.4 Synthesis of EPA-oxy-acetate 16

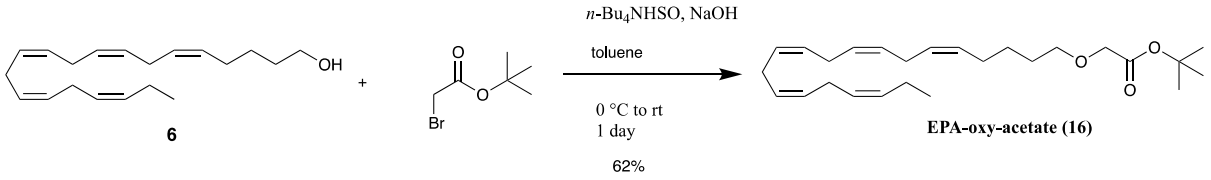

The EPA alcohol 6 (2.097 g, 7.27 mmol) was dissolved in toluene (94 mL). At 0 °C, 50% NaOH (94 mL) was added to the reaction mixture while stirring. *n*Bu_4NHSO_4 (0.247 g, 0.727 mmol) was added and the reaction was stirred for 1 hour. Subsequently, *t*-butyl 2-bromoacetate (2.02 mL, 13.66 mmol) was added dropwise to the stirred solution. The reaction mixture was stirred at ambient temperature overnight.The biphasic solution was separated and the aqueous was extracted with diethyl ether (5 x 40 mL). The organic layers were combined and dried over Na_2SO_4 and solvent were removed aqueous *in vacuo*. The crude product was purified by flash chromatography on silica gel (EtOAc/hexane 5:95) and the unsaturated *t*-butyl ester 7 was obtained as a yellow oil. **Yield**: 1.808 g (62 %); **TLC** (EtOAc/hexane 5:95, $KMnO_4$ stain) R_f = 0.32 ;**^{1}H NMR** (400 MHz, $CDCl_3$) δ 5.27 – 5.44 (m, 10H), 3.94 (s, 2H), 3.51 (t, *J* = 6.5 Hz, 2H), 2.76 – 2.89 (m, 8H), 2.03 – 2.13 (m, 4H), 1.59 – 1.68 (m, 2H), 1.48 (s, 9H), 1.40 – 1.46 (m, 2H), 0.97 (t, *J* = 7.5 Hz, 3H); **^{13}C NMR** (101 MHz, $CDCl_3$) δ 170.0, 132.2, 130.1, 128.7, 128.6, 128.4, 128.3, 128.1 (3C), 127.2, 81.6, 71.8, 68.9, 29.4, 28.3 (3C), 27.1, 26.2, 25.8 (3C), 25.7, 20.7, 14.4. **HRMS (ESI)**: calculated for $[M+Na]^+$: 425.3026, found: 425.3025.

There is no reference data available for this compound. The spectral data were in agreement with previous synthetic routes made in the LIPCHEM group.

4.2.5 Synthesis of EPA acid 10

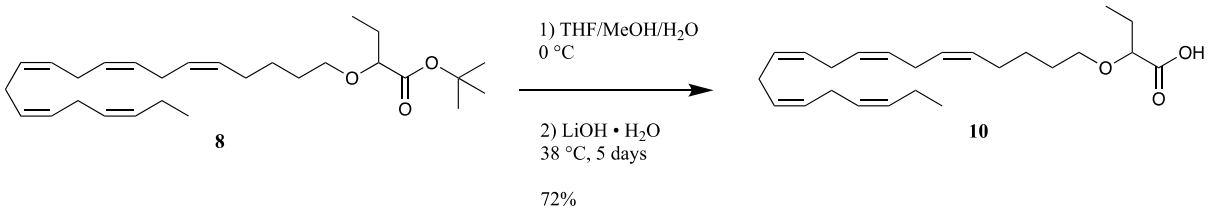

8 **10**

A solution of the EPA ethyl ether **8** (0.59 g, 1.38 mmol) and THF/MeOH/H_2O (33 mL, 33 mL, 17 mL) was chilled to 0 °C. To this solution, LiOH • H_2O (2.03g, 48.3 mmol, 35 eq.) was added and reaction mixture was heated to 38 °C and stirred for 5 days. To quench the reaction, saturated aqueous NaH_2PO_4 (92 mL) was added followed by EtOAc (92 mL). The biphasic solution was separated and the aqueous was extracted with EtOAc (5 x 30 mL). The organic layers were combined and dried over Na_2SO_4 and the solvent was removed *in vacuo*. The crude product was purified by flash chromatography on silica gel (MeOH/DCM 5:95) and the unsaturated *t*-butyl ester **8** was obtained as a yellow oil. **Yield**: 0.368 g (72%); **TLC** (MeOH/DCM 5:95, $KMnO_4$ stain and UV light) R_f = 0.29; **^{1}H NMR** (400 MHz, $CDCl_3$) δ 5.27 – 5.46 (m, 10H), 3.84 – 3.91 (m, 1H), 3.55 (m, 2H), 2.75 – 2.91 (m, 8H), 2.03 – 2.14 (m, 4H), 1.78 – 1.88 (m, 2H), 1.62 – 1.68 (m, 2H), 1.43 – 1.50 (m, 2H), 0.95 – 1.01 (m, 6H); **^{13}C NMR** (101 MHz, $CDCl_3$) δ 173.8, 132.2, 129.8, 128.7, 128.5 (2C), 128.4, 128.3 (2C), 128.0, 127.2, 79.8, 71.0, 29.4, 27.0, 26.2, 25.8 (3C), 25.7, 25.3, 20.7 14.4, 9.1. **HRMS (ESI)**: calculated for $[M+Na]^+$: 397.2713, found: 397.2713.

The recorded ^{1}H NMR spectrum is in agreement with previously recorded ^{1}H NMR spectrum.[14] There is no recorded ^{13}C NMR available for this compound. The ^{13}C NMR data are in accordance with the structure.

4.2.6 Synthesis of named (2*S*,4*S*,5*R*)-diastereomer-17 and (2*R*,4*S*,5*R*)-diastereomer-18

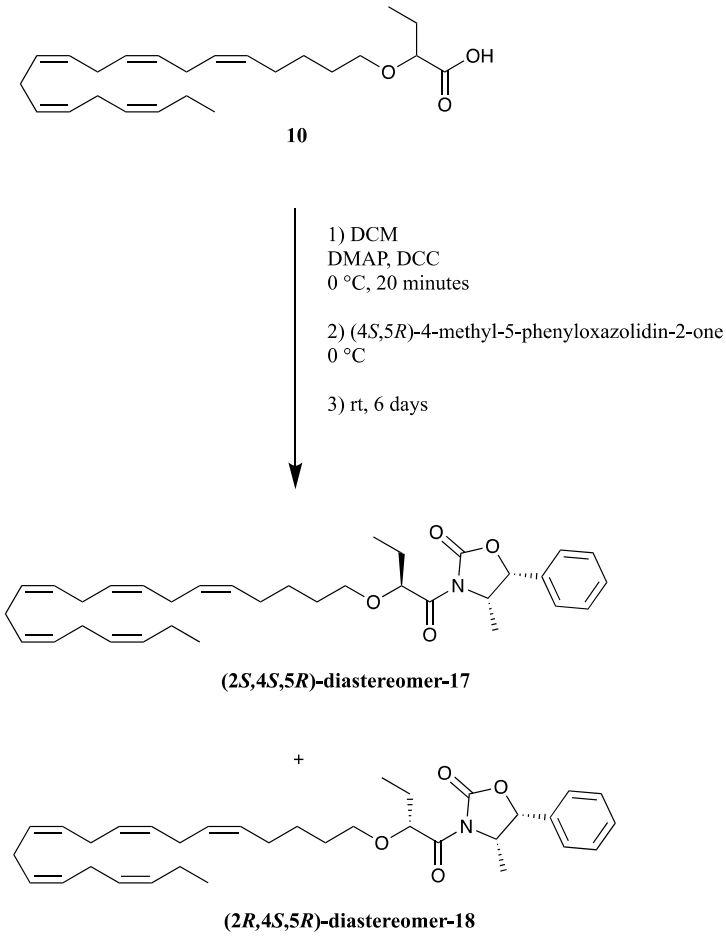

The acid **10** (0.211 g, 0.56 mmol) was transferred to a flame dried round-bottom flask and dry DCM (6.6 mL) was added. DMAP (73 mg, 0.6 mmol) and DCC (0.126 g, 0.61 mmol) were added to the stirred mixture at 0 °C and under argon. The mixture was then stirred at 0 °C for 20 minutes. (4*S*,5*R*)-4-methyl-5-phenyloxazolidin-2-one (99 mg, 0.56 mmol) was added which was still held at 0 °C. The ice-bath was removed after 2,5 hours. The turbid mixture was stirred for six days. The reaction mixture was filtrated under reduced pressure. The crude product was purified by flash chromatography on silica gel (EtOAc/heptane 15:85). The two diastereomers **(2*S*,4*S*,5*R*)-diastereomer-17** and **(2*R*,4*S*,5*R*)-diastereomer-18** were separated and the equal fractions were merged. Several purifications by flash chromatography was done to obtain pure fractions. **(2*S*,4*S*,5*R*)-diastereomer-17** was eluted first and was obtained as an oil. Then, **(2*R*,4*S*,5*R*)-diastereomer-18** was eluted and obtained as an oil.

(**2*S*,4*S*,5*R*)-diastereomer-17**: **HPLC analysis** (Eclipse XBD-C_{18}, MeOH/H_2O 90:10, 1.0 mL/min, t_r(major) = 40.55 min and t_r(minor) = 44.45 min. **Yield**: 0.0430 g (29 %); *de*: 98%; *dr*: 96:1; **TLC** (EtOAc/heptane 15:85, $KMnO_4$ stain and UV light) R_f = 0.34; $\boldsymbol{[\alpha]_D^{20}}$= 26.9 (c = 0.01, EtOH); **^{1}H NMR** (400 MHz, $CDCl_3$) δ 7.35 – 7.46 (m, 3H), 7.27 – 7.32 (m, 2H), 5.73 (d, *J* = 7.5 Hz, 1H), 5.29 – 5.46 (m, 10H), 4.81 – 4.92 (m, 2H), 3.56 (dt, *J* = 9.0, 6.4 Hz, 1H), 3.35 (dt, *J* = 8.9, 6.6 Hz, 1H), 2.75 – 2.91 (m, 8H), 2.02 – 2.14 (m, 4H), 1.81 – 1.93 (m, 1H), 1.61 – 1.74 (m, 3H), 1.42 – 1.52 (m, 2H), 1.05 (t, *J* = 7.3 Hz, 3H), 0.97 (t, *J* = 7.5 Hz, 3H), 0.88 (d, *J* = 6.6 Hz, 3H); **^{13}C NMR** (101 MHz, $CDCl_3$) δ 173.2, 152.8, 133.4, 132.2, 130.2, 129.0, 128.9 (2C), 128.7, 128.6, 128.4, 128.3, 128.1 (3C), 127.2, 125.8 (2C), 79.6, 79.4, 70.6, 54.7, 29.6, 27.1, 26.4, 26.3, 25.8 (3C), 25.7, 20.7, 14.7, 14.4, 10.1. **HRMS (ESI):** Exact mass calculated for $[M+Na]^+$: 556.3397, found : 556.3397.

The recorded ^{1}H NMR spectrum is in agreement with previously recorded ^{1}H NMR spectrum.[14] There is no recorded ^{13}C NMR available for this compound. The ^{13}C NMR data are in accordance with the structure.

(**2*R*,4*S*,5*R*)-diastereomer-18: HPLC analysis** (Eclipse XBD-C_{18}, MeOH/H_2O 90:10, 1.0 mL/min, t_r(major) = 43.19 min and t_r(minor) = 40.29 min. **Yield**: 0.0830 g (55 %); *de*: 98%; *dr*: 120:1; TLC (EtOAc/heptane 15:85, $KMnO_4$ stain and UV light) R_f = 0.27; $\boldsymbol{[\alpha]_D^{20}}$= -35.1 (c = 0.01, EtOH); **^{1}H NMR** (400 MHz, $CDCl_3$) δ 7.35 – 7.46 (m, 3H), 7.28 – 7.33 (m, 2H), 5.69 (d, *J* = 7.2 Hz, 1H), 5.23 – 5.48 (m, 10H), 4.92 – 4.98 (m, 1H), 4.77 (p, *J* = 6.7 Hz, 1H), 3.51 – 3.60 (m, 1H), 3.31 – 3.39 (m, 1H), 2.74 – 2.89 (m, 8H), 2.05 – 2.13 (m, 4H), 1.78 – 1.89 (m, 1H), 1.60 – 1.75 (m, 3H), 1.40 – 1.51 (m, 2H), 1.06 (t, *J* = 7.3 Hz, 3H), 0.92 – 1.00 (m, 6H); **^{13}C NMR** (101 MHz, $CDCl_3$) δ 173.4, 152.9, 133.2, 132.2, 130.2, 129.0, 128.9 (2C), 128.7, 128.6, 128.3(2C), 128.1 (3C), 127.2, 125.7 (2C), 79.6 (2C), 70.6, 55.3, 29.6, 27.1, 26.7, 26.2, 25.8 (3C), 25.7, 20.7, 14.7, 14.4, 10.3. **HRMS (ESI**): Exact mass calculated for $[M+Na]^+$: 556.3397, found: 556.3396.

The recorded ^{1}H NMR spectrum is in agreement with previously recorded ^{1}H NMR spectrum.[14] There is no recorded ^{13}C NMR available for this compound. The ^{13}C NMR data are in accordance with the structure.

4.2.7 Synthesis of EPA amide 19

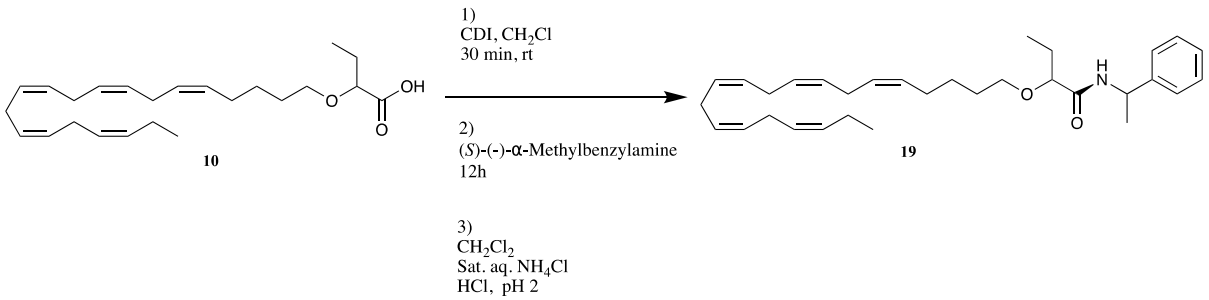

A solution of EPA acid **10** (25,7 mg, 0.0686 mmol, 1.0 equiv.) and CH_2Cl_2 (0.34 mL) was stirred, followed by addition of CDI (12.2 mg, 0.0754 mmol, 1.1 equiv.). After 30 minutes, (*S*)-(-)-alpha-methylbenzylamine (9.19 mL, 1.1 mmol, 1.1 equiv.) at room temperature. Then, CH_2Cl_2 (0.343 mL) was added after 12 h. Saturated aqueous NH_4Cl was added, followed by 2M HCl to acidify the mixture to pH 2. The organic phase and the aqueous phase were separated. Then, the aqueous phase was extracted with CH_2Cl_2 (3 x 0.5 mL). The organic layers were combined and dried over Na_2SO_4 and solvent were removed aqueous *in vacuo*. The crude product was purified by micro scale flash chromatography on silica gel increasing polarity (EtOAc:Heptane, 5:95 → 25:75). TLC (EtOAc/heptane 25:75, $KMnO_4$ stain) R_f = 0.39; **HRMS (ESI):** Exact mass calculated for $[M+Na]^+$: 500.3499, found: 500.3398.

The recorded NMR spectra were too complex too give any information.

4.2.8 Synthesis of *tert*-butyl 2-bromobutanoate (5)

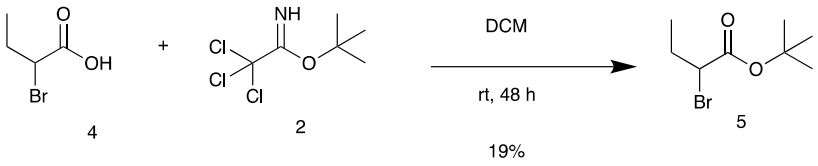

Trichloroacetimidate **(2)** (0.430 mL, 0.534 g, 2.40 mmol, 2 eq.) was dissolved in 0.25 M DCM (9.6 mL) in a flame-dried flask filled with argon. 2-bromobutanoic acid **(4)** (0.200 mg, 1.2 mmol, 1 eq.) was added to the mixture and stirred at room temperature. After 48 hours, the reaction was quenched by adding an aqueous solution of 2 M NaOH (8 mL). The mixture was extracted with DCM (3x10 mL). The organic layers were combined and dried over Na_2SO_4 and the solvent was removed aqueous *in vacuo* and the crude product was concentrated. The unsaturated *t*-butyl ester **5** was obtained. **Yield**: 0.049 g (19 %).

4.2.9 Attempt of synthesis of EPA acid (*R*)-10

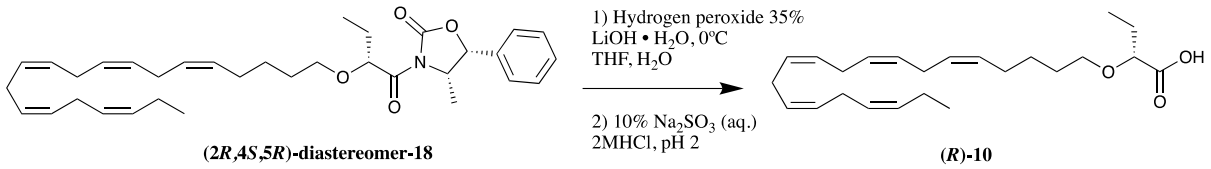

(2*R*,4*S*,5*R*)-diastereomer-18 **(*R*)-10**

The following procedure for synthesis of EPA acid **(*R*)-10** was described in a patent belonging to BASF AS in 2019.[14] A solution was made of **(2*R*,4*S*,5*R*)-diastereomer-18** (6.9 mg, 0.0129 mmol) in tetrahydrofuran (84 µL) and water (28 µL). The solution was held at 0°C under argon, when hydrogen peroxide (35% in water, 4.6 µL, 0.129 mmol) and lithium hydroxide monohydrate (1.05 mg, 0.0129 mmol) were added. For 30 minutes, the reaction mixture was stirred. Then, 10% Na_2SO_3 (aq.) (210 µL) was added. 2M HCl was added to adjust the pH to 2. Heptane (210 µL) was used to extract the mixture twice. The organic phases were combined and dried over Na_2SO_4, followed by filtration and concentration. The crude product was purified by micro scale flash chromatography on silica gel using gradient elution (Heptane:EtOAc, 98:2 → 50:50).

5 References

1. Y. Tian, M. Aursnes, T. V. Hansen, J. E. Tungen, J. D. Galpin, L. Leisle, C. A. Ahern, R. Xu, S. H. Heinemann and T. Hoshi, *PNAS USA*, 2016, **113**, 13905-13910.
2. D. R. Ferrier, in *Biochemistry Lippincott's illustrated reviews*, Wolters Kluwer, Philadelphia, 6th edn., 2014, pp. 181-182
3. P. M. Dewick, in *Medicinal natural products : a biosynthetic approach*, Wiley, Chichester, U.K., 3rd edn., 2009, pp. 39-53.
4. N. Siriwardhana, N. S. Kalupahana and N. Moustaid-Moussa, *Adv Food Nutr Res*, 2012, **65**, 211-222.
5. D. Fontaine, S. Figiel, R. Félix, S. Kouba, G. Fromont, K. Mahéo, M. Potier-Cartereau, A. Chantôme and C. Vandier, *J Lipid Res*, 2020, **61**, 840-858.
6. P. C. Calder and P. Yaqoob, *Postgrad Med*, 2009, **121**, 148-157.
7. G. Henderson, R. J. Flower, J. M. Ritter, M. M. Dale and H. P. Rang, *Journal*, 2016, 291.
8. D. Bhatnagar and F. Hussain, *Future Lipidol.*, 2007, **2**, 263-270.
9. T.-C. Su, J.-J. Hwang, K.-C. Huang, F.-T. Chiang, K.-L. Chien, K.-Y. Wang, M.-J. Charng, W.-C. Tsai, L.-Y. Lin, R. Vige, J. E. R. Olivar and C.-D. Tseng, *JAT*, 2017, **24**, 275-289.
10. M. Alves-Bezerra and D. E. Cohen, *Compr Physiol*, 2017, **8**, 1-8.
11. U.S. Food and Drug Administration; SPC for Omacor, https://www.accessdata.fda.gov/drugsatfda_docs/label/2004/21654lbl.pdf, (accessed 05.04.2021).
12. E. S. Kim and P. L. McCormack, *American journal of cardiovascular drugs : drugs, devices, and other interventions*, 2014, **14**, 471-478.
13. U.S. Food and Drug Administration; SPC for VASCEPA®, https://www.accessdata.fda.gov/drugsatfda_docs/label/2019/202057s035lbl.pdf, (accessed 14.04.2021, 2021).
14. H. H. Steineger, T. Skjæret, D. A. Fraser, PCT Int.Apl. 2019111048 A1, 2019
15. B. Alberts, Garland Science, New York, 3rd edn., 2010, pp. 387-407.
16. J. F. Cordero-Morales and V. Vásquez, *Curr. Opin. Struct. Biol.* , 2018, **51**, 92-98.
17. J. Teng, S. Loukin, A. Anishkin and C. Kung, *Pflügers Arch.*, 2015, **467**, 27-37.
18. F. Elinder and S. I. Liin, *Front Physiol*, 2017, **8**, 43-43.
19. J. E. Larsson, D. J. A. Frampton and S. I. Liin, *Frontiers in physiology*, 2020, **11**, 641-641.
20. H. Yang, G. Zhang and J. Cui, *Front Physiol*, 2015, **6**, 29-29.
21. B. Wang, Q. H. Chen and R. Brenner, in *Encyclopedia of Basic Epilepsy Research*, vol. 2, pp. 662-669.
22. F. Vetri, M. Saha Roy Choudhury, P. Sundivakkam and D. A. Pelligrino, *Journal of receptor, ligand and channel research*, 2014, **7**, 3.
23. A. S. Kshatri, A. Gonzalez-Hernandez and T. Giraldez, *Frontiers in molecular neuroscience*, 2018, **11**, 258-258.
24. U. S. Lee and J. Cui, *Trends Neurosci*, 2010, **33**, 415-423.
25. J. C. Sheehan and G. P. Hess, *J. Am. Chem. Soc*, 1955, **77**, 1067-1068.

26. G. T. Hermanson, San Diego: Elsevier Science & Technology, San Diego, 2013, pp. 267-268.
27. D. C. Hobbs and A. R. English, *J Med Pharm Chem*, 1961, **4**, 207-210.
28. D. R. Klein, *Organic Chemistry*, Wiley, Hoboken, N.J, 2nd ed. edn., 2015.
29. G. P. Moss, *Pure and applied chemistry*, 1996, **68**, 2193-2222.
30. M. M. Heravi, V. Zadsirjan and B. Farajpour, *RSC Adv.* , 2016, **6**, 3498-3551.
31. D. A. Evans, J. Bartroli and T. L. Shih, *J. Am. Chem. Soc*, 1981, **103**, 2127-2129.
32. B. Neises and W. Steglich, *Angew. Chem. Int. Ed. Engl*, 1978, **17**, 522-524.
33. T. Itoh, A. Tomiyasu and K. Yamamoto, *Lipids*, 2011, **46**, 455-461.
34. M. K. Pangopoulos, Y. Stenstrøm and T. V. Hansen, *Journal*, 2016, 26-58.
35. C. M. Starks, *J. Am. Chem. Soc*, 1971, **93**, 195-199.
36. M. G. Jakobsen, A. Vik and T. V. Hansen, *Tetrahedron Lett.*, 2012, **53**, 5837-5839.
37. S. J. R. Johansson, T. Johannessen, C. F. Ellefsen, M. S. Ristun, S. Antonsen, T. V. Hansen, Y. Stenstrøm and J. M. J. Nolsøe, *Synlett*, 2019, **30**, 213-217.
38. N. S. Mahajani, R. I. L. Meador, T. J. Smith, S. E. Canarelli, A. A. Adhikari, J. P. Shah, C. M. Russo, D. R. Wallach, K. T. Howard, A. M. Millimaci and J. D. Chisholm, *J. Org. Chem*, 2019, **84**, 7871-7882.

6 Appendix

6.1 $^{1}H^{-}$ and ^{13}C- NMR spectra of the synthesized compounds

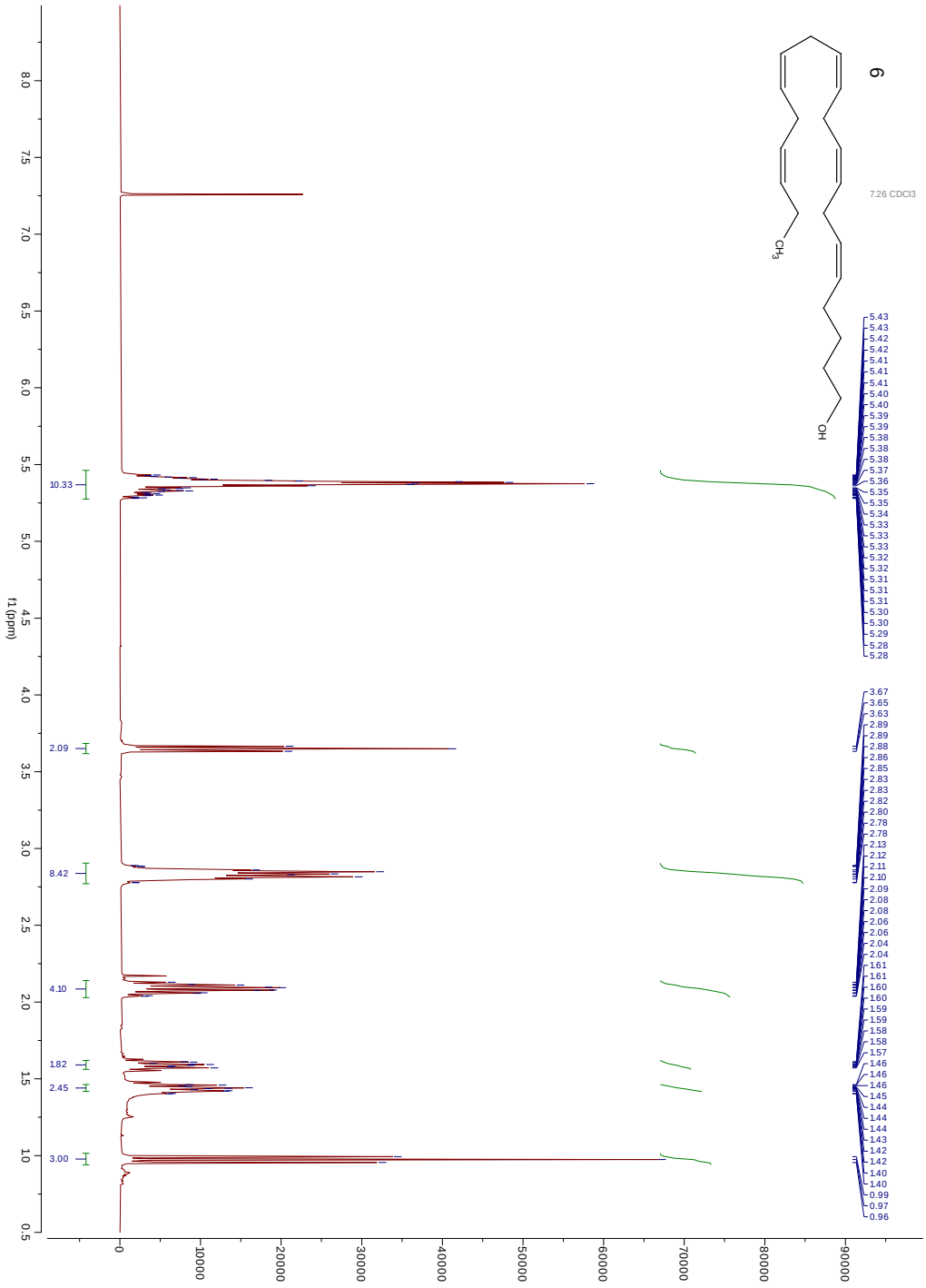

Figure 6.1: ^{1}H NMR spectrum of compound **6.**

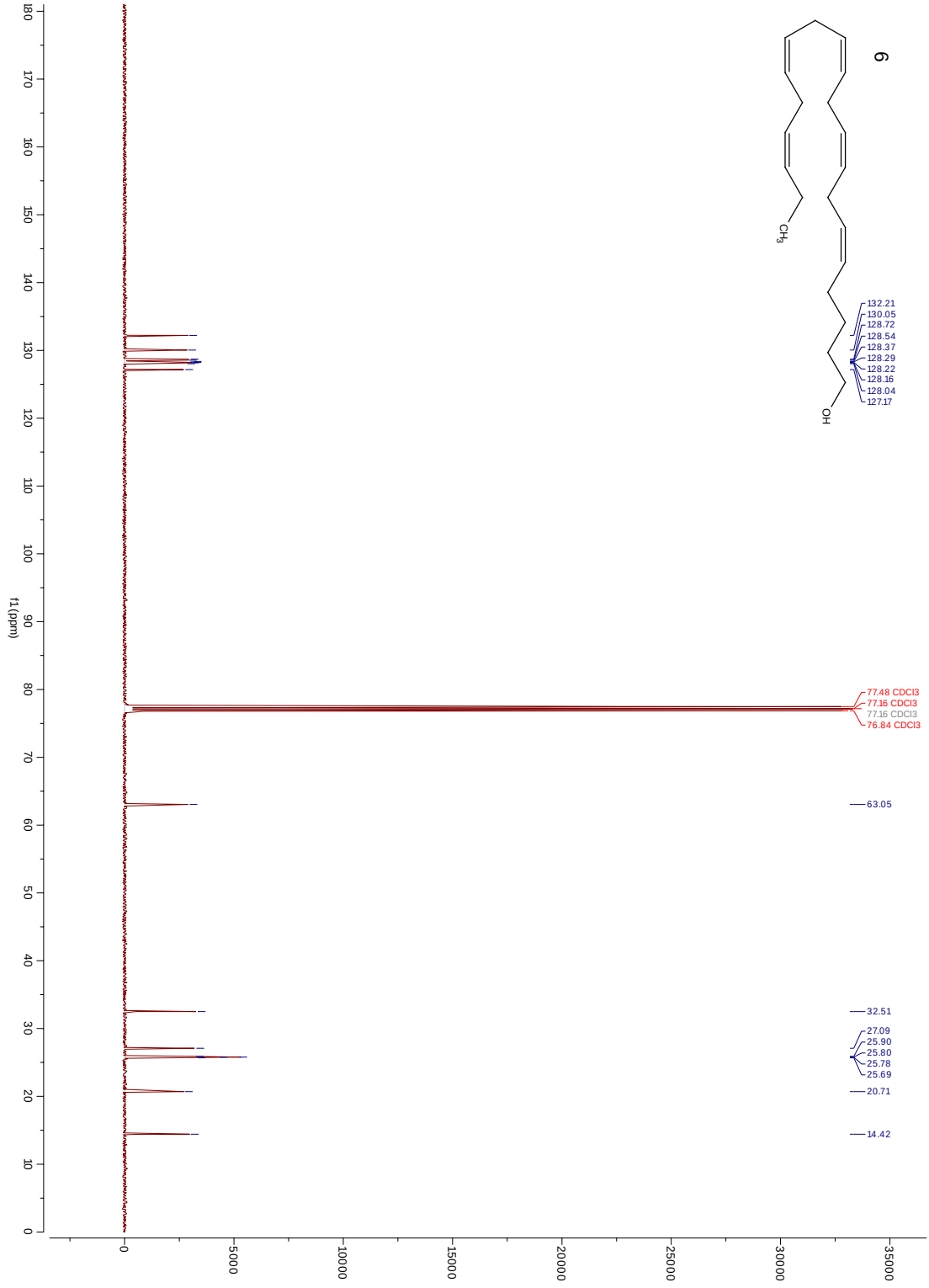

Figure 6.2: ^{13}C NMR spectrum of compound **6**

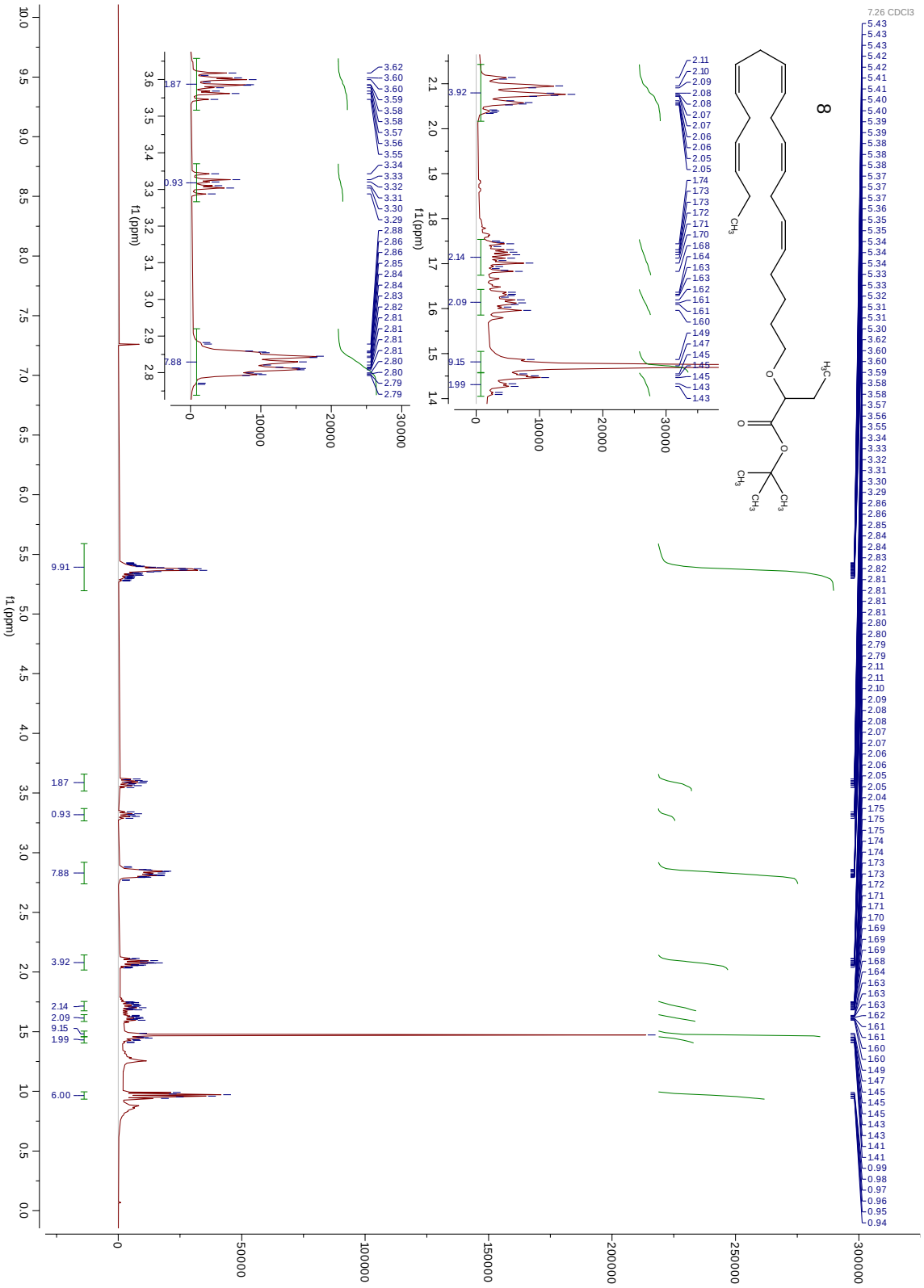

Figure 6.3: ^{1}H NMR spectrum of compound **8.**

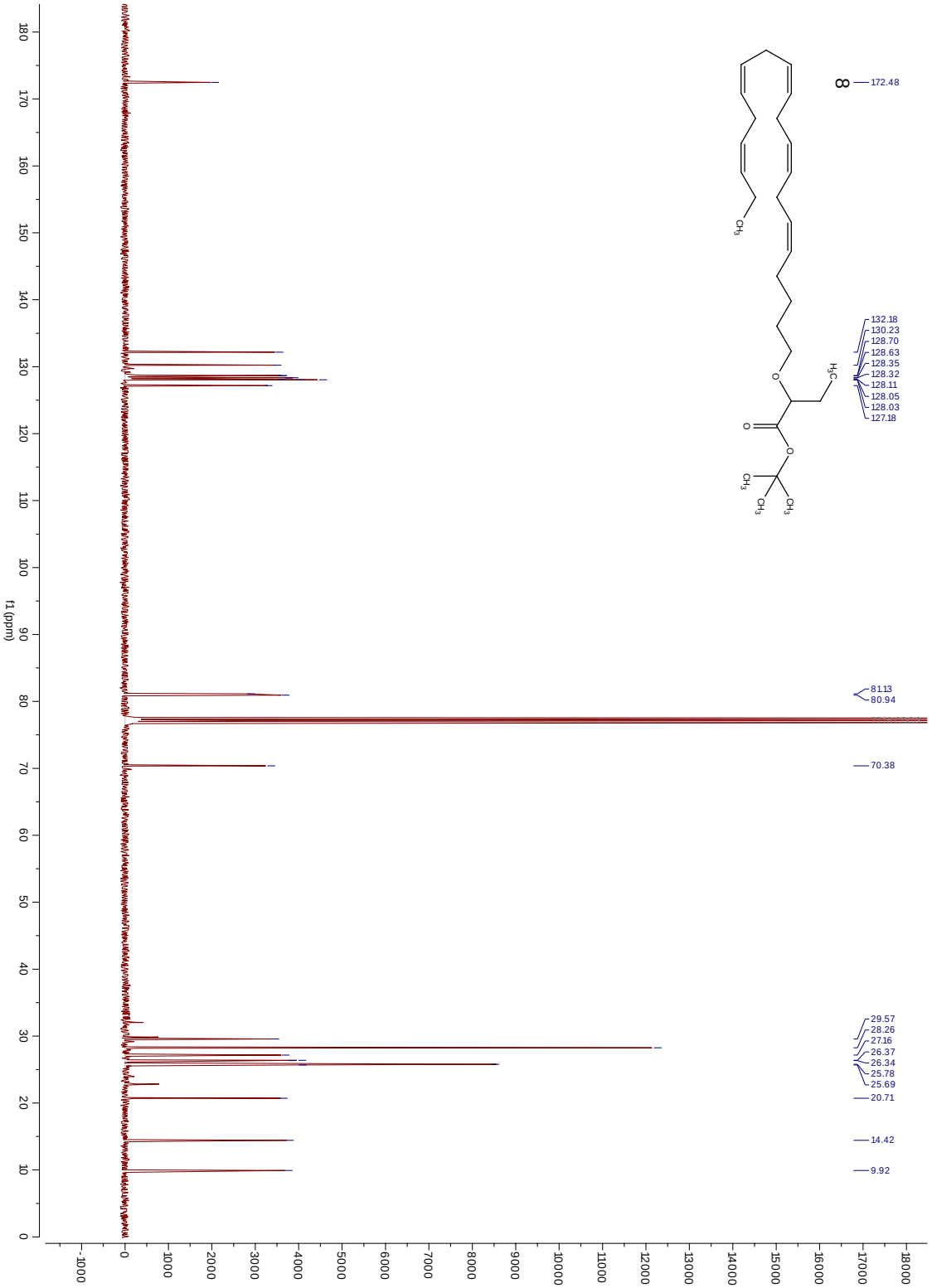

Figure 6.4: ^{13}C NMR spectrum of compound **8.**

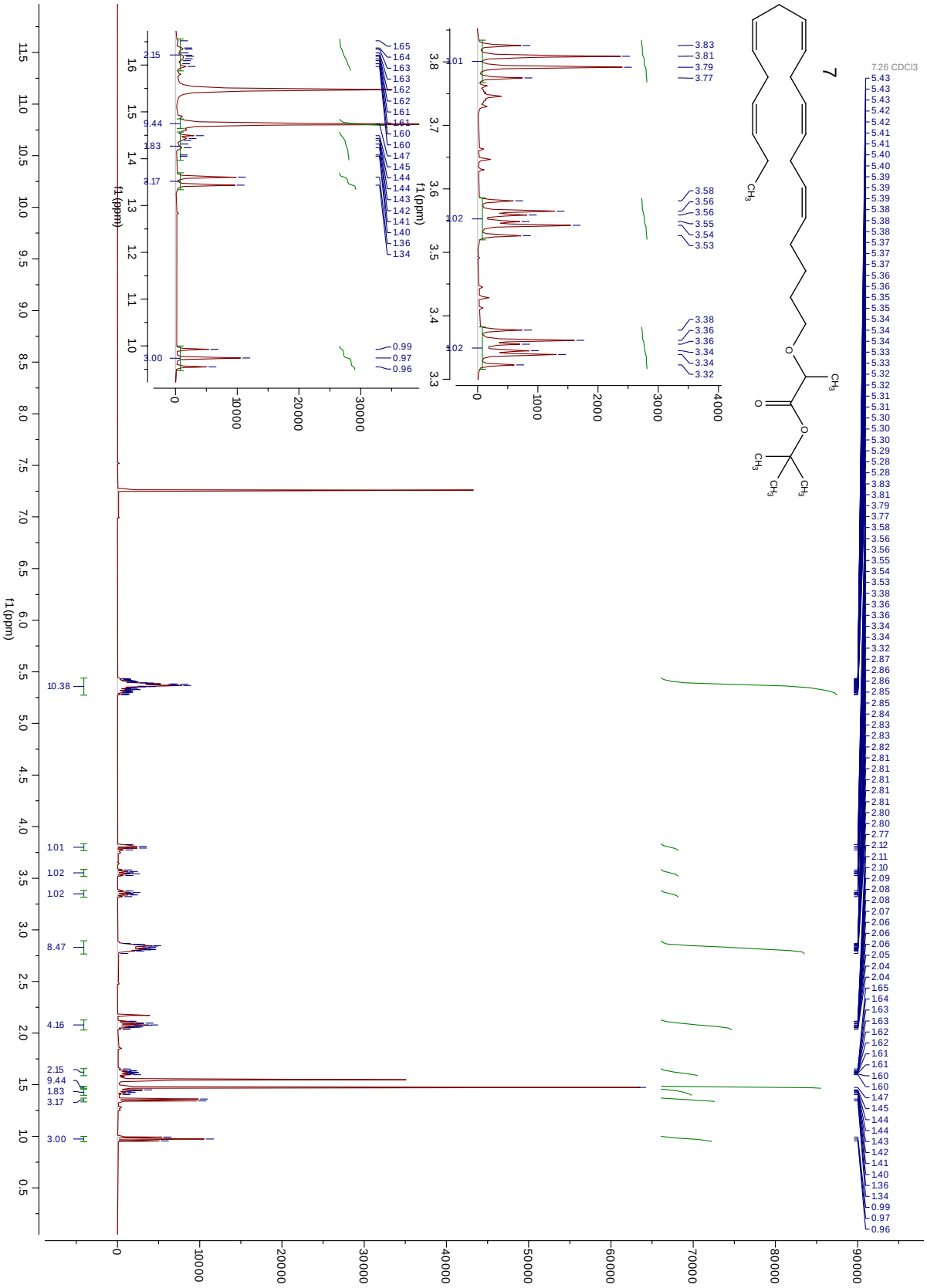

Figure 6.5: ^{1}H NMR spectrum of compound **7.**

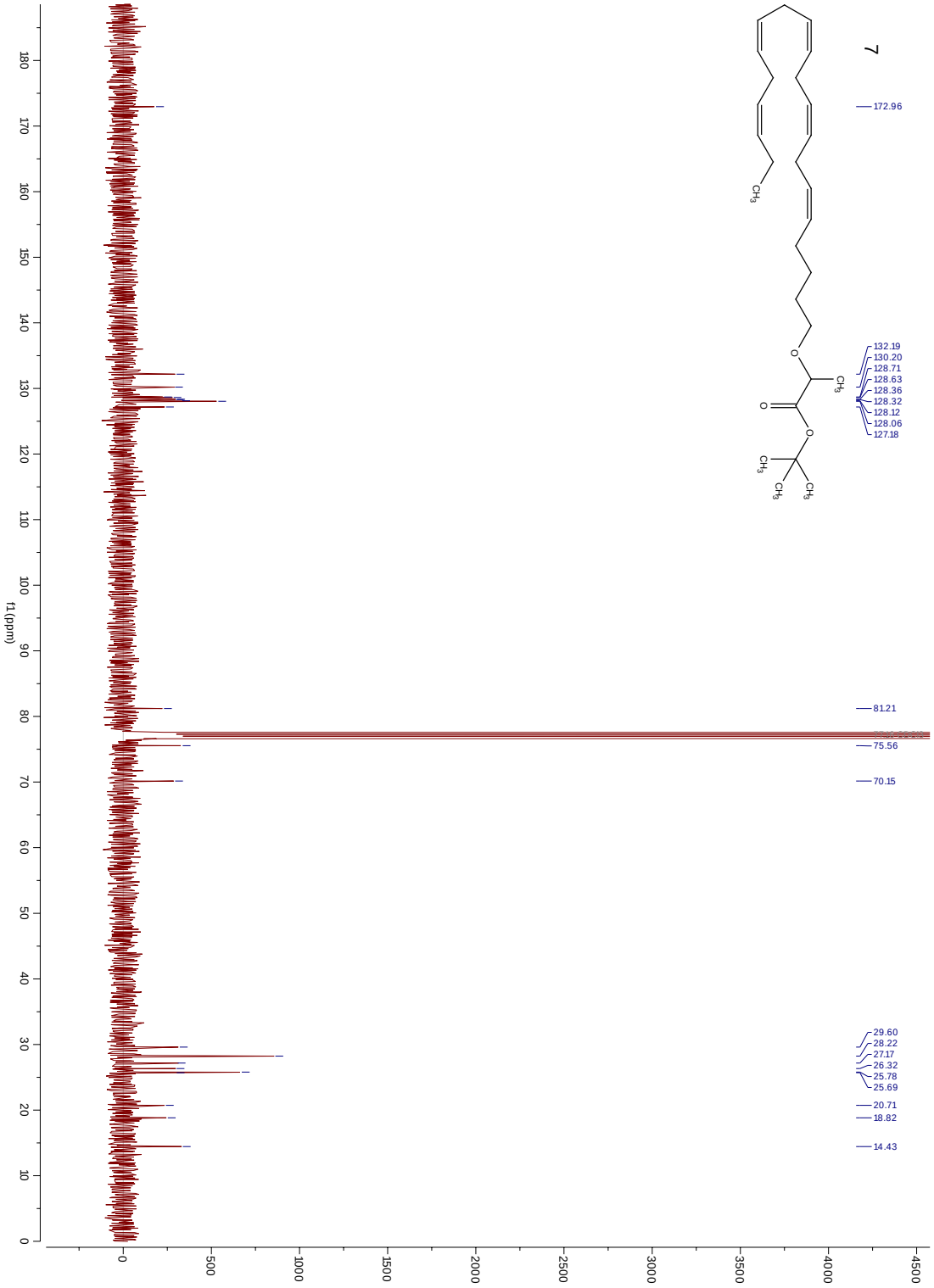

Figure 6.6: ^{13}C NMR spectrum of compound **7**

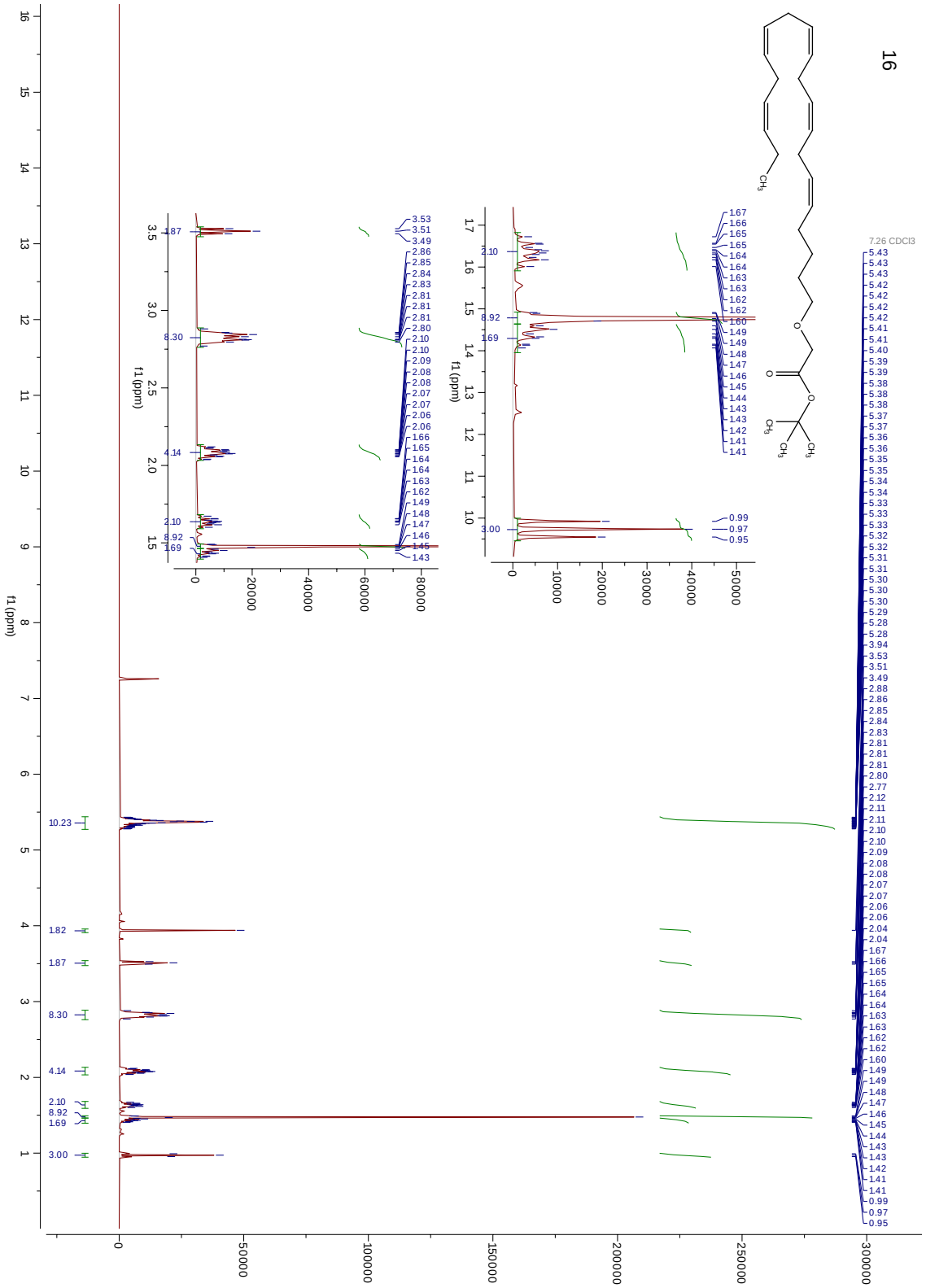

Figure 6.7: ^{1}H NMR spectrum of compound **16.**

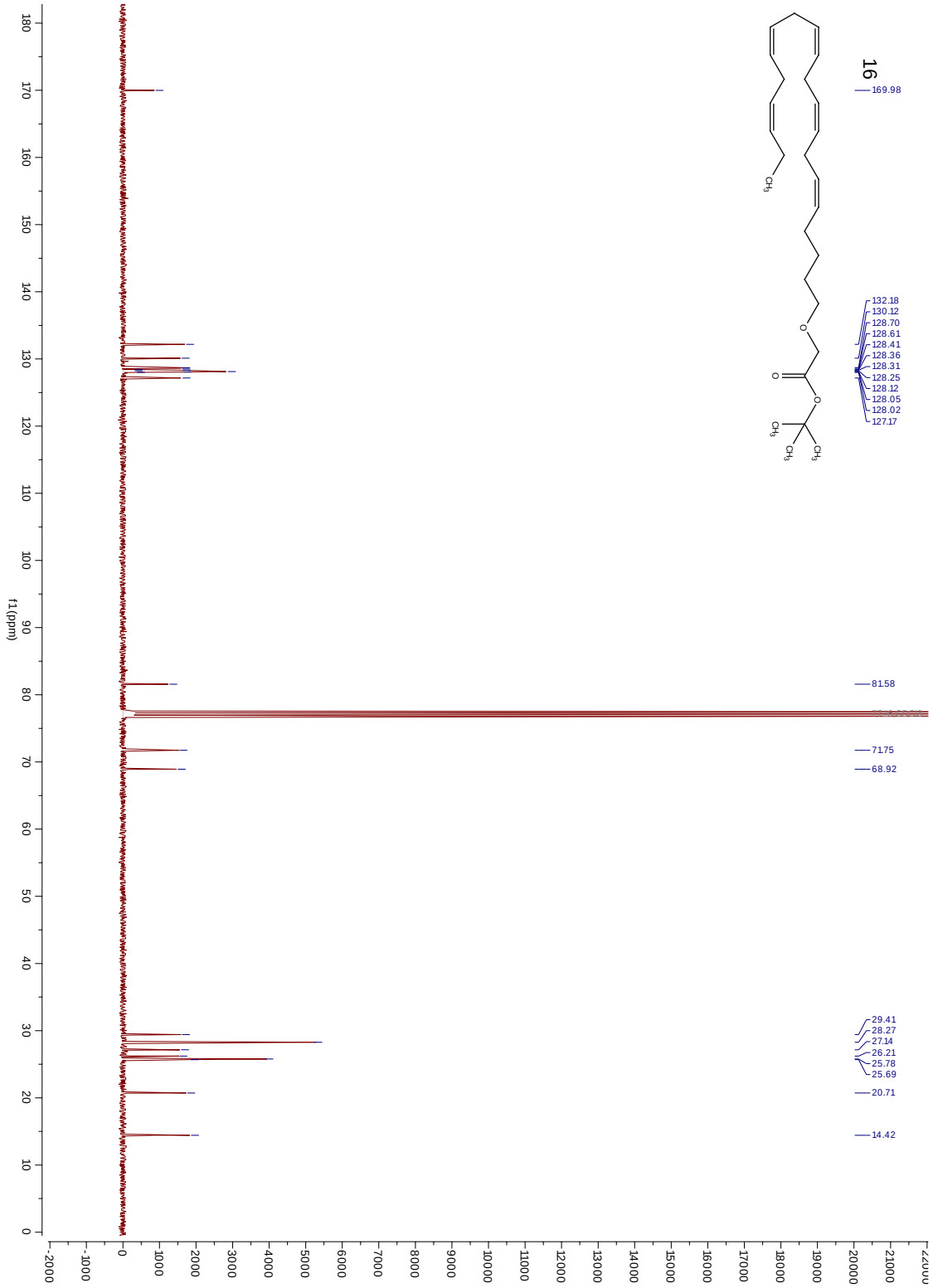

Figure 6.8: ^{13}C NMR spectrum of compound **16.**

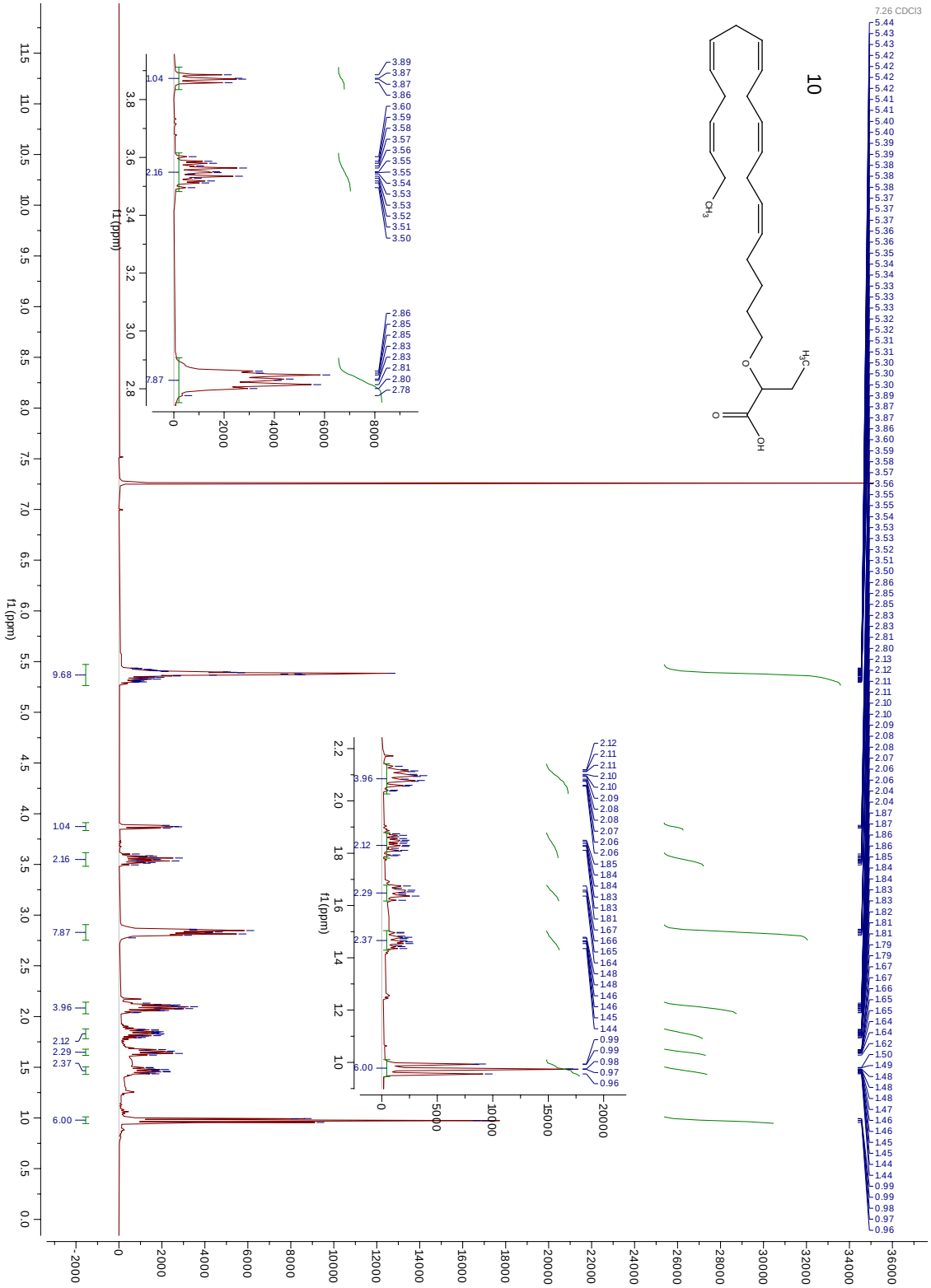

Figure 6.9: ^{1}H NMR spectrum of compound **10.**

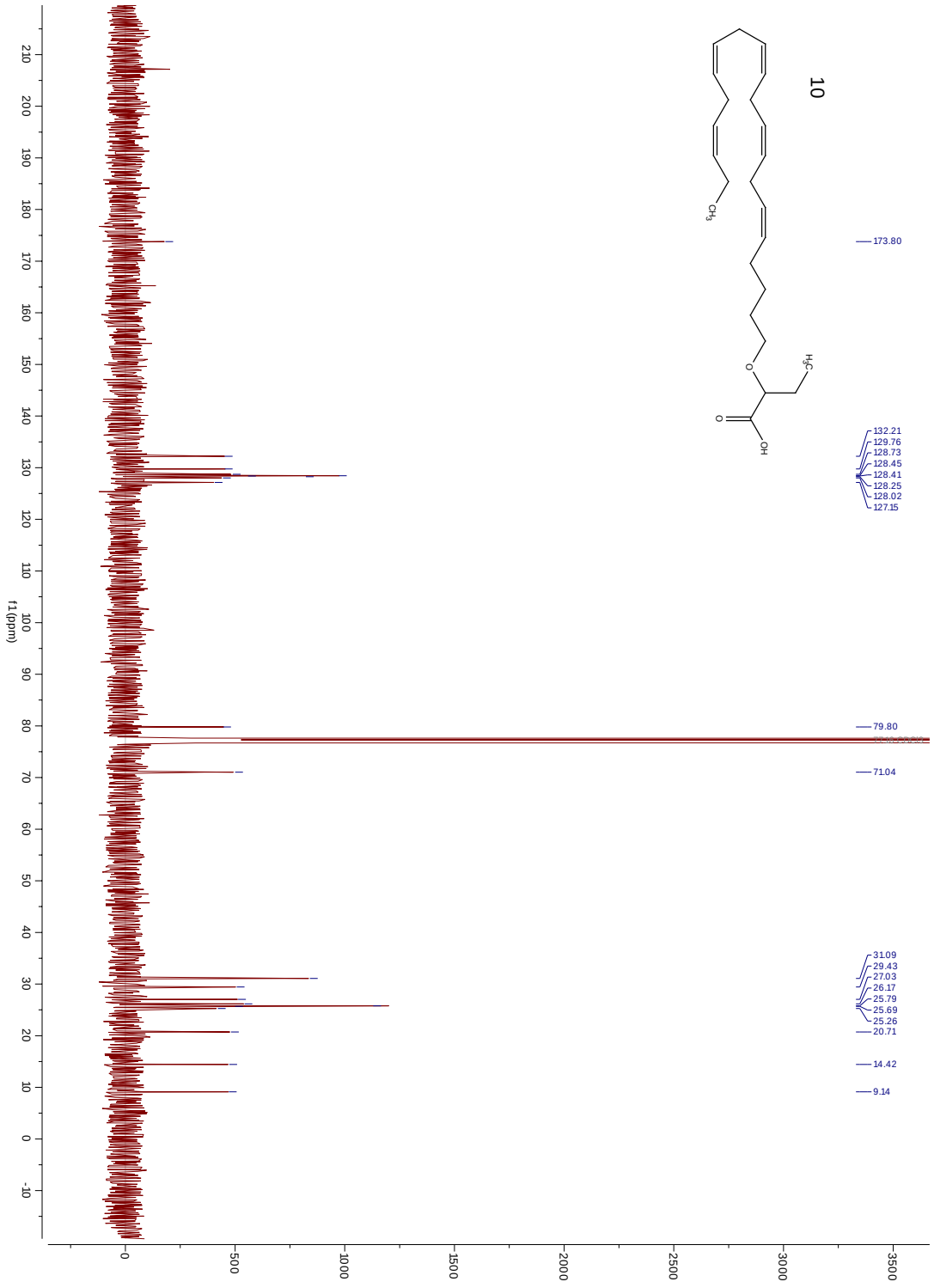

Figure 6.10: ^{13}C NMR spectrum of compound **10.**

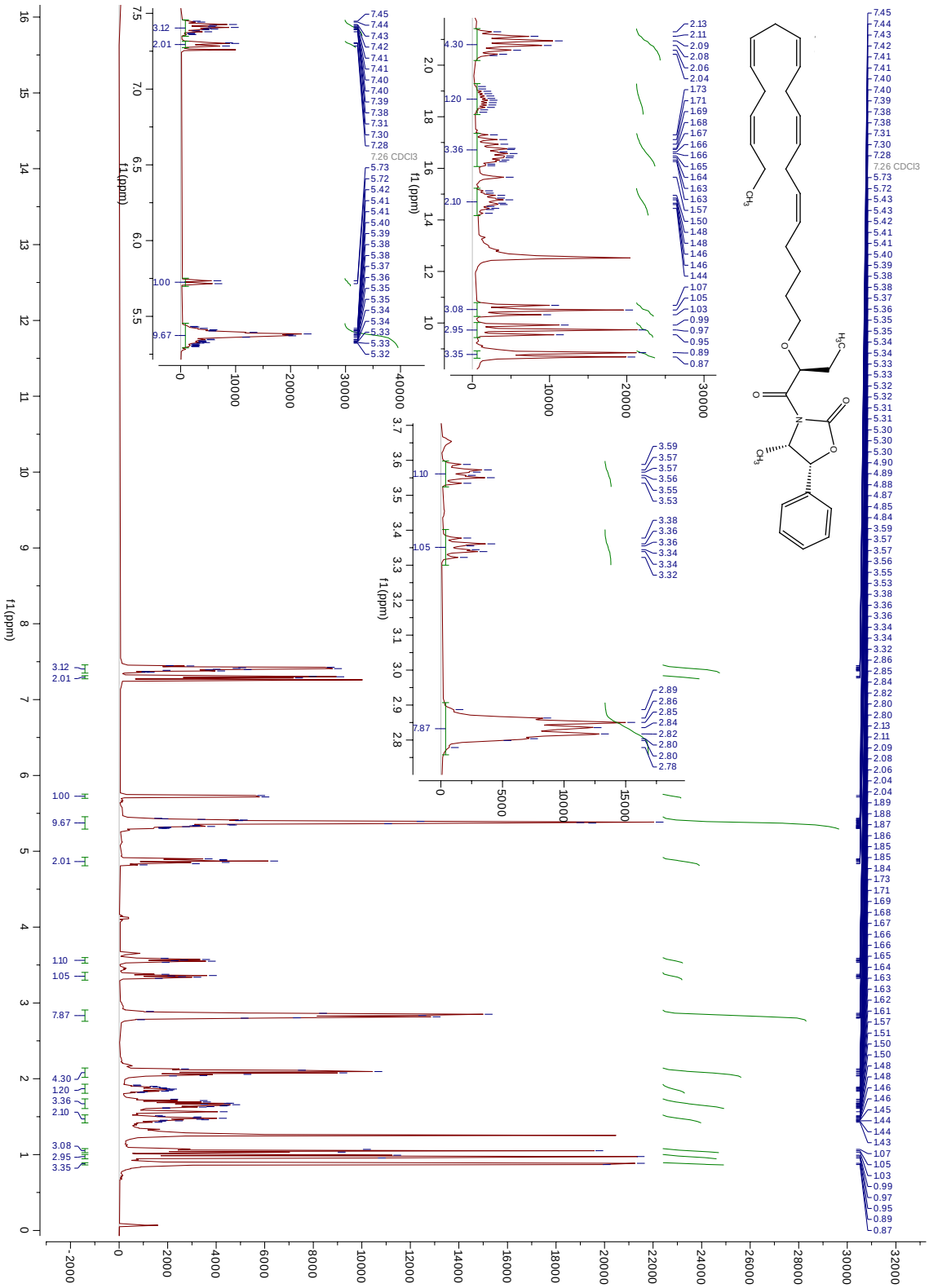

Figure 6.11: ^{1}H NMR spectrum of compound **(2*S*,4*S*,5*R*)-diastereomer-17**

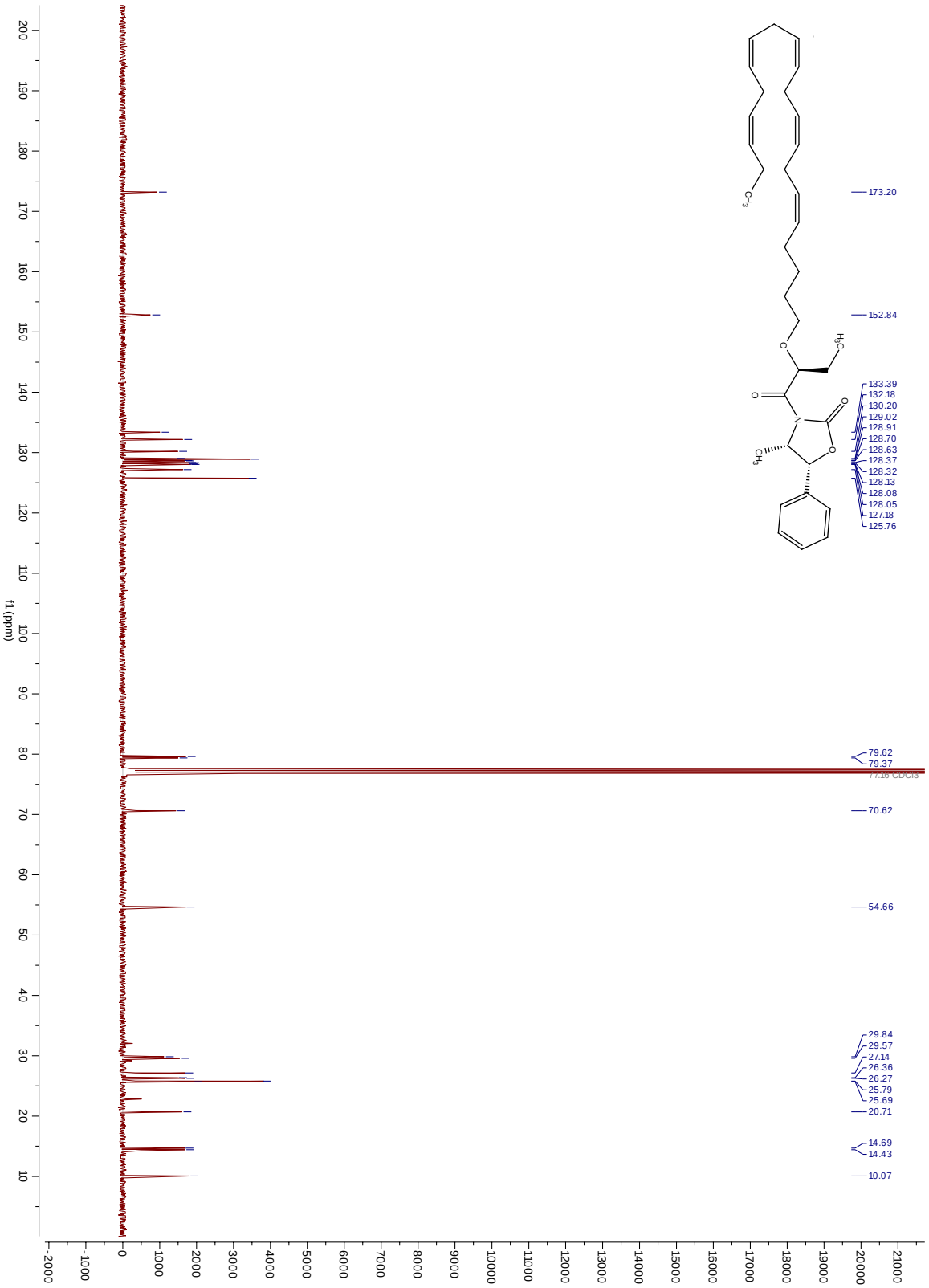

Figure 6.12: ^{13}C NMR spectrum of compound **(2*S*,4*S*,5*R*)-diastereomer-17.**

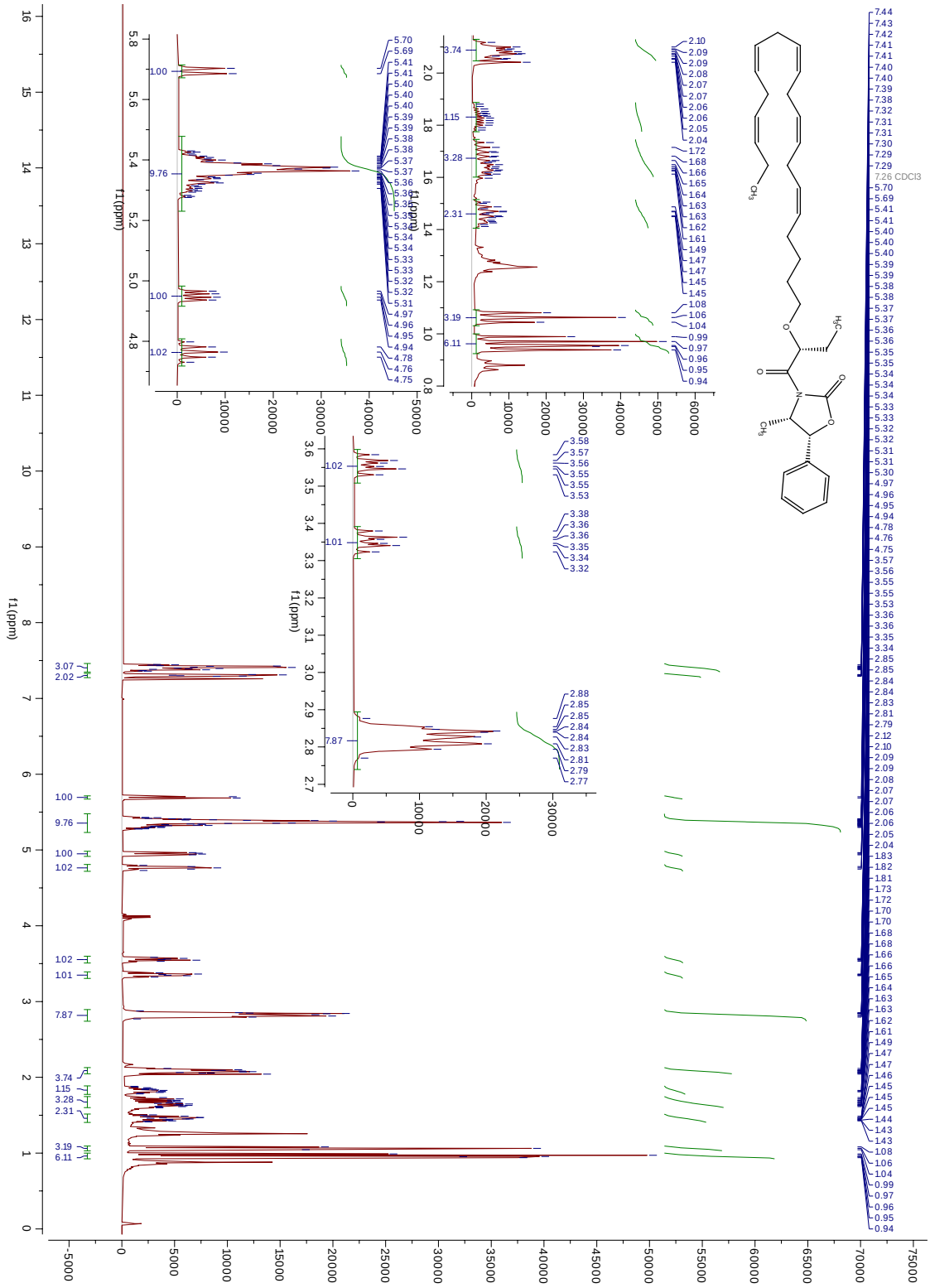

Figure 6.13: ^{1}H NMR spectrum of compound **(2*R*,4*S*,5*R*)-diastereomer-18**

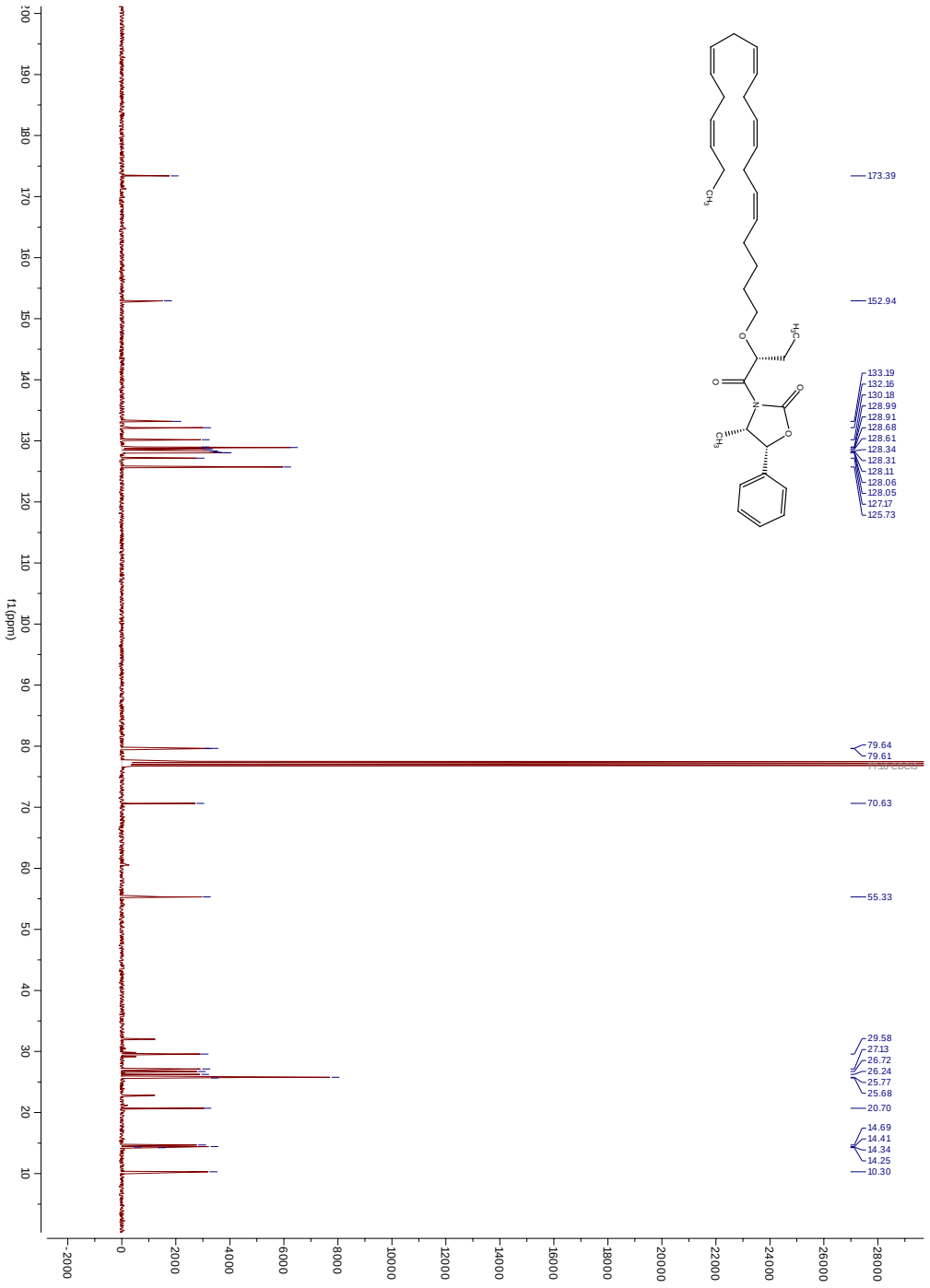

Figure 6.14: ^{13}C NMR spectrum of compound **(2*R*,4*S*,5*R*)-diastereomer-18**

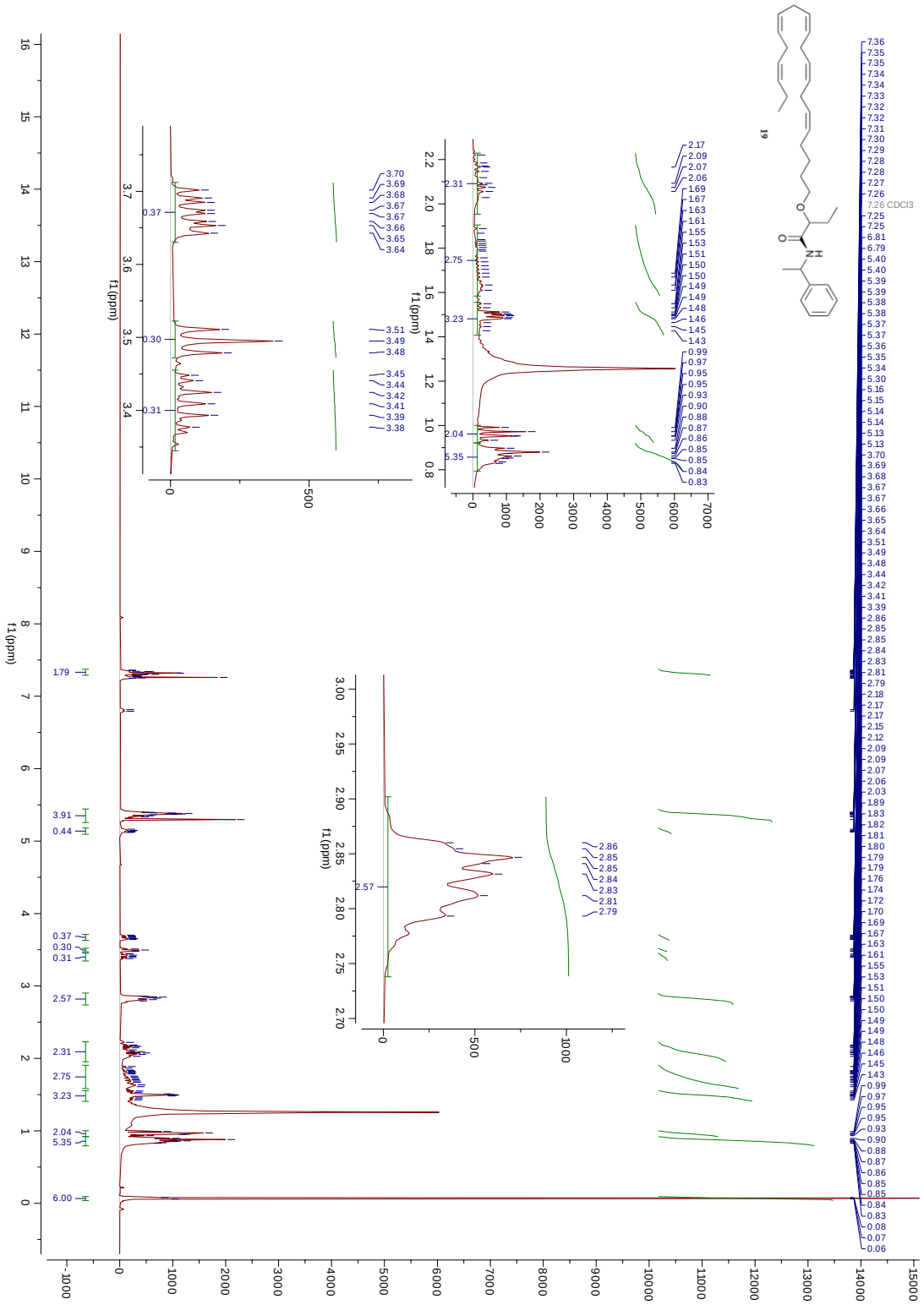

Figure 6.15: ^{1}H NMR spectrum of compound **19.**

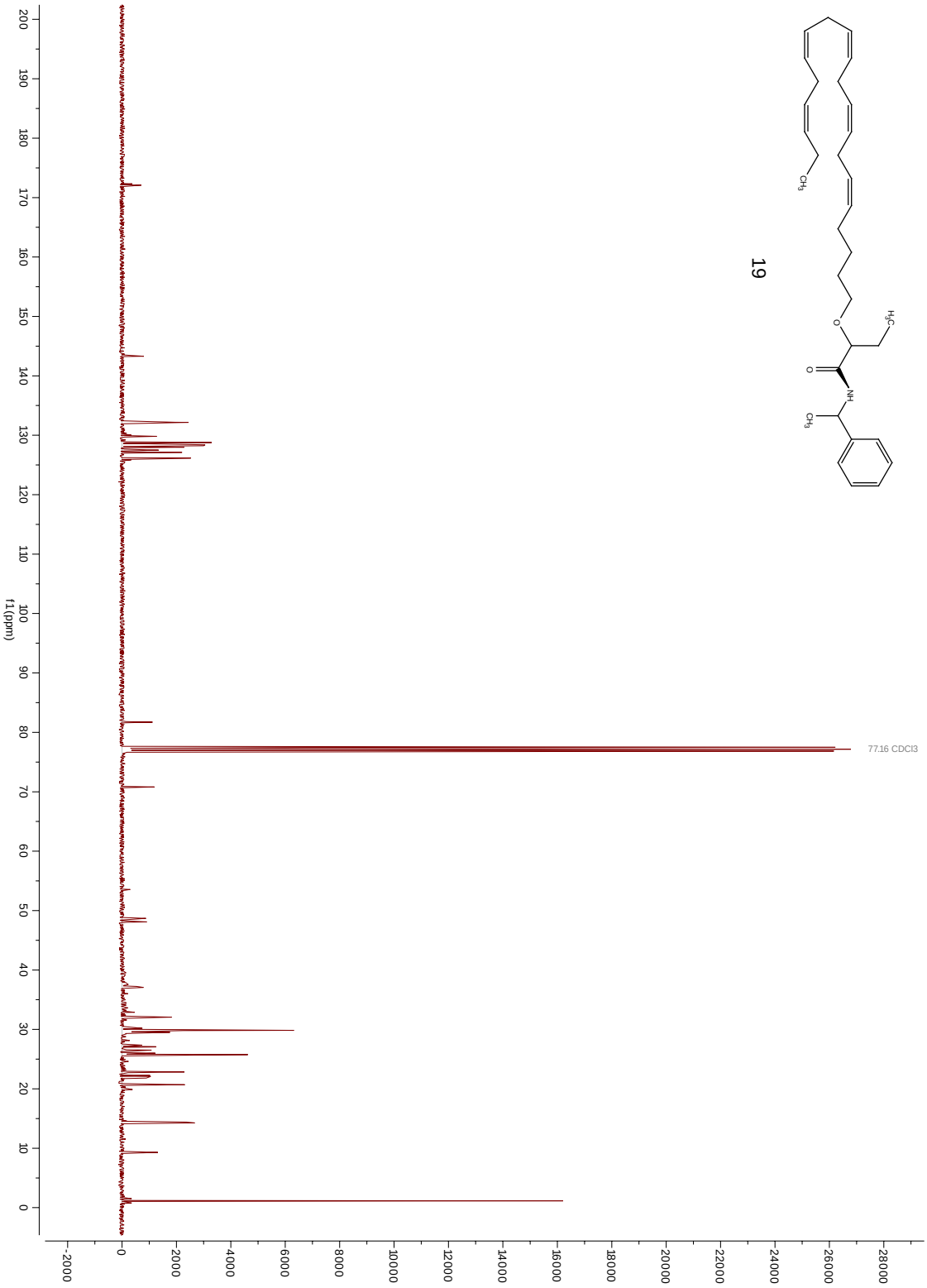

Figure 6.16: ^{13}C NMR spectrum of compound **19**.

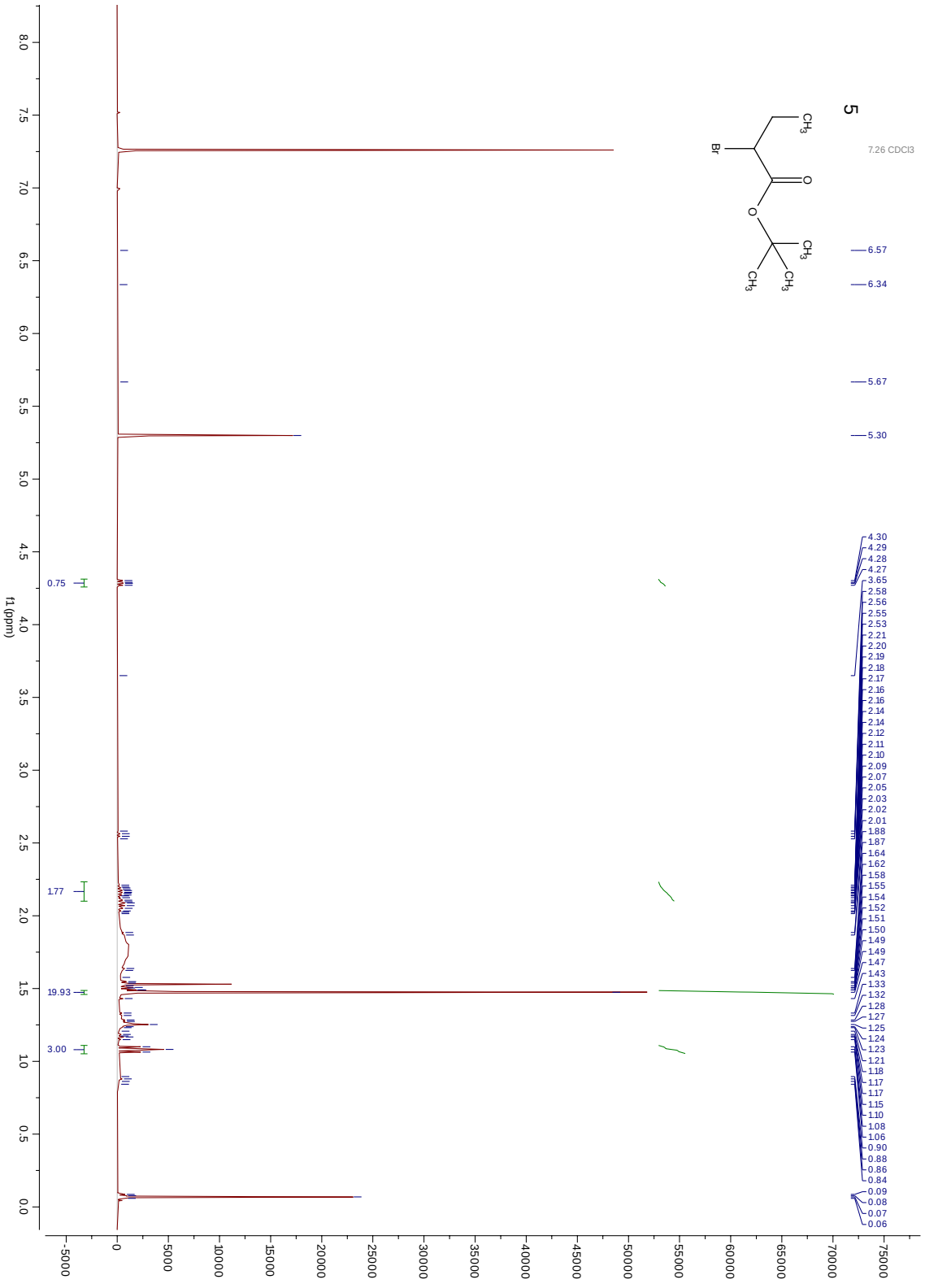

Figure 6.17: ^{1}H NMR spectrum of compound **5.**

6.2 MS- and HRMS spectra of synthesized compounds

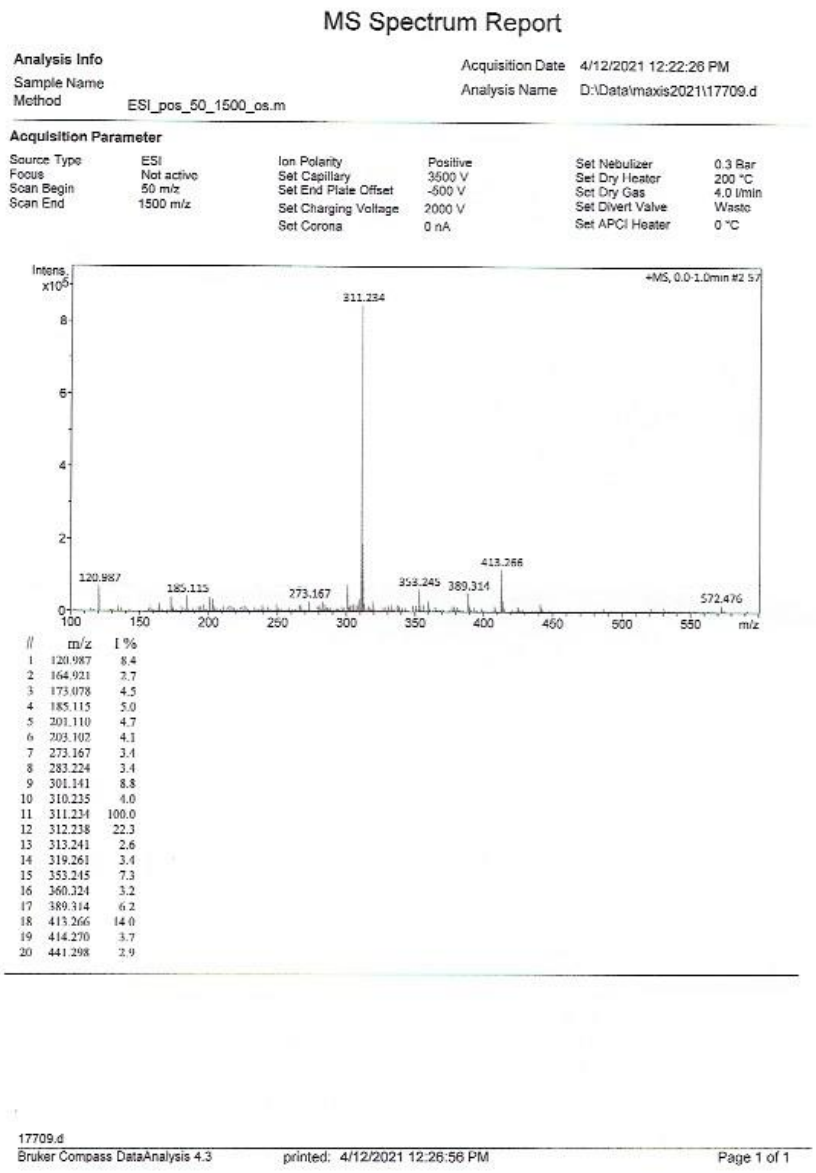

#	m/z	I %
1	120.987	8.4
2	164.921	3.7
3	173.078	4.5
4	185.115	5.0
5	201.110	4.7
6	203.102	4.1
7	273.167	3.4
8	283.224	3.4
9	301.141	8.8
10	310.235	4.0
11	311.234	100.0
12	312.238	22.3
13	313.241	2.6
14	319.261	3.4
15	353.245	7.3
16	360.324	3.2
17	389.314	6.2
18	413.266	14.0
19	414.270	3.7
20	441.298	2.9

Figure 6.18 MS spectrum of compound **6.**

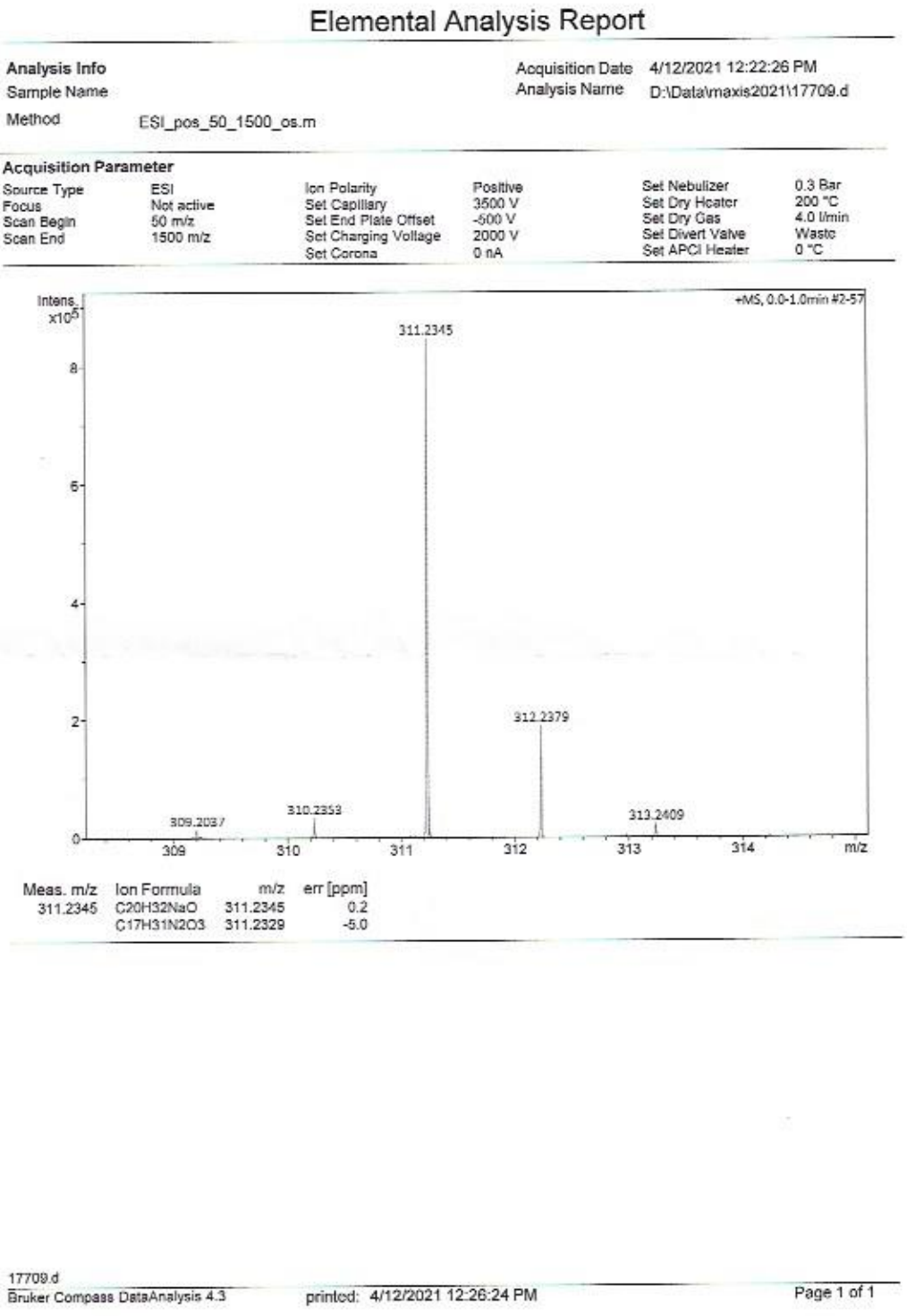

Figure 6.19 HRMS spectrum of compound **6.**

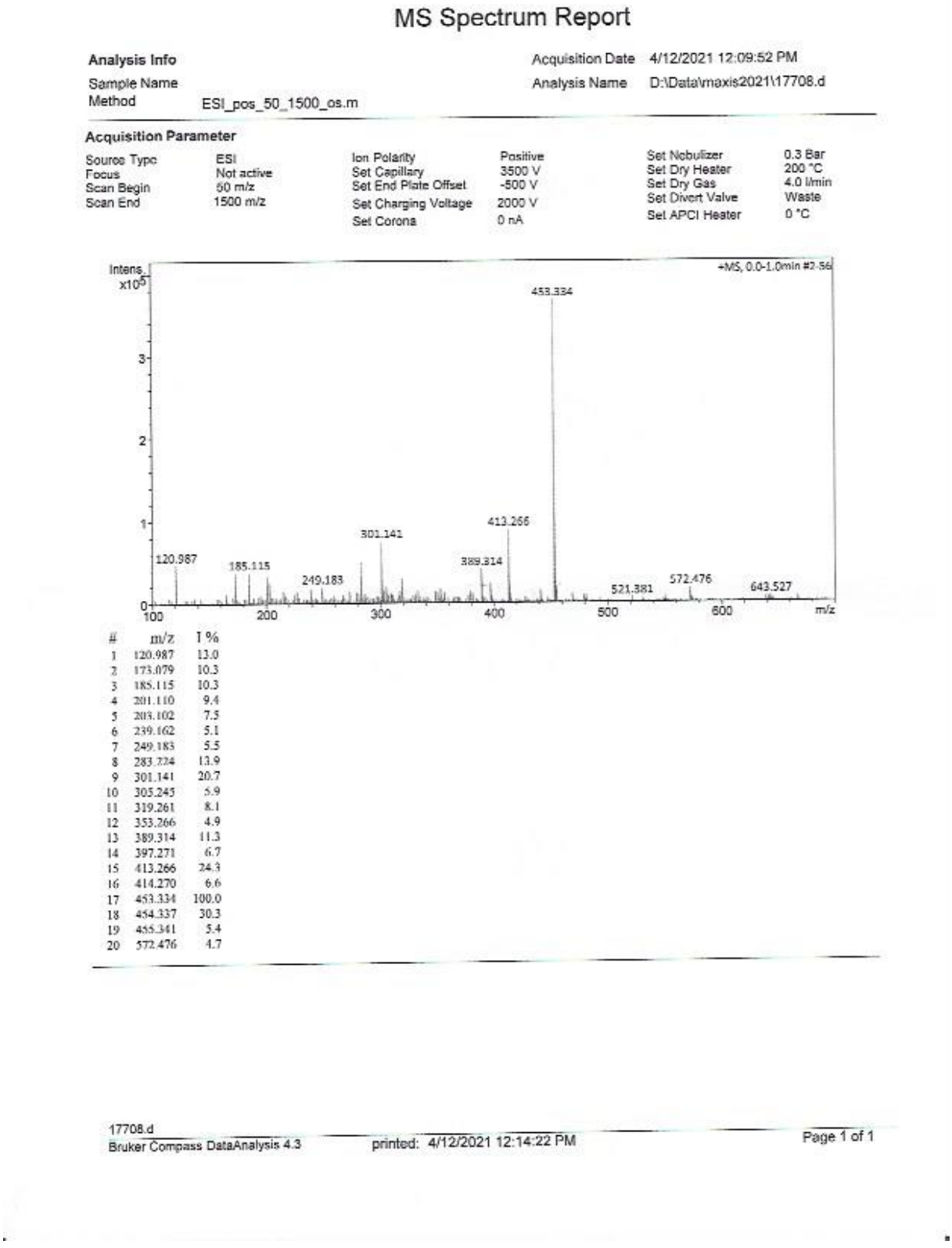

Figure 6.20 MS spectrum of compound **8.**

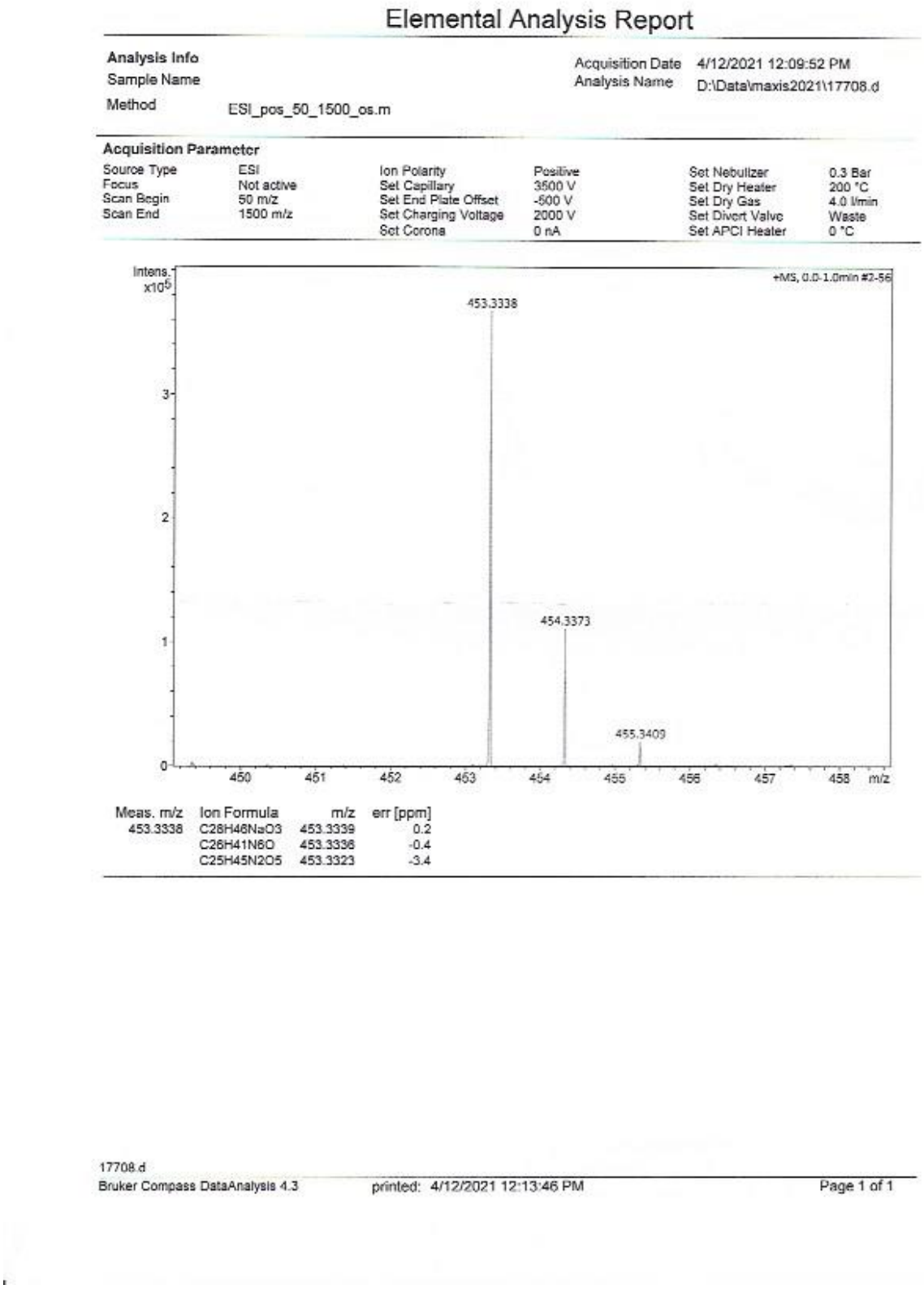

Figure 6.21 HRMS spectrum of compound **8.**

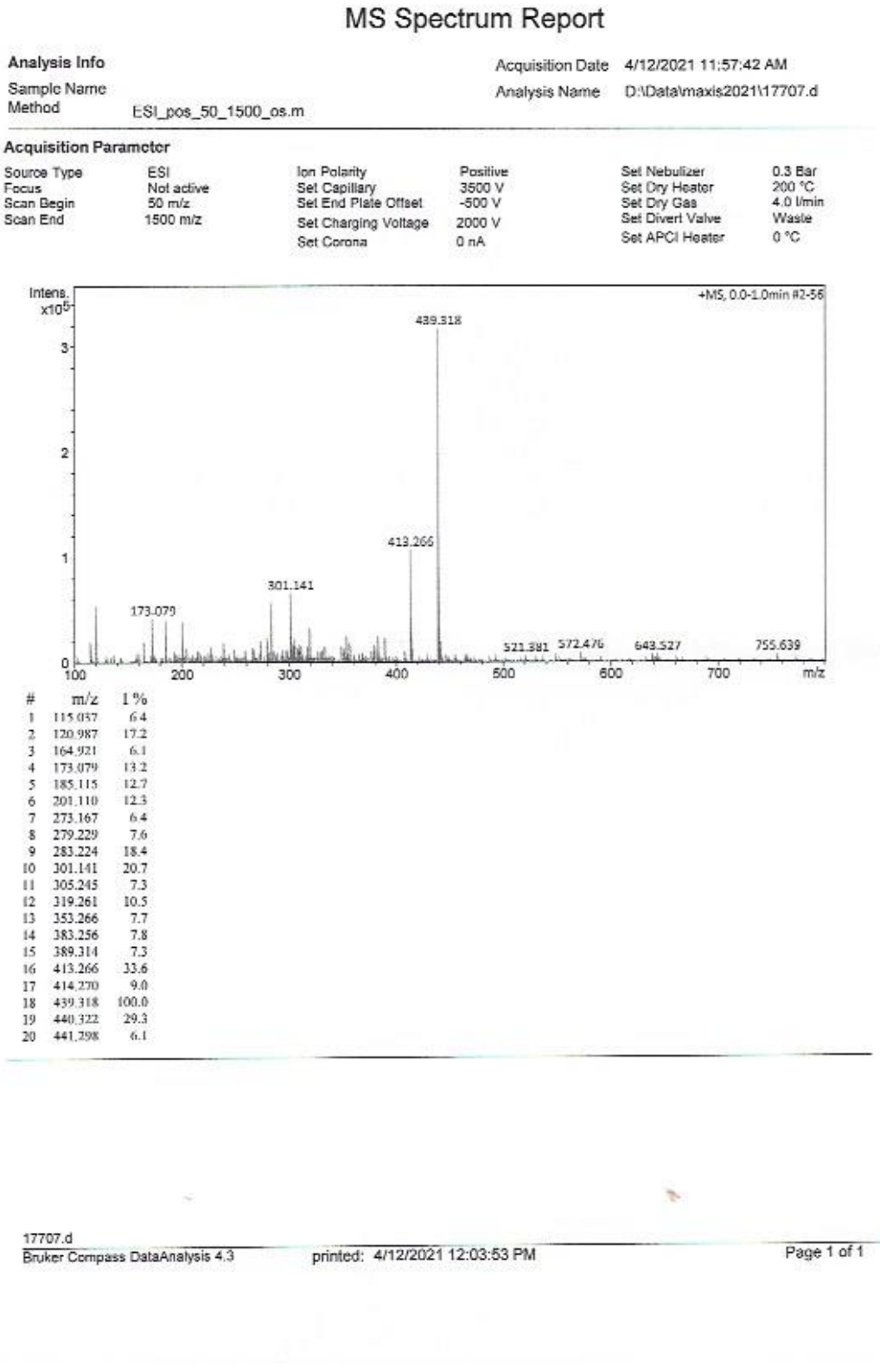

Figure 6.22 MS spectrum of compound **7.**

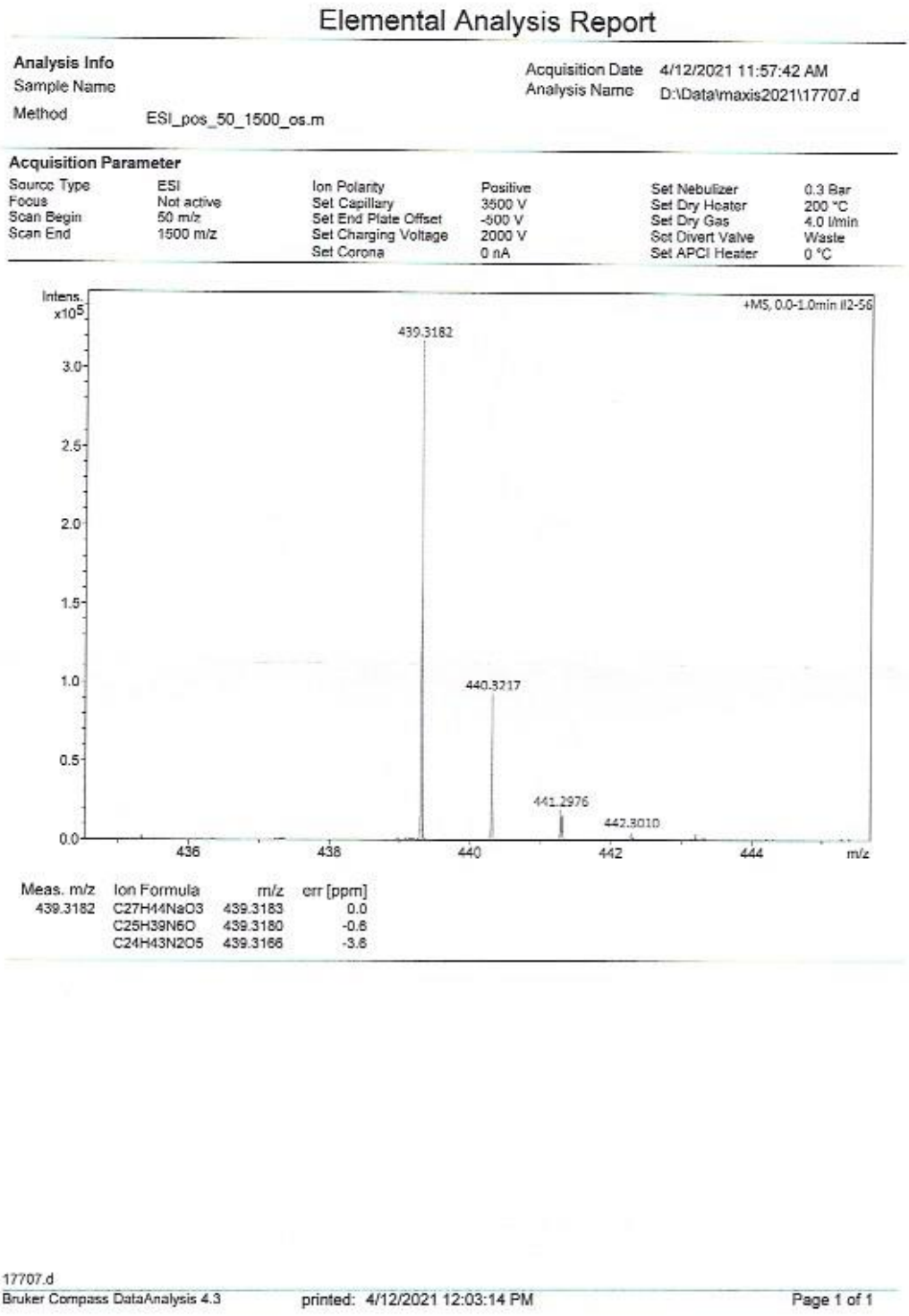

Figure 6.23 HRMS spectrum of compound **7.**

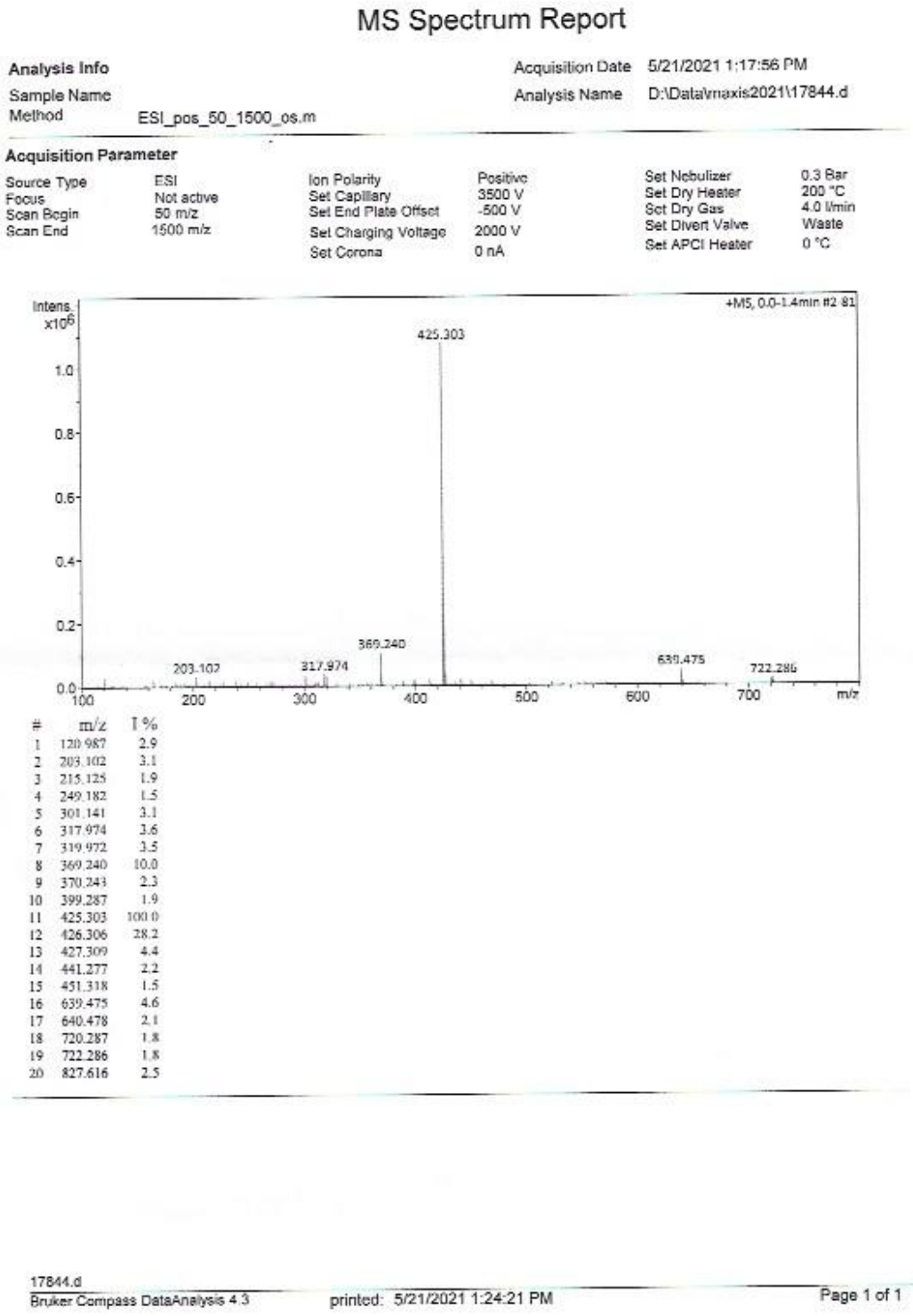

Figure 6.24 MS spectrum of compound **16.**

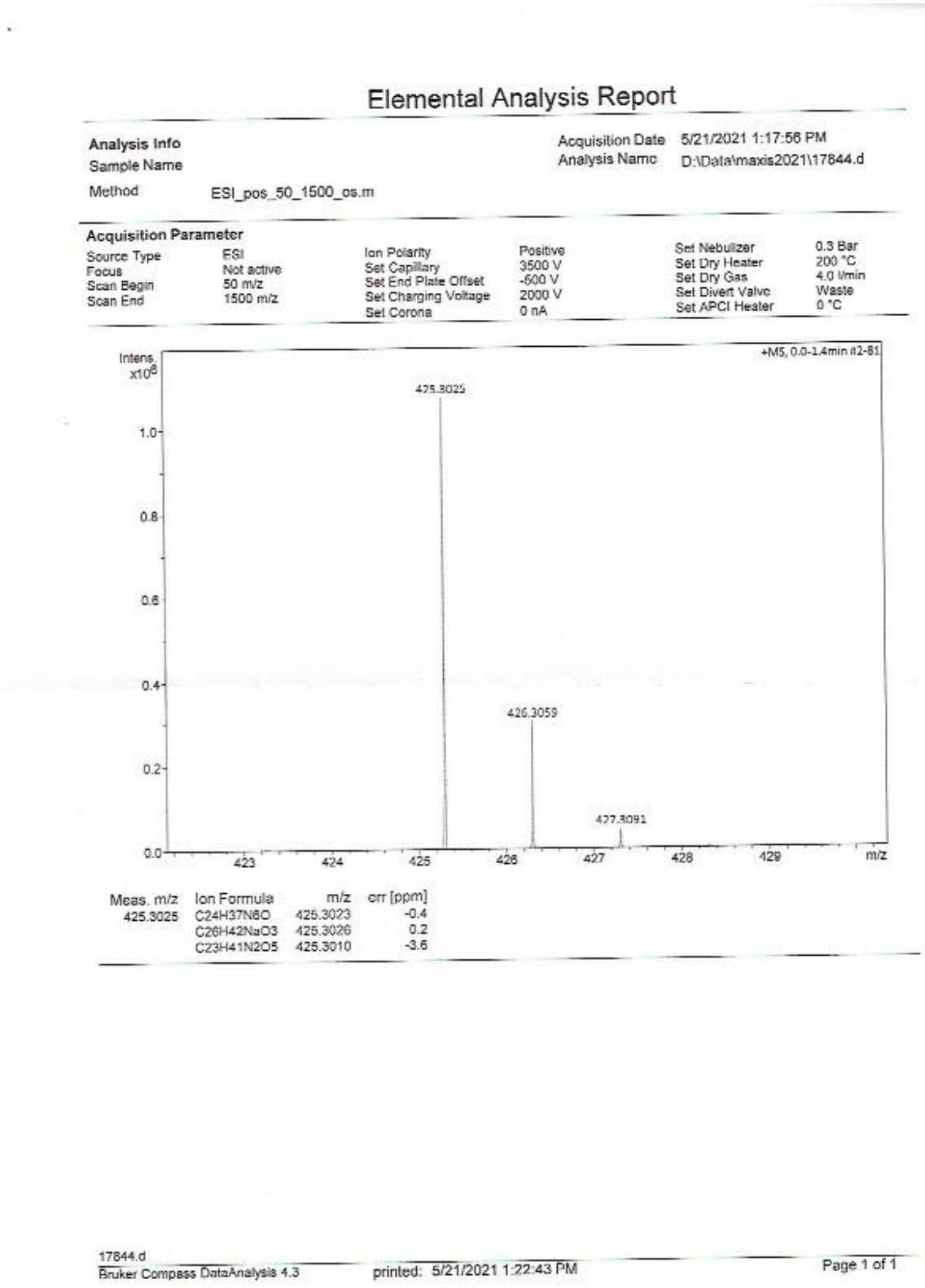

Figure 6.25 HRMS spectrum of compound **16.**

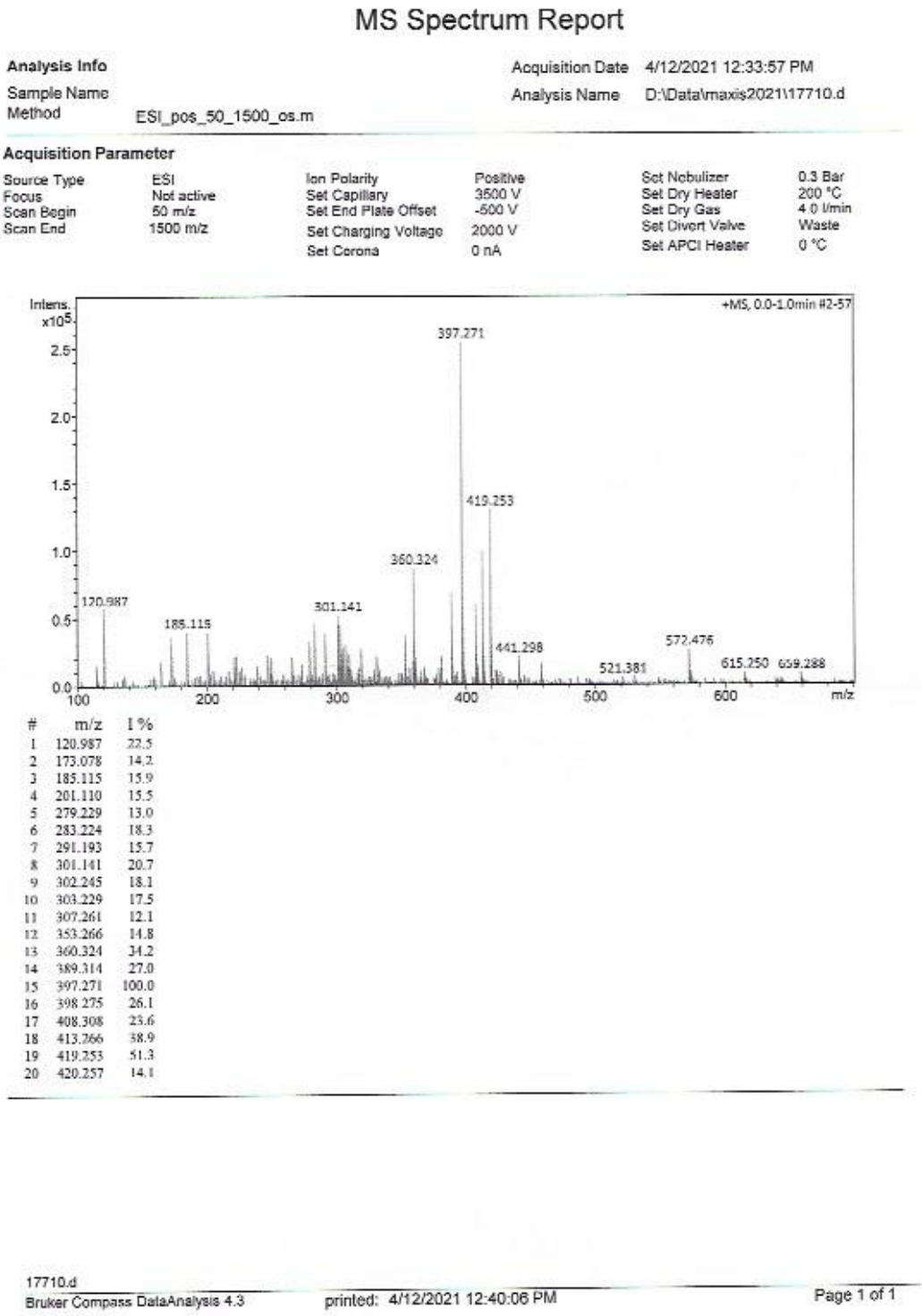

Figure 6.26 MS spectrum of compound **10.**

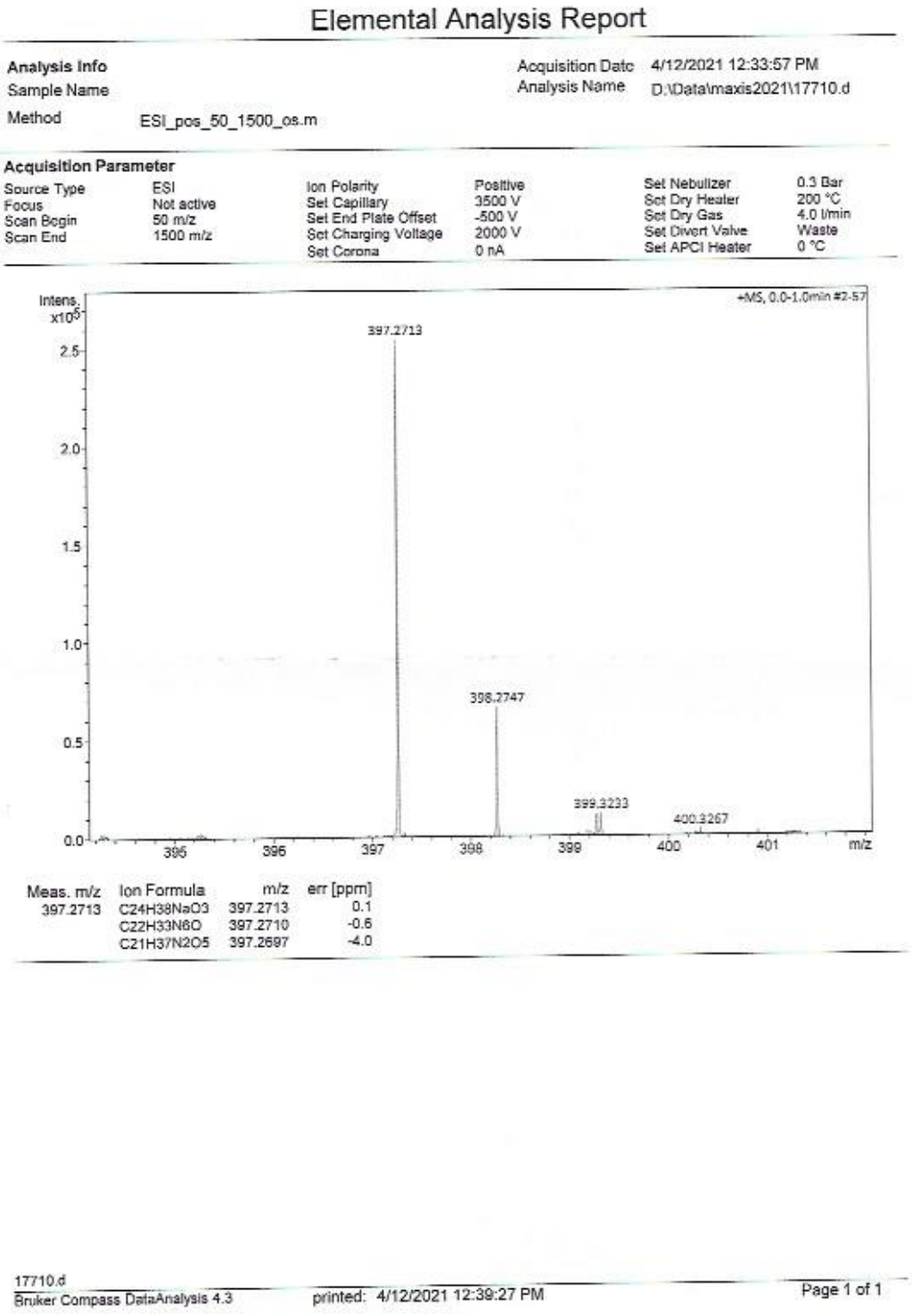

Figure 6.27 HRMS spectrum of compound **10.**

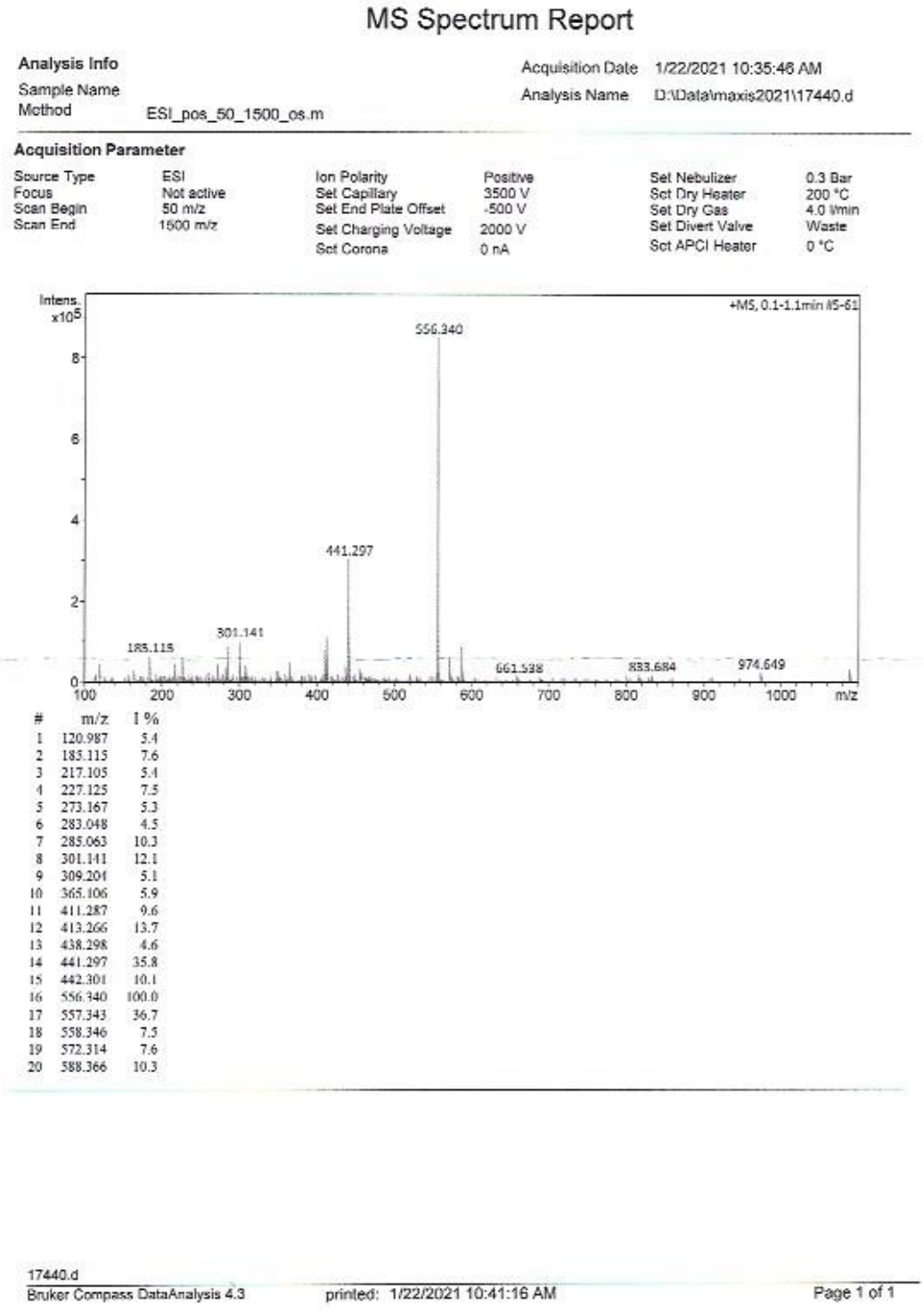

Figure 6.28 MS spectrum of compound **(2*S*,4*S*,5*R*)-diastereomer-17.**

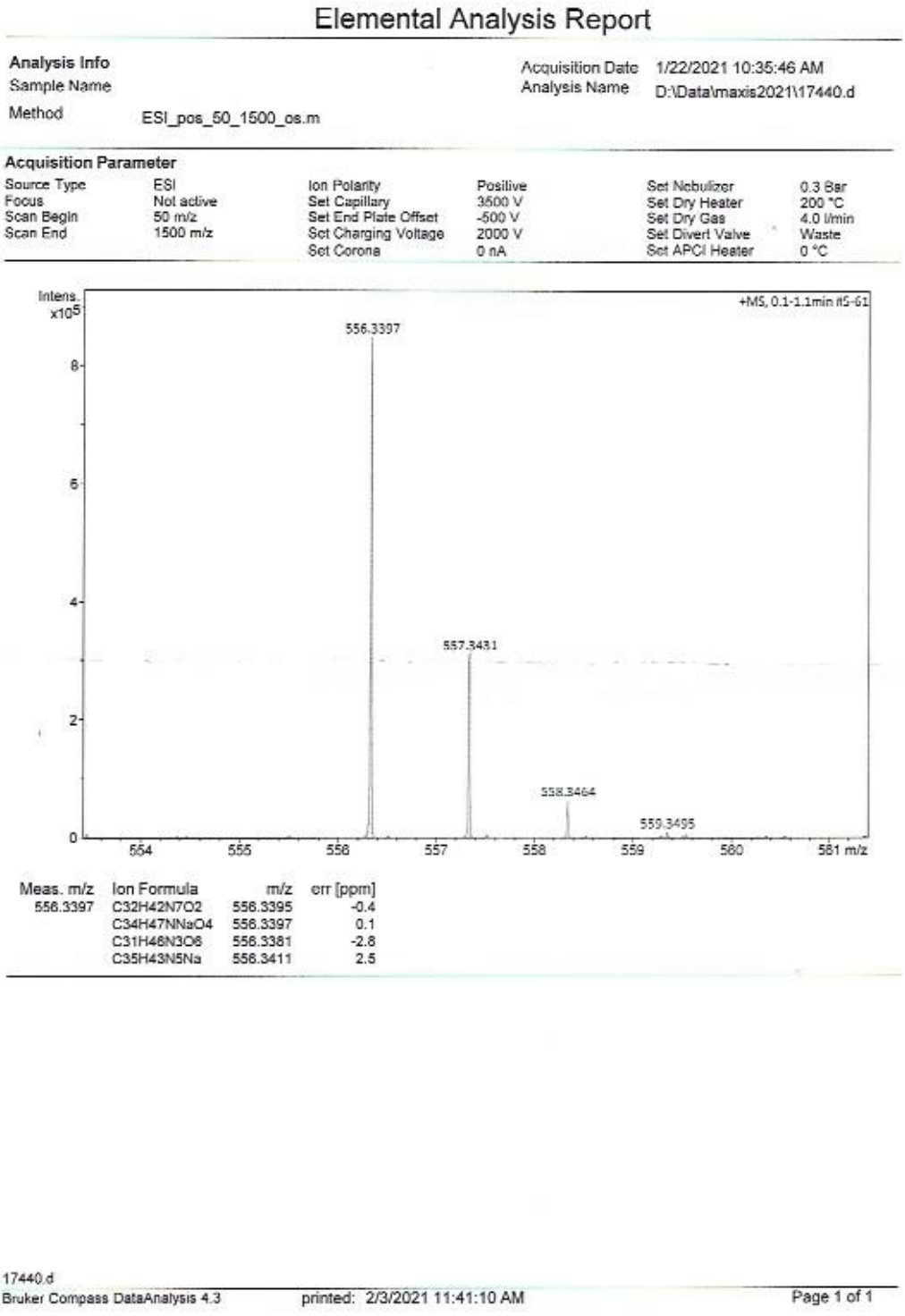

Figure 6.29 HRMS spectrum of compound **(2*S*,4*S*,5*R*)-diastereomer-17.**

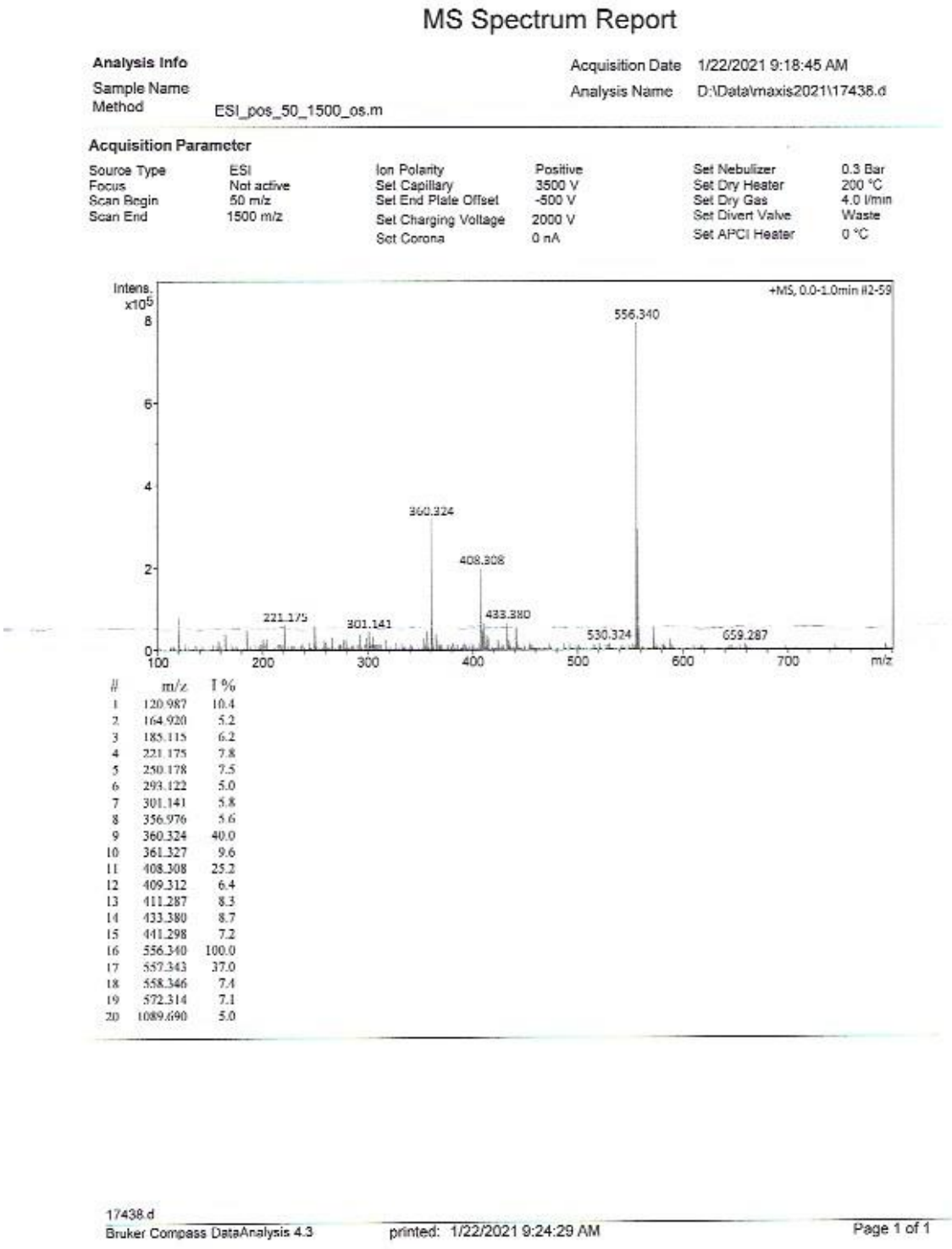

Figure 6.30 MS spectrum of compound **(2*R*,4*S*,5*R*)-diastereomer-18**

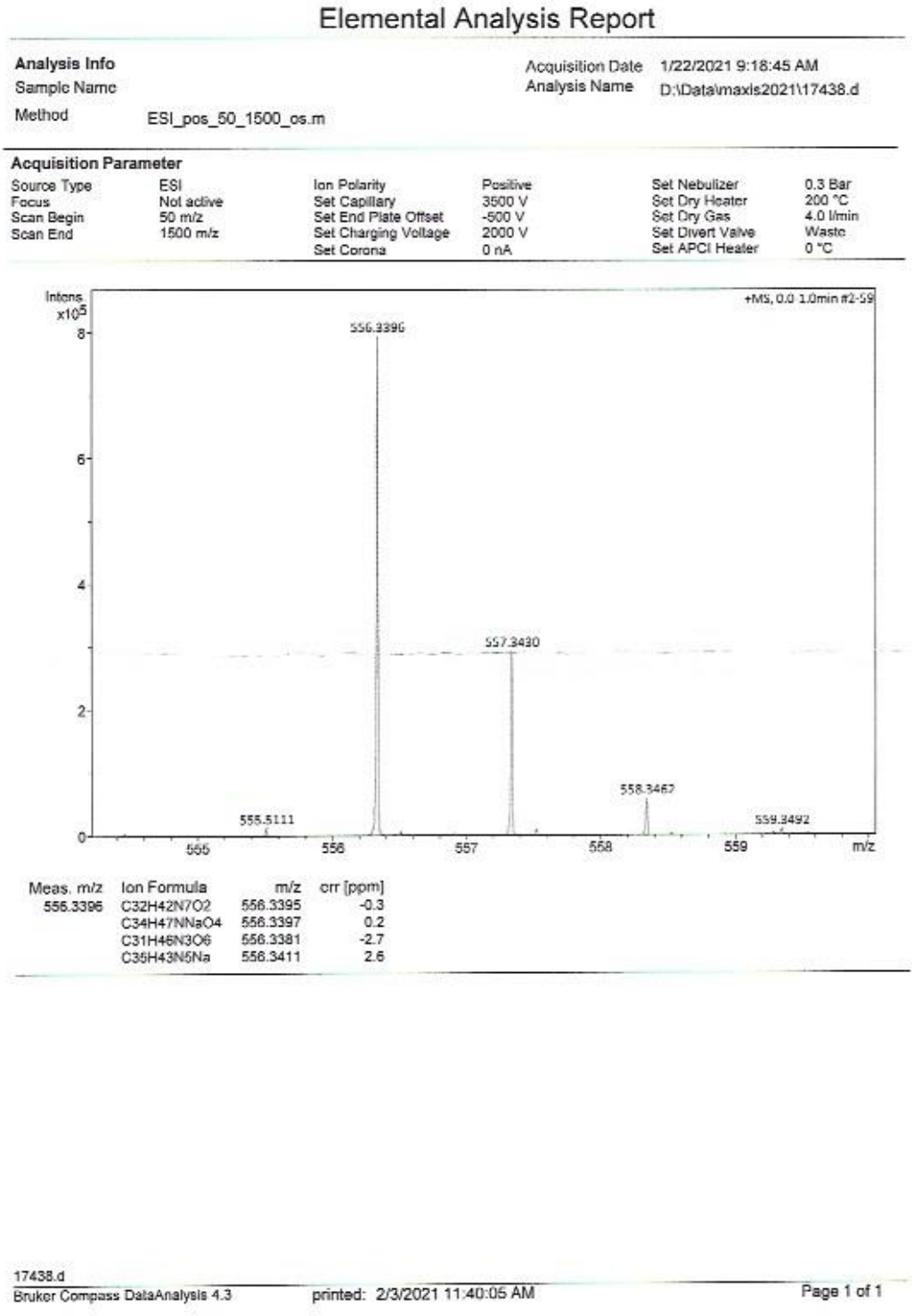

Figure 6.31 HRMS spectrum of compound **(2*R*,4*S*,5*R*)-diastereomer-18**

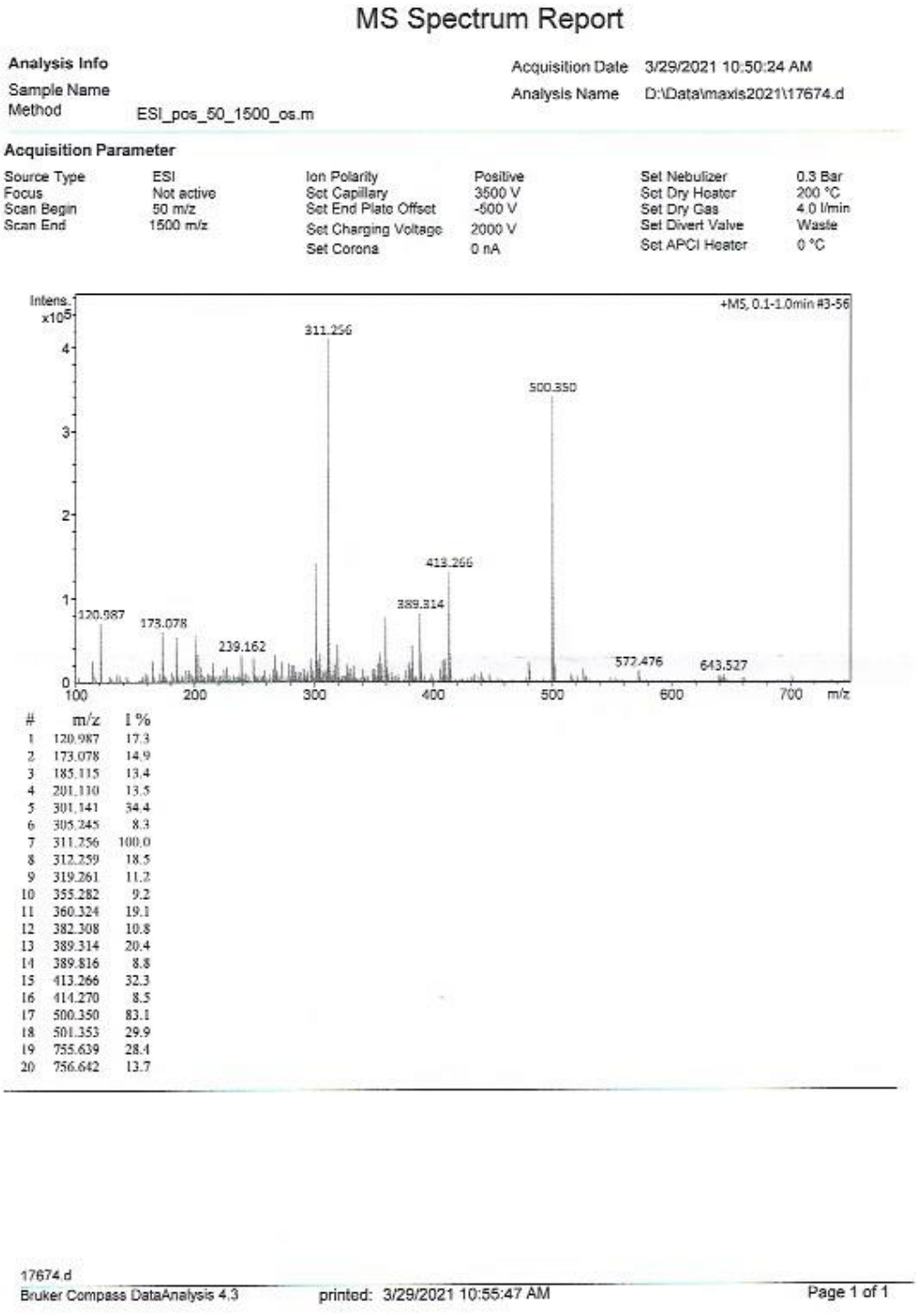

Figure 6.32 MS spectrum of compound **19.**

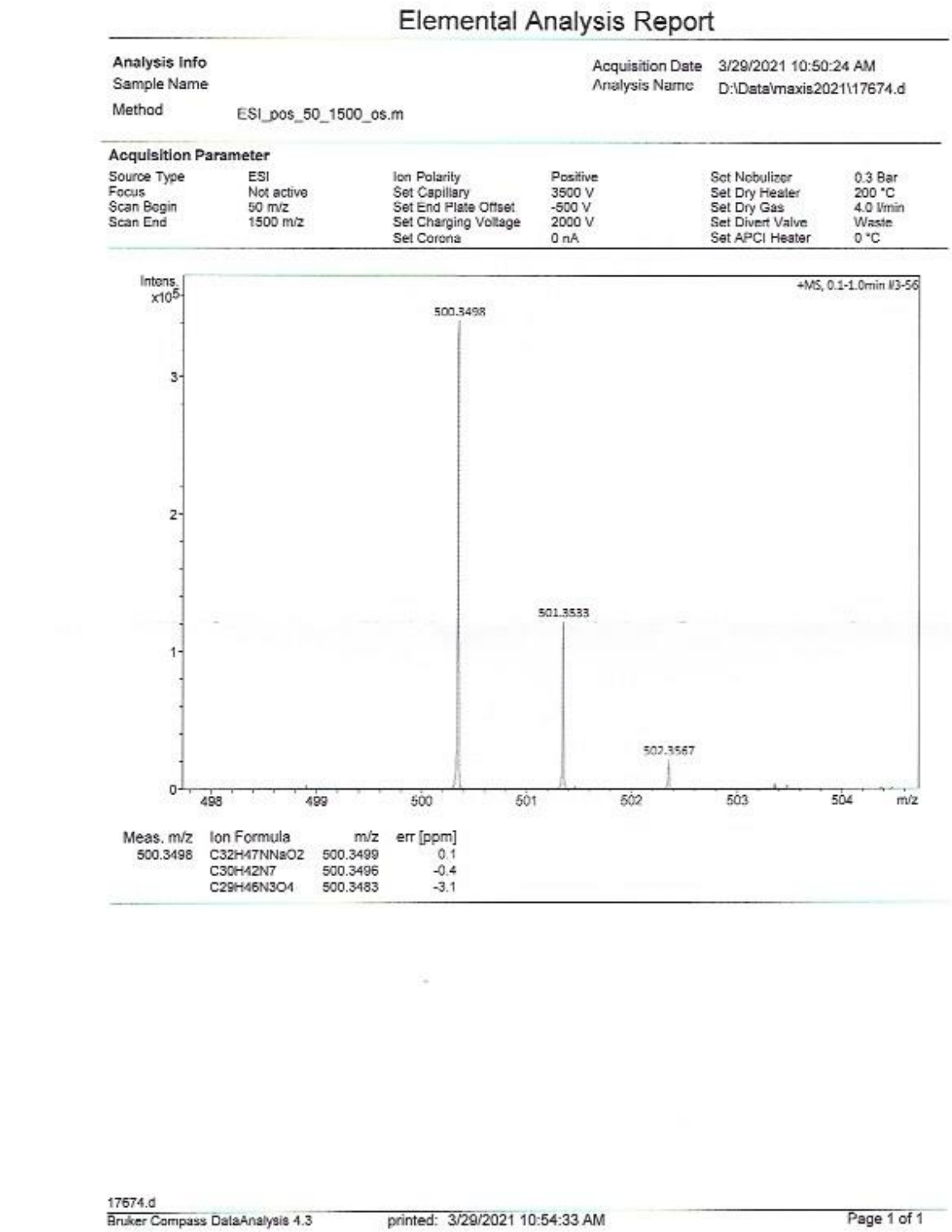

Figure 6.33 HRMS spectrum of compound **19.**

6.3 HPLC chromatograms of synthesized compounds

```
Data File C:\Chem32\2\Data\LA-racemisk 2021-04-08 13-51-16.D
Sample Name: LA-racemisk

    ======================================================================
    Acq. Operator   : SYSTEM
    Sample Operator : SYSTEM
    Acq. Instrument : LC1260-1                      Location :   P1-A-01
    Injection Date  : 4/8/2021 1:51:54 PM
                                                  Inj Volume : 5.000 µl
    Acq. Method     : C:\CHEM32\2\METHODS\uio-test.M
    Last changed    : 4/8/2021 1:41:05 PM by SYSTEM
                      (modified after loading)
    Analysis Method : C:\CHEM32\2\METHODS\uio-test.M
    Last changed    : 4/8/2021 3:07:27 PM by SYSTEM
                      (modified after loading)
    Sample Info     : 1 ml/min, C-18 column, 90% MeOH i H2O, UV-210

    Additional Info : Peak(s) manually integrated
```

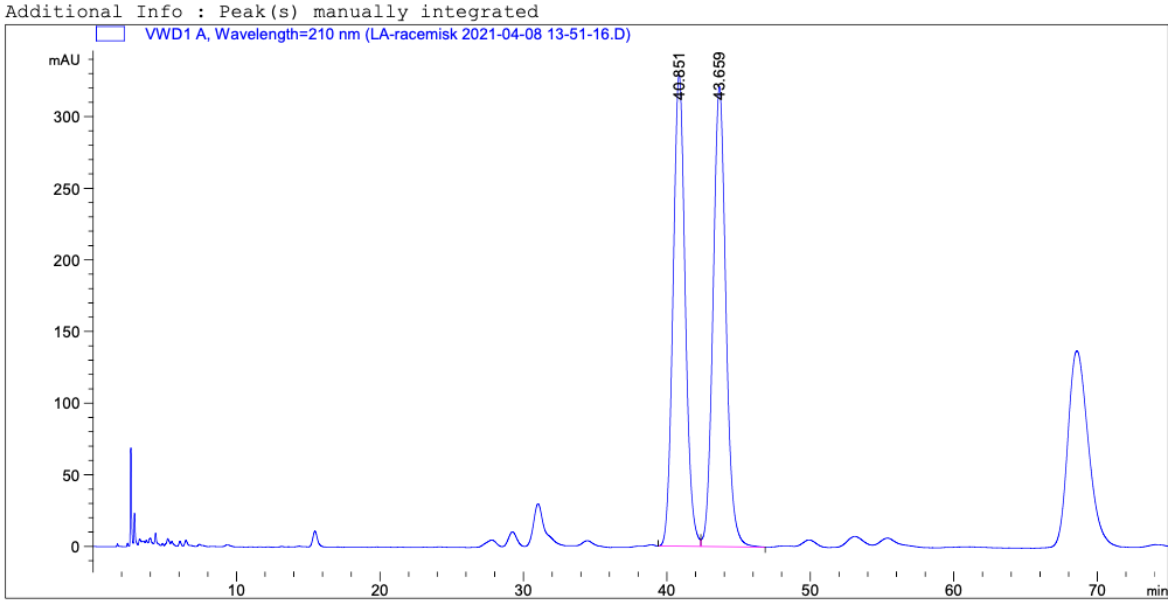


```
    ======================================================================
                              Area Percent Report
    ======================================================================

    Sorted By             :      Signal
    Multiplier            :      1.0000
    Dilution              :      1.0000
    Use Multiplier & Dilution Factor with ISTDs


    Signal 1: VWD1 A, Wavelength=210 nm

    Peak RetTime Type  Width     Area      Height     Area
      #   [min]        [min]   [mAU*s]     [mAU]       %
    ----|-------|----|-------|----------|----------|--------|
       1  40.851 BV    0.9089 1.93871e4   329.28293  49.2430
       2  43.659 VB    0.9518 1.99832e4   321.22903  50.7570

    Totals :                  3.93702e4   650.51196

LC1260-1 4/8/2021 3:07:54 PM SYSTEM                          Page   1 of 2
```

Figure 6.35 HPLC chromatogram of **(2*S*,4*S*,5*R*)-diastereomer-17** and **(2*R*,4*S*,5*R*)-diastereomer-18**

Data File C:\Chem32\2\Data\LA-20.1 2021-04-08 12-15-40.D
Sample Name: LA-20.1

```
==========================================================================
Acq. Operator    : SYSTEM
Sample Operator  : SYSTEM
Acq. Instrument  : LC1260-1                          Location :    P1-A-01
Injection Date   : 4/8/2021 12:16:18 PM
                                                     Inj Volume : 5.000 µl
Acq. Method      : C:\CHEM32\2\METHODS\uio-test.M
Last changed     : 4/8/2021 12:15:11 PM by SYSTEM
                   (modified after loading)
Analysis Method  : C:\CHEM32\2\METHODS\uio-test.M
Last changed     : 4/8/2021 3:07:27 PM by SYSTEM
                   (modified after loading)
Sample Info      : 1 ml/min, C-18 column, 90% MeOH i H2O, UV-210

Additional Info  : Peak(s) manually integrated
```

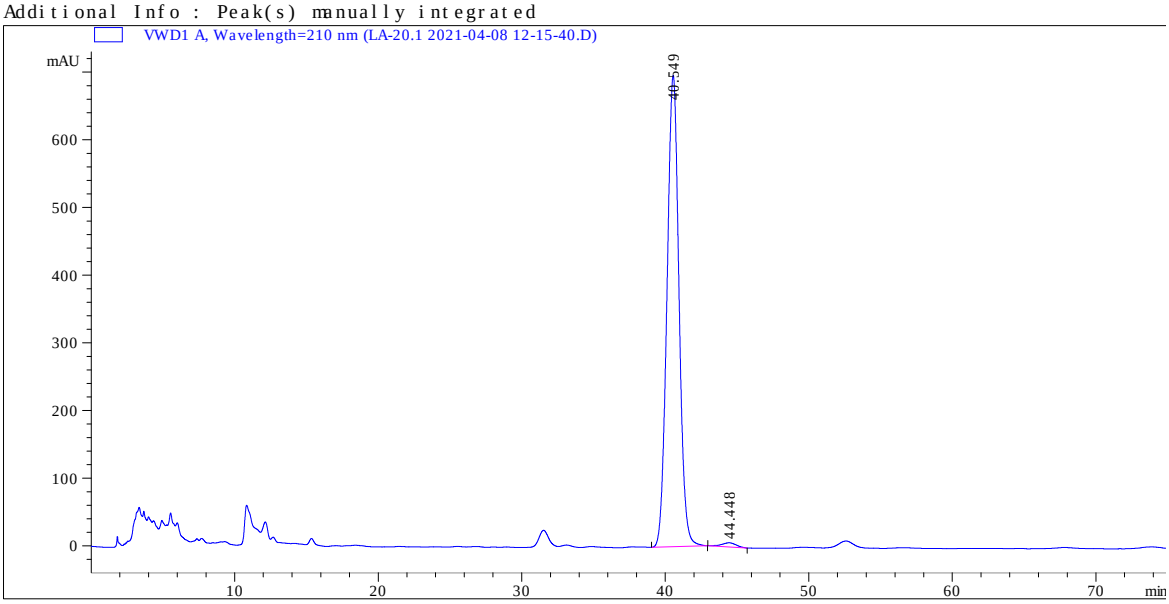


```
==========================================================================
                          Area Percent Report
==========================================================================

Sorted By             :      Signal
Multiplier            :      1.0000
Dilution              :      1.0000
Use Multiplier & Dilution Factor with ISTDs


Signal 1: VWD1 A, Wavelength=210 nm

Peak  RetTime  Type  Width      Area       Height      Area
  #    [min]         [min]   [mAU*s]      [mAU]        %
----|-------|----|-------|----------|----------|--------|
   1  40.549  BB    0.8955 4.03007e4   696.00183  98.9708
   2  44.448  BB    0.9794   419.10123    6.01130   1.0292

Totals :                   4.07198e4   702.01313
```


Figure 6.36 HPLC chromatogram of compound **(2*S*,4*S*,5*R*)-diastereomer-17.**

Data File C:\Chem32\2\Data\LA-spiking racemisk+ LA20.1 2021-04-09 08-08-41.D
Sample Name: LA-spiking racemisk+ LA20.1

```
======================================================================
Acq. Operator   : SYSTEM
Sample Operator : SYSTEM
Acq. Instrument : LC1260-1                      Location :   P1-A-01
Injection Date  : 4/9/2021 8:09:19 AM
                                                Inj Volume : 5.000 µl
Method          : C:\CHEM32\2\METHODS\uio-test.M
Last changed    : 4/9/2021 8:03:01 AM by SYSTEM
                  (modified after loading)
Sample Info     : 1 ml/min, C-18 column, 90% MeOH i H2O, UV-210
```

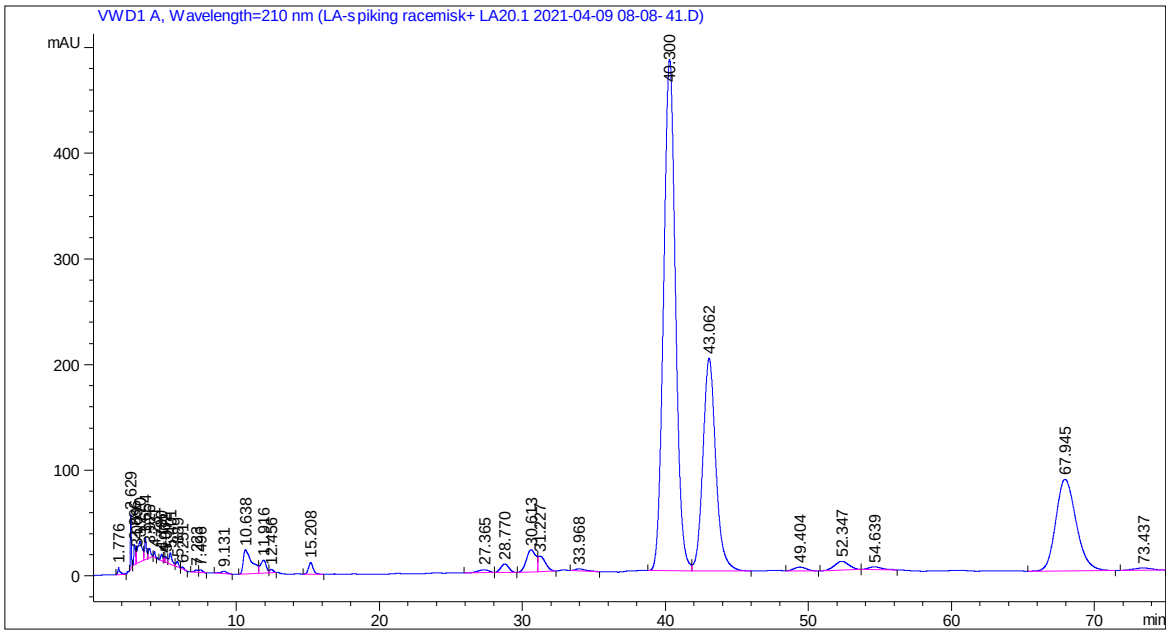


```
======================================================================
                        Area Percent Report
======================================================================

Sorted By             :      Signal
Multiplier            :      1.0000
Dilution              :      1.0000
Use Multiplier & Dilution Factor with ISTDs


Signal 1: VWD1 A, Wavelength=210 nm

Peak RetTime Type  Width     Area      Height     Area
  #   [min]        [min]   [mAU*s]     [mAU]       %
----|-------|----|-------|----------|----------|--------|
   1   1.776 BV R  0.1617   82.81100    6.81945   0.1482
   2   2.629 BB    0.0719  235.74541   51.02007   0.4220
   3   2.886 BV    0.1067  146.52995   19.48216   0.2623
   4   3.009 VV    0.0411   34.12981   12.02432   0.0611
   5   3.270 VV    0.3193  444.76007   19.33774   0.7961
   6   3.654 VV    0.1331  188.42087   20.33096   0.3373
   7   3.926 VB    0.1806  105.54649    8.82095   0.1889
```

Data File C:\Chem32\2\Data\LA-spiking racemisk+ LA20.1 2021-04-09 08-08-41.D
Sample Name: LA-spiking racemisk+ LA20.1

Peak #	RetTime [min]	Type	Width [min]	Area [mAU*s]	Height [mAU]	Area %
8	4.281	BV	0.1049	35.95911	5.24808	0.0644
9	4.780	BV	0.1567	62.93491	6.03434	0.1127
10	4.962	VV	0.0844	25.19025	4.29603	0.0451
11	5.072	VV	0.1497	57.06867	5.33904	0.1022
12	5.401	VV	0.2135	162.12587	10.77710	0.2902
13	5.889	VB	0.1827	61.27803	4.97421	0.1097
14	6.251	BB	0.1670	21.47854	1.98824	0.0384
15	7.223	BV	0.2103	36.06553	2.45559	0.0646
16	7.496	VB	0.2619	47.01632	2.70308	0.0842
17	9.131	BB	0.4365	66.36015	2.24759	0.1188
18	10.638	BV	0.5417	938.54150	22.91988	1.6800
19	11.916	VV	0.4184	339.62900	12.13897	0.6079
20	12.456	VB	0.2899	55.37603	2.97801	0.0991
21	15.208	BB	0.3563	256.70755	10.95848	0.4595
22	27.365	BB	0.7141	149.46248	2.86271	0.2675
23	28.770	BB	0.6070	314.81009	8.07283	0.5635
24	30.613	BV	0.6849	968.80750	20.97502	1.7342
25	31.227	VB	0.5468	519.36908	14.46663	0.9297
26	33.968	BB	0.7296	103.66857	1.86460	0.1856
27	40.300	BV	0.8951	2.80414e4	483.90482	50.1943
28	43.062	VB	0.9555	1.26257e4	201.08484	22.6001
29	49.404	BB	0.8849	208.09471	3.44399	0.3725
30	52.347	BB	1.0381	588.37946	8.30910	1.0532
31	54.639	BB	0.7888	165.86397	2.67710	0.2969
32	67.945	BB	1.5240	8594.35449	86.81369	15.3839
33	73.437	BBA	1.0203	182.13899	2.08892	0.3260
Totals :				5.58658e4	1069.45852	

*** End of Report ***

Figure 6.37 HPLC chromatogram of compound **(2*S*,4*S*,5*R*)-diastereomer-17** spiked with **racemic compound**

Data File C:\Chem32\2\Data\LA20.3 2021-04-09 09-31-21.D
Sample Name: LA20.3

```
=====================================================================
Acq. Operator   : SYSTEM
Sample Operator : SYSTEM
Acq. Instrument : LC1260-1                      Location :   P1-A-01
Injection Date  : 4/9/2021 9:32:00 AM
                                                Inj Volume : 5.000 µl
Method          : C:\CHEM32\2\METHODS\uio-test.M
Last changed    : 4/9/2021 8:03:01 AM by SYSTEM
                  (modified after loading)
Sample Info     : 1 ml/min, C-18 column, 90% MeOH i H2O, UV-210
```

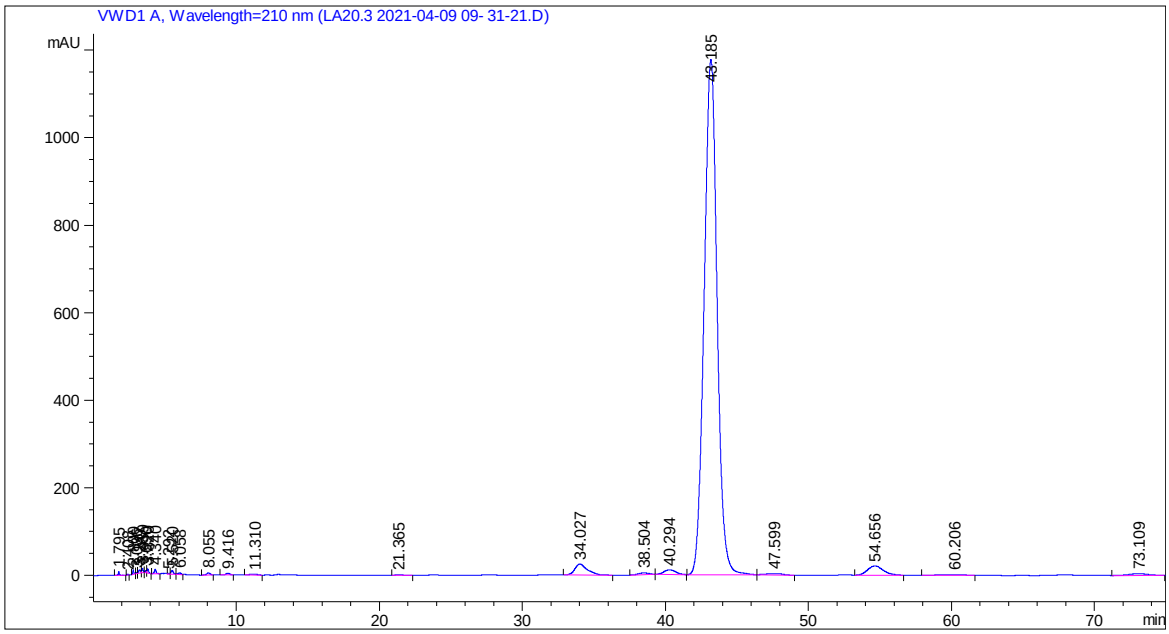


```
=====================================================================
                        Area Percent Report
=====================================================================

Sorted By             :      Signal
Multiplier            :      1.0000
Dilution              :      1.0000
Use Multiplier & Dilution Factor with ISTDs


Signal 1: VWD1 A, Wavelength=210 nm

Peak RetTime Type  Width     Area      Height     Area
  #   [min]        [min]   [mAU*s]     [mAU]       %
----|-------|----|-------|----------|----------|--------|
   1   1.795 BV R  0.0805   50.03836    8.65308   0.0629
   2   2.408 BB    0.0743   10.57545    2.19005   0.0133
   3   2.800 BV    0.0790   53.50050   10.07329   0.0673
   4   3.036 VV    0.0973   17.76920    2.64908   0.0223
   5   3.247 VV    0.1512   72.48302    7.47310   0.0911
   6   3.439 VB    0.0967   69.28200   10.67139   0.0871
   7   3.690 BV    0.0910   33.44498    5.65751   0.0420
```

Data File C:\Chem32\2\Data\LA20.3 2021-04-09 09-31-21.D
Sample Name: LA20.3

Peak #	RetTime [min]	Type	Width [min]	Area [mAU*s]	Height [mAU]	Area %
8	3.820	VB	0.1081	68.16933	9.24097	0.0857
9	4.340	BB	0.1343	95.25529	10.45386	0.1197
10	5.292	VV	0.1487	21.18527	2.06489	0.0266
11	5.520	VV	0.1662	102.73215	8.99997	0.1291
12	6.058	VV	0.2108	62.39336	4.23749	0.0784
13	8.055	BB	0.2224	70.44462	4.85026	0.0886
14	9.416	BB	0.2557	67.56167	4.02791	0.0849
15	11.310	BB	0.4947	75.33118	2.07450	0.0947
16	21.365	BB	0.4601	55.52138	1.80872	0.0698
17	34.027	BB	0.9127	1537.96619	24.79198	1.9332
18	38.504	BB	0.7444	200.53044	4.24251	0.2521
19	40.294	BB	0.8608	607.48969	10.71001	0.7636
20	43.185	BB	0.9627	7.38369e4	1177.23792	92.8142
21	47.599	BB	0.9081	223.28308	2.93657	0.2807
22	54.656	BB	1.1384	1609.08875	21.15586	2.0227
23	60.206	BB	1.3250	222.48117	2.00904	0.2797
24	73.109	BB	1.2012	390.01718	4.08019	0.4903
Totals :				7.95535e4	1342.29015	

*** End of Report ***

Figure 6.38 HPLC chromatogram of compound **(2*R*,4*S*,5*R*)-diastereomer-18**

Data File C:\Chem32\2\Data\LA spiking racemisk + 20.3 2021-04-09 12-08-13.D
Sample Name: LA spiking racemisk + 20.3

```
======================================================================
Acq. Operator   : SYSTEM
Sample Operator : SYSTEM
Acq. Instrument : LC1260-1                      Location :   P1-A-01
Injection Date  : 4/9/2021 12:08:51 PM
                                              Inj Volume : 5.000 µl
Method          : C:\CHEM32\2\METHODS\uio-test.M
Last changed    : 4/9/2021 8:03:01 AM by SYSTEM
                  (modified after loading)
Sample Info     : 1 ml/min, C-18 column, 90% MeOH i H2O, UV-210
```

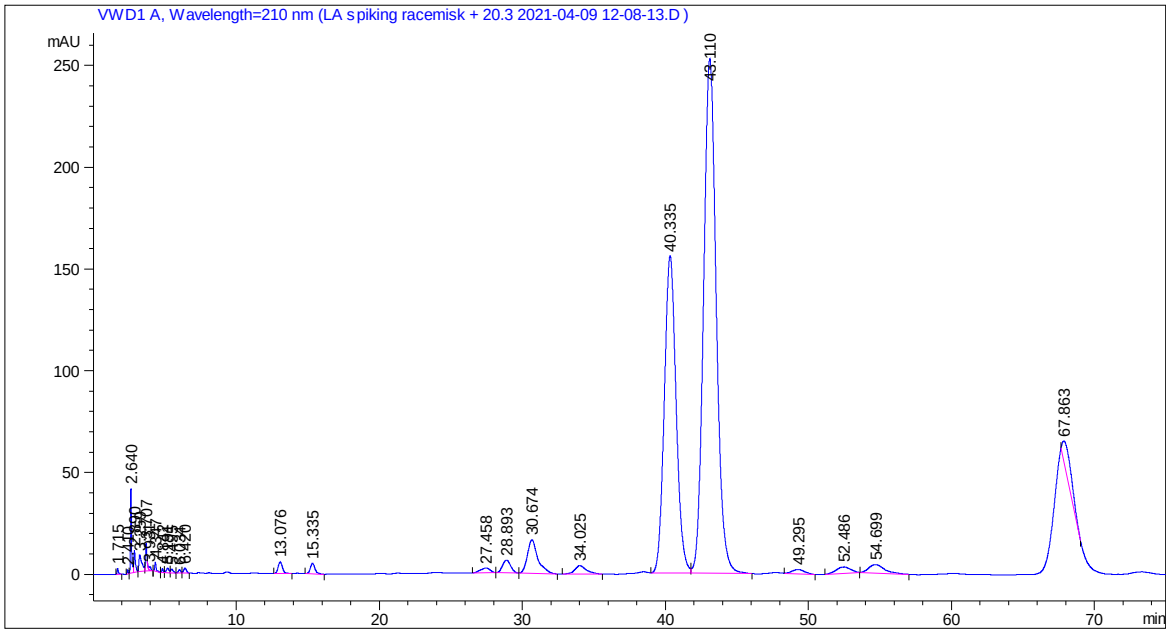


```
======================================================================
                        Area Percent Report
======================================================================

Sorted By             :      Signal
Multiplier            :      1.0000
Dilution              :      1.0000
Use Multiplier & Dilution Factor with ISTDs


Signal 1: VWD1 A, Wavelength=210 nm

Peak RetTime Type  Width     Area      Height     Area
  #   [min]        [min]   [mAU*s]     [mAU]       %
----|-------|----|-------|----------|----------|--------|
   1   1.715 BB    0.0907   18.74676    2.96756   0.0667
   2   2.410 BB    0.0755   10.56014    2.18192   0.0376
   3   2.640 BV R  0.0786  220.03807   41.65591   0.7826
   4   2.890 VB    0.0976   76.32295   10.90794   0.2715
   5   3.259 BV    0.2009  114.73219    8.11938   0.4081
   6   3.707 VV R  0.1117  104.42706   13.72873   0.3714
   7   3.931 VB E  0.1469   19.43867    1.73285   0.0691
```

Data File C:\Chem32\2\Data\LA spiking racemisk + 20.3 2021-04-09 12-08-13.D
Sample Name: LA spiking racemisk + 20.3

Peak #	RetTime [min]	Type	Width [min]	Area [mAU*s]	Height [mAU]	Area %
8	4.347	BB	0.1128	32.53146	4.37342	0.1157
9	4.842	BV	0.1143	14.12027	1.88792	0.0502
10	5.191	VV	0.1829	32.47088	2.41488	0.1155
11	5.495	VB	0.1798	23.74540	1.95335	0.0845
12	6.034	BV	0.1624	18.94191	1.77661	0.0674
13	6.420	VB	0.2041	32.32690	2.44709	0.1150
14	13.076	BB	0.3278	121.81360	5.71245	0.4333
15	15.335	BB	0.3435	116.73274	5.16789	0.4152
16	27.458	BB	0.6136	109.99619	2.33503	0.3912
17	28.893	BB	0.6053	245.91734	6.27374	0.8747
18	30.674	BB	0.7354	833.68085	16.50069	2.9652
19	34.025	BB	0.8296	233.10573	4.09795	0.8291
20	40.335	BV	0.8837	8932.92383	155.85475	31.7720
21	43.110	VB	0.9453	1.55449e4	252.84682	55.2888
22	49.295	BB	0.7564	128.40274	2.17598	0.4567
23	52.486	BB	0.8884	215.37869	3.13535	0.7660
24	54.699	BB	1.0377	315.82935	4.16938	1.1233
25	67.863	BB	0.8902	598.69464	9.99026	2.1294
Totals :				2.81158e4	564.40786	

*** End of Report ***

Figure 6.39 HPLC chromatogram of compound **(2*R*,4*S*,5*R*)-diastereomer-18** spiked with **racemic mixture.**

Data File C:\Chem32\2\Data\LA22.8 2021-03-29 15-16-00.D
Sample Name: LA22.8

```
=====================================================================
Acq. Operator    : SYSTEM
Sample Operator  : SYSTEM
Acq. Instrument  : LC1260-1                          Location :   P1-A-01
Injection Date   : 3/29/2021 3:16:44 PM
                                                     Inj Volume : 10.000 µl
Acq. Method      : C:\CHEM32\2\METHODS\uio-test.M
Last changed     : 3/29/2021 3:50:06 PM by SYSTEM
                   (modified after loading)
Analysis Method  : C:\CHEM32\2\METHODS\uio-test.M
Last changed     : 4/21/2021 2:57:18 PM by SYSTEM
                   (modified after loading)
Sample Info      : 1 ml/min, C-18 column, 80% i MeOH in H2O, UV-201
```

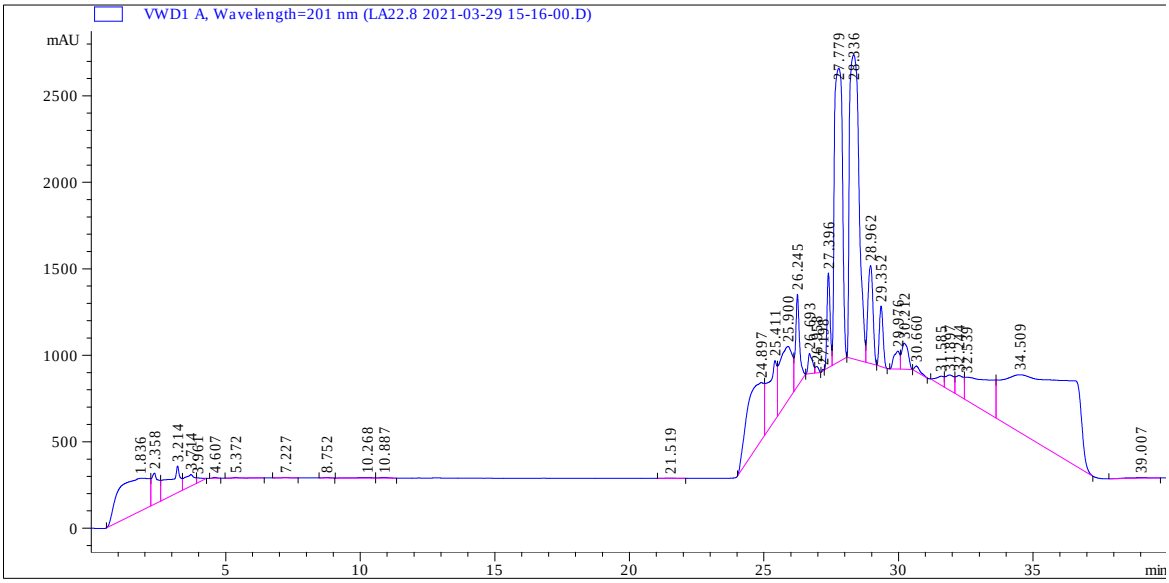


```
=====================================================================
                        Area Percent Report
=====================================================================

Sorted By             :      Signal
Multiplier            :      1.0000
Dilution              :      1.0000
Use Multiplier & Dilution Factor with ISTDs


Signal 1: VWD1 A, Wavelength=201 nm

Peak  RetTime Type  Width     Area      Height     Area
  #    [min]      [min]    [mAU*s]     [mAU]       %
----|-------|----|-------|----------|----------|--------|
   1   1.836 BV    1.0022 1.60802e4  190.02675   6.2689
   2   2.358 VV    0.2446 3204.17676 179.16457   1.2491
   3   3.214 VV    0.4040 5089.57568 155.04546   1.9842
   4   3.714 VV    0.3418 1804.72754  66.47211   0.7036
   5   3.961 VB    0.1662  349.21371  28.06161   0.1361
   6   4.607 BB    0.1532   49.00303   4.92174   0.0191
```

Data File C:\Chem32\2\Data\LA22.8 2021-03-29 15-16-00.D
Sample Name: LA22.8

Peak #	RetTime [min]	Type	Width [min]	Area [mAU*s]	Height [mAU]	Area %
7	5.372	BV R	0.2550	82.93858	4.41926	0.0323
8	7.227	BB	0.3077	44.76363	2.07521	0.0175
9	8.752	BB	0.2394	32.67757	2.17312	0.0127
10	10.268	BV	0.6704	125.76963	2.37669	0.0490
11	10.887	VB	0.3041	78.89742	3.86648	0.0308
12	21.519	BB	0.4083	47.11846	1.70586	0.0184
13	24.897	BV	0.5907	1.61336e4	335.12473	6.2897
14	25.411	VV	0.3039	8200.31250	343.00909	3.1969
15	25.900	VV	0.4507	1.06463e4	310.78101	4.1504
16	26.245	VB	0.1495	5497.28955	532.39673	2.1431
17	26.693	BV	0.1496	1280.71045	118.02924	0.4993
18	26.958	VB	0.1408	329.28519	37.75554	0.1284
19	27.198	BB	0.0691	36.19468	8.60865	0.0141
20	27.396	BV	0.1242	4368.99170	547.09839	1.7032
21	27.779	VB	0.3368	3.45974e4	1697.67822	13.4878
22	28.336	BV	0.3947	4.32002e4	1758.04468	16.8416
23	28.962	VB	0.2130	7419.55713	565.65918	2.8925
24	29.352	BB	0.1514	3355.45581	351.26038	1.3081
25	29.976	BV	0.2070	1596.24683	104.61337	0.6223
26	30.212	VB	0.2696	2508.39038	150.35497	0.9779
27	30.660	BB	0.2173	451.97672	31.90953	0.1762
28	31.585	BV	0.2663	973.02429	51.75824	0.3793
29	31.897	VV	0.3133	1905.96423	87.79926	0.7430
30	32.244	VV	0.2932	2471.03052	117.10073	0.9633
31	32.539	VV	1.1317	1.20031e4	135.20708	4.6794
32	34.509	VB	2.7025	7.22653e4	333.43115	28.1726
33	39.007	BB	0.8637	279.96771	4.06894	0.1091
Totals :				2.56509e5	8261.99798	

*** End of Report ***

LC1260-1 4/21/2021 3:03:32 PM SYSTEM Page 2 of 2

Figure 6.40 HPLC chromatogram of compound **19.**

6.4 UV Spectra of synthesized compounds

Hardcopy view Date 4/7/2021 Time 09:40:18 Page 1 of 1

Overlaid Sample Spectra

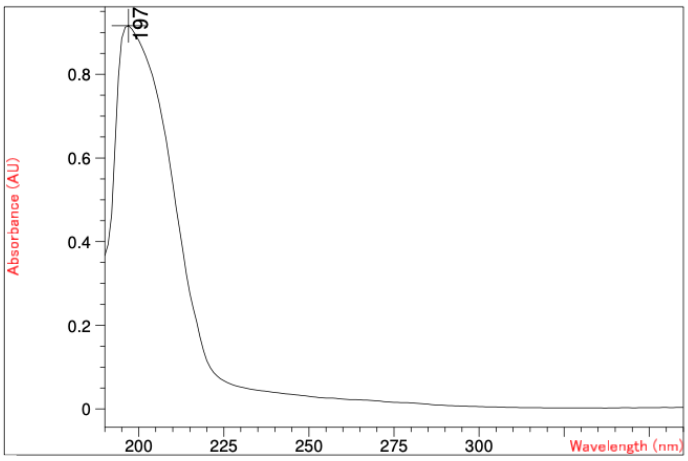

Sample/Result Table

#	Name	Peaks(nm)	Abs(AU)
1		197.0	0.91572

*** End Hardcopy view ***

Figure 6.41 UV spectrum of compound **racemic mixture** of **(2*S*,4*S*,5*R*)-diastereomer-17 and (2*R*,4*S*,5*R*)-diastereomer-18**

Hardcopy view Date 3/29/2021 Time 15:22:12 Page 1 of 1

Last Blank Spectrum

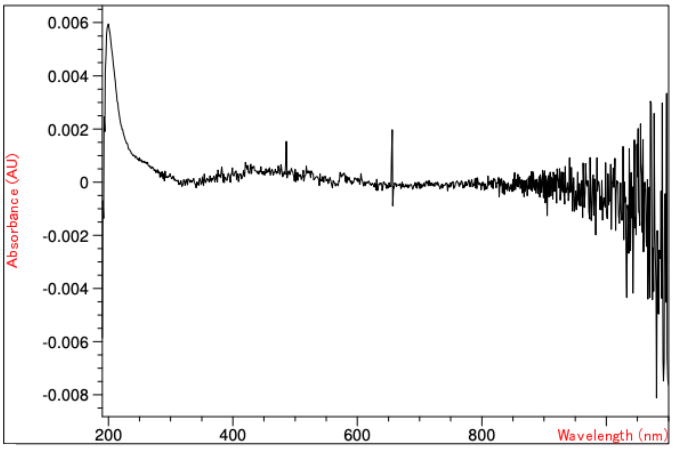

Overlaid Sample Spectra

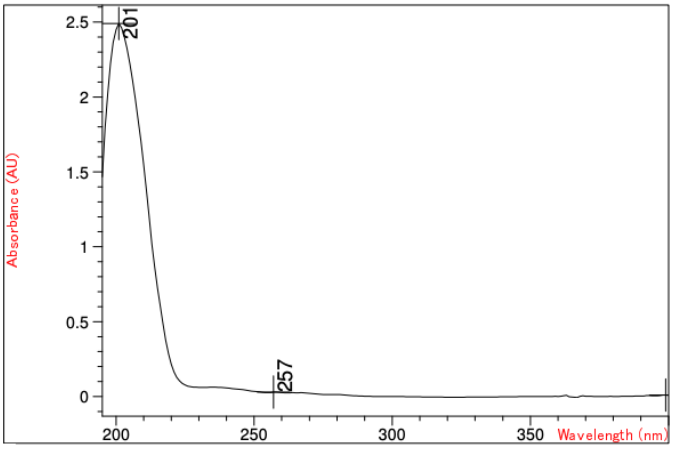

Sample/Result Table

#	Name	Peaks(nm)	Abs(AU)	#	Name	Peaks(nm)	Abs(AU)
1		201.0	2.48980	1		399.0	1.0251E-2
1		257.0	2.9261E-2				

*** End Hardcopy view ***

Figure 6.42 UV spectrum of compound **19.**